

LA-8085-MS
Informal Report
UC-34b
Issued: October 1979

Solar Photo Rate Coefficients

W. F. Huebner
C. W. Carpenter*



*Graduate Research Assistant. Department of Chemistry, University of Wisconsin,
Madison, WI 53706.



SOLAR PHOTO RATE COEFFICIENTS

by

W. F. Huebner and C. W. Carpenter

ABSTRACT

Photo rate coefficients based on wavelength-dependent solar photon flux at 1 AU heliocentric distance have been determined for atomic hydrogen, carbon, nitrogen, and oxygen, and for some molecules formed from these elements. Branching ratios are considered for the various modes of decay of these molecules. Rates for some metastable states have been estimated.

I. INTRODUCTION

Photo rate coefficients for atomic and molecular species found or suspected in the atmospheres of planets, satellites (moons) and comets are needed in analysis and modeling. Lifetimes for possible mother molecules of observed radicals in comets were determined by Potter and del Duca¹ and more recently by Jackson.^{2,3} Some rate coefficients for several atomic and simple molecular constituents of lunar and planetary atmospheres have been calculated by Siscoe and Mukherjee,⁴ McElroy and Hunten,⁵ McElroy and McConnell,⁶ and McElroy et al.,⁷ and for solar wind physics by Axford.⁸ In addition, lifetimes (reciprocals of rate coefficients) for some isolated species or rate coefficients in very limited wavelength bands -- e.g., the solar hydrogen Lyman alpha line -- have been obtained by various investigators for special situations and applications.

If the chief concern is the prediction of potential mother molecules of observed radicals, then only the main decay branch needs to be considered.¹ For

molecules the main branch is almost always a dissociation, very seldom ionization, and never photodissociative ionization. This is immediately apparent from the magnitude of the threshold values for these processes (see Table I) -- although a small photodissociation and a large ionization cross section near the respective thresholds can invalidate such an oversimplified analysis. Predissociation and autoionization significantly increase rate coefficients (decrease lifetimes) and, if known, are included in the evaluations presented here.

The dissociation rate coefficients presented in Refs. 1-3 are based on averages over bandwidths of 100 Å or more, at wavelengths down to that of the hydrogen Lyman alpha line (1215.7 Å). No details about branching ratios are given in Refs. 1-4 and 7. For terrestrial atmospheric constituents, cross sections and rate constants have been compiled by Huffman⁹ and by Baurer and Bortner,¹⁰ respectively. They also list many references.

In this report photo rate coefficients are plotted for small wavelength bands and the summed values are listed for atomic hydrogen, carbon, nitrogen and oxygen and for simple molecules formed from these elements. Most of the known branching ratios are taken into account, but where necessary, some have been estimated. In addition rate coefficients are estimated for a few metastable states. In Sec. II the solar spectrum is presented. Section III presents the computed rate coefficients for each photoprocess and plots of the rates in each solar flux bin together with the sources for the cross sections, the thresholds, and the branching ratios. For easy reference the rate coefficients for each process and summed for all processes operating on a mother species are presented in Table I. The last column in this table gives the mean excess energy of the solar photolysis products. Species without state designation always refer to the ground state. Since cross sections are measured typically around 300 °K, rotationally excited levels in the ground state of molecules will effectively lower the photothreshold. The molecular rate coefficients presented here include this contribution caused by the shift to the effective threshold. Larger contributions from excited states occur at higher temperatures.

The rate constants scale approximately with the solar flux, i.e., with r_h^{-2} , where r_h is the heliocentric distance in AU. At small r_h the rate constants can increase more rapidly with increasing r_h^{-2} because of the contributions from thermally excited states.

TABLE I
PHOTO RATE COEFFICIENTS

Mother Species	Decay Products	Threshold (Å)	Rate Coefficient (10^{-6} s^{-1})	Total Rate Coefficient (10^{-6} s^{-1})	Photolysis Products Excess Energy (eV)
H	$\text{H}^+ + \text{e}$	911.75	0.073	0.073	3.6
$\text{C}(^3\text{P})$	$\text{C}^+ + \text{e}$	1101.1	0.41	0.41	5.8
$\text{C}(^1\text{D})$	$\text{C}^+ + \text{e}$	1240.	3.6	3.6	1.0
$\text{C}(^1\text{S})$	$\text{C}^+ + \text{e}$	1446.	4.3	4.3	2.1
N	$\text{N}^+ + \text{e}$	853.06	0.19	0.19	14.8
$\text{O}(^3\text{P})$	$\text{O}^+ + \text{e}$	910.44	0.21	0.21	21.5
$\text{O}(^1\text{D})$	$\text{O}^+ + \text{e}$	827.9	0.18	0.18	21.5
$\text{O}(^1\text{S})$	$\text{O}^+ + \text{e}$	858.3	0.20	0.20	18.8
H_2	$\text{H} + \text{H}$	970.0	0.044		2.2
	$\text{H}_2^+ + \text{e}$	803.67	0.054		6.6
	$\text{H} + \text{H}^+ + \text{e}$	685.8	0.0095		24.7
				0.11	

TABLE I (cont)

Mother Species	Decay Products	Threshold (Å)	Rate Coefficient (10^{-6} s^{-1})	Total Rate Coefficient (10^{-6} s^{-1})	Photolysis Products Excess Energy (eV)
CH	C + H	3589.9	12000.	12000.	0.5 ⁻
	CH ⁺ + e	1170.	0.76		6.4
CO(X ¹ Σ ⁺)	C + O	1117.8	0.28	0.65	2.6
	C(¹ D) + O(¹ D)	863.4	0.041		5.9
	CO ⁺ + e	884.79	0.31		10.2
	O + C ⁺ + e	554.7	0.0080		28.1
	C + O ⁺ + e	501.8	0.0060		31.0
CO(a ³ Π)	C + O	2431.8	79.	88.	2.1
	CO ⁺ + e	1549.1	8.6		2.0
	O + C ⁺ + e	758.3	0.011		28.6
	C + O ⁺ + e	662.7	0.0084		32.6
N ₂	N + N	1021.4	0.66	1.0	1.0
	N ₂ ⁺ + e	796.	0.35		17.8
	N + N ⁺ + e	510.4	0.015		28.7
NO	N + O	1910.	2.1	3.5	1.8
	NO ⁺ + e	1340.	1.3		8.2
	N + O ⁺ + e	616.2	0.0018		18.5
	O + N ⁺ + e	589.3	0.032		25.0

TABLE I (cont)

Mother Species	Decay Products	Threshold (Å)	Rate Coefficient (10^{-6} s^{-1})	Total Rate Coefficient (10^{-6} s^{-1})	Photolysis Products Excess Energy (eV)
O_2	$\text{O}(^3\text{P}) + \text{O}(^3\text{P})$	2454.	0.060		8.3
	$\text{O}(^3\text{P}) + \text{O}(^1\text{D})$	1759.	4.2		1.3
	$\text{O}(^1\text{S}) + \text{O}(^1\text{S})$	923.	0.042		0.8
	$\text{O}_2^+ + \text{e}$	1027.8	0.51		17.2
	$\text{O} + \text{O}^+ + \text{e}$	585.	0.053		26.8
				4.9	
H_2O	$\text{H} + \text{OH}$	1860.	10.		1.9
	$\text{H}_2 + \text{O}(^1\text{D})$	1450.	1.4		1.9
	$\text{H}_2\text{O}^+ + \text{e}$	984.	0.33		12.3
	$\text{H} + \text{OH}^+ + \text{e}$	684.4	0.055		18.5
	$\text{H}_2 + \text{O}^+ + \text{e}$	664.8	0.0058		36.3
	$\text{OH} + \text{H}^+ + \text{e}$	662.3	0.013		24.9
				12.	
HCN	$\text{H} + \text{CN}$	1950.	13.		4.3
				13.	
CO_2	$\text{CO}(\text{X}^1\Sigma^+) + \text{O}(^1\text{D})$	1990.	0.94		5.5
	$\text{CO}(\text{a}^3\Pi) + \text{O}$	1070.	0.28		1.9
	$\text{CO}_2^+ + \text{e}$	899.22	0.66		16.9
	$\text{O} + \text{CO}^+ + \text{e}$	636.93	0.050		26.9
	$\text{CO} + \text{O}^+ + \text{e}$	650.26	0.064		27.7
	$\text{O}_2 + \text{C}^+ + \text{e}$	546.55	0.029		30.0
				2.0	

TABLE I (cont)

Mother Species	Decay Products	Threshold (Å)	Rate Coefficient (10^{-6} s^{-1})	Total Rate Coefficient (10^{-6} s^{-1})	Photolysis Products Excess Energy (eV)
NH_3	$\text{NH} + \text{H}_2$	3170.	63.		2.3
	$\text{NH}_2^+ + \text{H}$	2798.	110.		2.0
	$\text{NH}_3^+ + \text{e}$	1220.	0.61		5.8
	$\text{H} + \text{NH}_2^+ + \text{e}$	786.2	0.18		11.2
	$\text{H}_2 + \text{NH}^+ + \text{e}$	~775.	0.0069		26.1
	$\text{H}_2 + \text{H} + \text{N}^+ + \text{e}$	~560.	0.0033		29.3
	$\text{NH}_2 + \text{H}^+ + \text{e}$	~387.	0.0034		19.8
				180.	
C_2H_2	$\text{H} + \text{C}_2\text{H}$	2306.	30.		3.5
	$\text{C}_2\text{H}_2^+ + \text{e}$	1086.	0.78		5.1
	$\text{H} + \text{C}_2\text{H}^+ + \text{e}$	697.	0.075		15.7
				31.	
H_2CO	$\text{H}_2 + \text{CO}$	3740.	160.		0.5
	$\text{H} + \text{HCO}$	3493.	85.		0.5
	$\text{H} + \text{H} + \text{CO}$	2750.	32.		3.0
	$\text{H}_2\text{CO}^+ + \text{e}$	1141.6	0.38		3.3
	$\text{H} + \text{HCO}^+ + \text{e}$	1043.	0.20		7.0
	$\text{H}_2 + \text{CO}^+ + \text{e}$	882.	0.12		28.4
				280.	

TABLE I (cont)

Mother Species	Decay Products	Threshold (Å)	Rate Coefficient (10^{-6} s^{-1})	Total Rate Coefficient (10^{-6} s^{-1})	Photolysis Products Excess Energy (eV)
CH ₄	CH ₃ + H	2800.	1.0		5.9
	CH ₂ + H ₂	1574.	5.6		2.5
	CH + H ₂ + H	1360.	0.50		1.8
	CH ₄ ⁺ + e	945.	0.36		5.4
	H + CH ₃ ⁺ + e	866.	0.20		8.0
	H ₂ + CH ₂ ⁺ + e	822.	0.021		19.5
	CH ₃ + H ⁺ + e	686.	0.0091		26.9
	H ₂ + H + CH ⁺ + e	545.	0.0042		24.9
				7.7	
HCOOH	CO ₂ + H ₂	2500.	270.		1.8
	HCO + OH	2500.	490.		1.8
	HCOOH ⁺ + e	1094.4	0.91		3.9
	OH + HCO ⁺ + e	902.	0.28		21.4
				760.	
HC ₃ N	HC ₂ + CN	1632.	28.		2.1
				28.	
C ₂ H ₄	C ₂ H ₂ + H ₂	1973.	41.		1.4
	C ₂ H ₂ + H + H	1226.	5.2		0.4
	C ₂ H ₄ ⁺ + e	1180.	0.58		7.3
	H ₂ + C ₂ H ₂ ⁺ + e	945.	0.20		12.1
	H + C ₂ H ₃ ⁺ + e	898.	0.23		13.0
				48.	

TABLE I (cont)

Mother Species	Decay Products	Threshold (Å)	Rate Coefficient (10^{-6} s^{-1})	Total Rate Coefficient (10^{-6} s^{-1})	Photolysis Products Excess Energy (eV)
CH ₃ OH	H ₂ CO + H ₂	2053.	250.		2.2
	CH ₃ + OH	2053.	13.		2.3
	CH ₃ OH ⁺ + e	1143.	0.50		2.6
	H + CH ₃ O ⁺ + e	1006.	0.12		3.5
	H ₂ + H ₂ CO ⁺ + e	976.	0.12		4.4
				270.	

II. SOLAR FLUX

The solar flux for the quiet sun has been compiled from many publications. To provide better resolution, it was sometimes necessary to interpolate by prorating the unresolved portions of flux measured in large wavelength intervals to smaller bins and then add the measured flux from emission lines with wavelengths that fall into these bins. Up to $\lambda = 10 \text{ \AA}$, data from Swider¹¹ were used. In the interval 10 \AA to 280 \AA measured fluxes were taken from Hinteregger.¹² From 270 \AA to 1163 \AA the data from Hall and Hinteregger¹³ were interpolated. In the range from 1163 \AA to 7350 \AA data from Ackerman¹⁴ were used with a correction by Simon¹⁵ in the interval 1961 \AA to 2299 \AA . Table II presents the details of the solar flux expressed as photons $\text{cm}^{-2} \text{ s}^{-1}$ in each wavelength bin. Figure 1 presents the same data but only up to 3975 \AA .

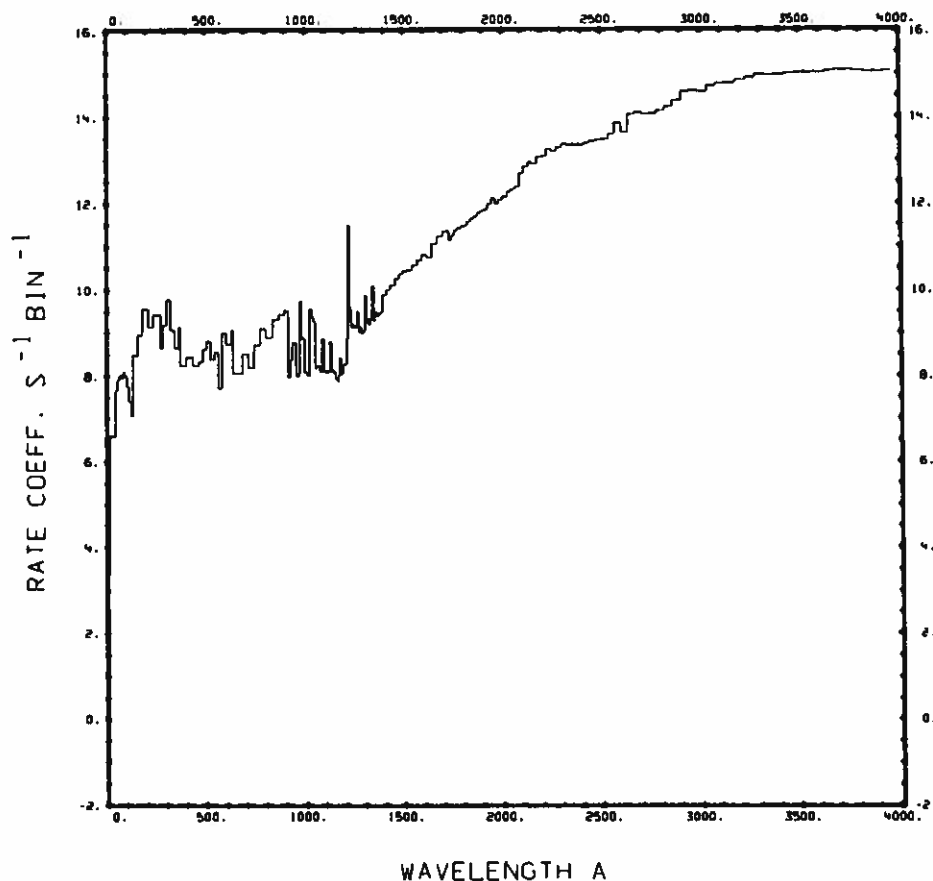


Fig. 1. Solar Flux.

TABLE II
SOLAR PHOTON FLUX [PHOTONS $\text{cm}^{-2} \text{s}^{-1}$] IN EACH BIN
BRACKETED BY WAVELENGTHS [Å]

WAVELENGTH	FLUX	WAVELENGTH	FLUX	WAVELENGTH	FLUX	WAVELENGTH	FLUX
0.00	1.00E-01	1057.00	1.70E+08	1852.00	4.95E+11	3975.00	1.54E+15
2.00	3.00E+01	1070.00	1.31E+08	1869.00	5.94E+11	4025.00	1.90E+15
4.00	2.50E+03	1080.00	7.21E+08	1887.00	6.59E+11	4075.00	1.99E+15
6.00	2.80E+04	1090.00	1.31E+08	1905.00	7.26E+11	4125.00	1.99E+15
8.00	1.80E+05	1100.00	1.31E+08	1923.00	9.85E+11	4175.00	2.02E+15
10.00	4.00E+06	1110.00	1.31E+08	1942.00	1.27E+12	4225.00	2.01E+15
40.00	4.70E+07	1120.00	6.21E+08	1961.00	1.01E+12	4275.00	1.94E+15
50.00	6.30E+07	1130.00	1.31E+08	1980.00	1.20E+12	4325.00	1.98E+15
60.00	1.05E+08	1140.00	1.31E+08	2000.00	1.44E+12	4375.00	2.25E+15
70.00	9.40E+07	1150.00	9.15E+07	2020.00	1.80E+12	4425.00	2.39E+15
80.00	1.20E+08	1157.00	7.84E+07	2041.00	2.08E+12	4475.00	2.48E+15
90.00	9.90E+07	1163.00	1.03E+08	2062.00	2.45E+12	4525.00	2.49E+15
100.00	5.60E+07	1170.00	2.66E+08	2083.00	3.09E+12	4575.00	2.48E+15
110.00	2.50E+07	1176.00	1.12E+08	2105.00	7.12E+12	4625.00	2.50E+15
120.00	1.20E+07	1183.00	1.24E+08	2128.00	9.23E+12	4675.00	2.55E+15
128.00	3.07E+08	1190.00	1.82E+08	2150.00	8.42E+12	4725.00	2.61E+15
153.00	9.00E+08	1198.00	1.90E+08	2174.00	1.20E+13	4775.00	2.59E+15
176.00	3.70E+09	1205.00	7.40E+08	2198.00	1.22E+13	4825.00	2.46E+15
205.00	1.40E+09	1212.00	3.02E+11	2222.00	1.77E+13	4875.00	2.44E+15
231.00	3.10E+09	1220.00	3.67E+09	2247.00	1.60E+13	4925.00	2.53E+15
270.00	4.50E+08	1227.00	1.36E+09	2273.00	1.96E+13	4975.00	2.48E+15
280.00	1.54E+09	1235.00	1.61E+09	2299.00	2.40E+13	5025.00	2.49E+15
300.00	5.84E+09	1242.00	1.32E+09	2326.00	2.25E+13	5075.00	2.50E+15
320.00	1.16E+09	1250.00	1.41E+09	2353.00	2.21E+13	5125.00	2.43E+15
340.00	4.50E+08	1258.00	3.11E+09	2381.00	2.32E+13	5175.00	2.43E+15
360.00	1.31E+09	1266.00	1.06E+09	2410.00	2.50E+13	5225.00	2.52E+15
370.00	1.77E+08	1274.00	1.37E+09	2439.00	2.73E+13	5275.00	2.58E+15
400.00	2.76E+08	1282.00	1.02E+09	2469.00	2.88E+13	5325.00	2.64E+15
430.00	1.77E+08	1290.00	1.14E+09	2500.00	3.02E+13	5375.00	2.67E+15
460.00	2.12E+08	1299.00	7.29E+09	2532.00	3.97E+13	5425.00	2.70E+15
480.00	4.32E+08	1307.00	2.20E+09	2564.00	7.13E+13	5475.00	2.68E+15
500.00	6.32E+08	1316.00	1.59E+09	2597.00	4.37E+13	5525.00	2.66E+15
520.00	2.42E+08	1324.00	2.21E+09	2632.00	1.12E+14	5575.00	2.66E+15
540.00	3.62E+08	1333.00	1.24E+10	2667.00	1.25E+14	5625.00	2.67E+15
560.00	5.17E+07	1342.00	1.99E+09	2703.00	1.16E+14	5675.00	2.67E+15
580.00	1.02E+09	1351.00	3.09E+09	2740.00	1.19E+14	5725.00	2.69E+15
600.00	5.52E+08	1360.00	2.57E+09	2778.00	1.38E+14	5775.00	2.71E+15
620.00	1.20E+09	1370.00	2.74E+09	2817.00	1.70E+14	5825.00	2.71E+15
630.00	1.15E+08	1379.00	3.10E+09	2857.00	2.46E+14	5875.00	2.71E+15
680.00	3.39E+08	1389.00	7.60E+09	2899.00	3.90E+14	5925.00	2.72E+15
710.00	1.59E+08	1408.00	1.01E+10	2941.00	3.99E+14	5975.00	2.72E+15
740.00	5.19E+08	1428.00	1.30E+10	2985.00	3.86E+14	6025.00	2.71E+15
770.00	1.28E+09	1449.00	1.82E+10	3030.00	5.08E+14	6075.00	2.70E+15
800.00	8.07E+08	1470.00	2.33E+10	3077.00	5.92E+14	6125.00	2.70E+15
830.00	2.05E+09	1492.00	2.66E+10	3125.00	6.05E+14	6175.00	2.70E+15
860.00	2.73E+09	1515.00	2.90E+10	3175.00	6.94E+14	6225.00	2.69E+15
890.00	3.34E+09	1538.00	3.60E+10	3225.00	8.12E+14	6275.00	2.68E+15
911.00	9.39E+07	1562.00	4.75E+10	3275.00	9.71E+14	6325.00	2.67E+15
920.00	2.34E+08	1587.00	6.40E+10	3325.00	8.97E+14	6375.00	2.66E+15
930.00	5.84E+08	1613.00	5.69E+10	3375.00	9.44E+14	6425.00	2.65E+15
940.00	5.94E+08	1639.00	1.19E+11	3425.00	1.01E+15	6475.00	3.05E+15
950.00	1.04E+08	1667.00	1.76E+11	3475.00	1.03E+15	6550.00	3.22E+15
960.00	1.04E+08	1695.00	2.32E+11	3525.00	1.03E+15	6650.00	3.18E+15
970.00	5.30E+09	1724.00	1.44E+11	3575.00	1.04E+15	6750.00	3.14E+15
980.00	7.56E+08	1739.00	1.83E+11	3625.00	1.18E+15	6850.00	3.09E+15
995.00	1.25E+08	1754.00	2.34E+11	3675.00	1.23E+15	6950.00	3.04E+15
1007.00	1.04E+08	1770.00	2.62E+11	3725.00	1.24E+15	7050.00	4.99E+15
1017.00	3.60E+09	1784.00	2.88E+11	3775.00	1.17E+15	7150.00	4.94E+15
1027.00	2.46E+09	1802.00	3.14E+11	3825.00	1.11E+15	7250.00	4.90E+15
1035.00	1.83E+09	1818.00	3.81E+11	3875.00	1.09E+15		
1045.00	1.57E+08	1835.00	4.43E+11	3925.00	1.19E+15		

III. PHOTO RATE COEFFICIENTS

The rate coefficient for wavelength interval $\Delta\lambda = \lambda_2 - \lambda_1$ is

$$k(\Delta\lambda) = \int_{\lambda_1}^{\lambda_2} \sigma(\lambda)\phi(\lambda)d\lambda ,$$

where $\sigma(\lambda)$ is a photo cross section and $\phi(\lambda)$ is the photon flux at wavelength λ . Since neither $\sigma(\lambda)$ nor $\phi(\lambda)$ are known as a continuous function of λ the rate coefficients are approximated by

$$k(\Delta\lambda) = \bar{\sigma}(\Delta\lambda)\phi(\Delta\lambda) ,$$

where $\bar{\sigma}(\Delta\lambda)$ denotes the wavelength averaged photo cross section in a bin with width $\Delta\lambda$ and $\phi(\Delta\lambda)$ is the photon flux in the same bin

$$\phi(\Delta\lambda) = \int_{\lambda_1}^{\lambda_2} \phi(\lambda)d\lambda .$$

In the following discussions the photon flux $\phi(\Delta\lambda)$ is the solar flux presented in Table II, except in the bin containing the threshold of a cross section where it is linearly prorated to the threshold wavelength.

The mean excess energy of solar photolysis products is

$$\bar{E} = \sum hc \left(\frac{2}{\lambda_1 + \lambda_2} - \frac{1}{\lambda_{th}} \right) k(\Delta\lambda)/k ,$$

where the summation is over all wavelength bins, λ_{th} is the threshold wavelength, and the photo rate coefficient is

$$k = \sum k(\Delta\lambda) .$$

Results for k are summarized in Table I in column 4 and for \bar{E} in column 6.

Atomic hydrogen, H

Cross section:

In the long wavelength region the Stobbe¹⁶ formula is used, in the short wavelength region the cross section is based on the Sauter¹⁷ formula. The transition from one to the other is made similar to that suggested by Bethe and Salpeter.¹⁸

Threshold:

$$\lambda = 911.75 \text{ \AA} \text{ from Moore.}^{19}$$

Rate coefficient:

$H + \nu \rightarrow H^+ + e$: $7.31 \times 10^{-8} \text{ s}^{-1}$, compares favorably with $7.1 \times 10^{-8} \text{ s}^{-1}$ obtained by Keller²⁰ and $7.0 \times 10^{-8} \text{ s}^{-1}$ obtained by Bertaux et al.²¹ The values $1.5 \times 10^{-7} \text{ s}^{-1}$ quoted by Axford⁸ and $4.5 \times 10^{-7} \text{ s}^{-1}$ obtained by Siscoe and Mukherjee⁴ are too high.

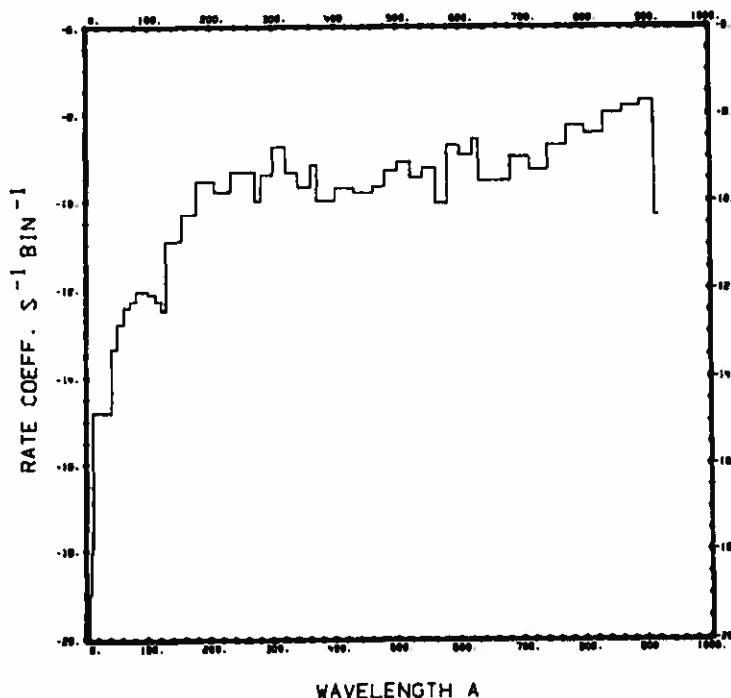


Fig. 2. $H + \nu \rightarrow H^+ + e$.

Atomic carbon, C(³P), C(¹D), C(¹S)

Cross sections:

From $\lambda = 110 \text{ \AA}$ to threshold the cross sections are calculated from fits made by Henry.²² At shorter wavelengths cross sections are based on fits made by Barfield et. al.²³

Thresholds:

The threshold values are obtained from Moore¹⁹

$$C(^3P) : \lambda = 1101.1 \text{ \AA}$$

$$C(^1D) : \lambda = 1240 \text{ \AA}$$

$$C(^1S) : \lambda = 1446 \text{ \AA}$$

Rate coefficients:

$$C(^3P) + v \rightarrow C^+ + e : 4.10 \times 10^{-7} \text{ s}^{-1}$$

$$C(^1D) + v \rightarrow C^+ + e : 3.58 \times 10^{-6} \text{ s}^{-1}$$

$$C(^1S) + v \rightarrow C^+ + e : 4.34 \times 10^{-6} \text{ s}^{-1}$$

The rate coefficient for the ground state quoted by Axford⁸ ($4.0 \times 10^{-6} \text{ s}^{-1}$) is wrong. Note that the large rates for the metastable states are caused by the hydrogen Ly α flux.

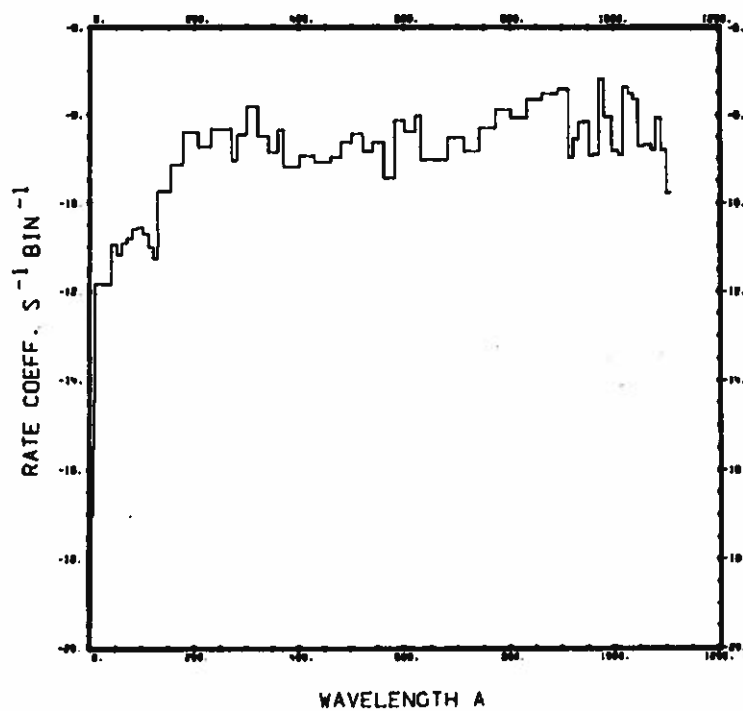


Fig. 3.
 $C(3P) + v \rightarrow C^+ + e.$

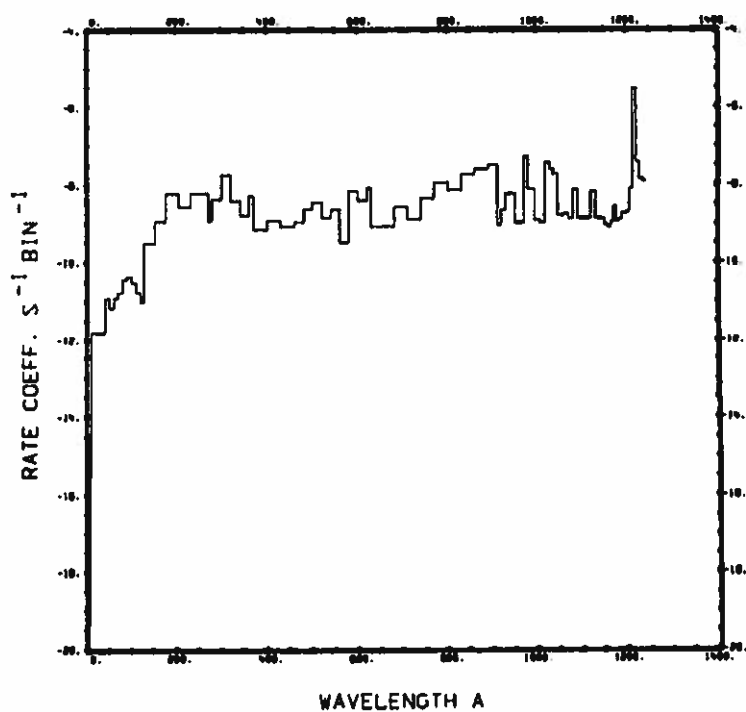


Fig. 4.
 $C(1D) + v \rightarrow C^+ + e.$

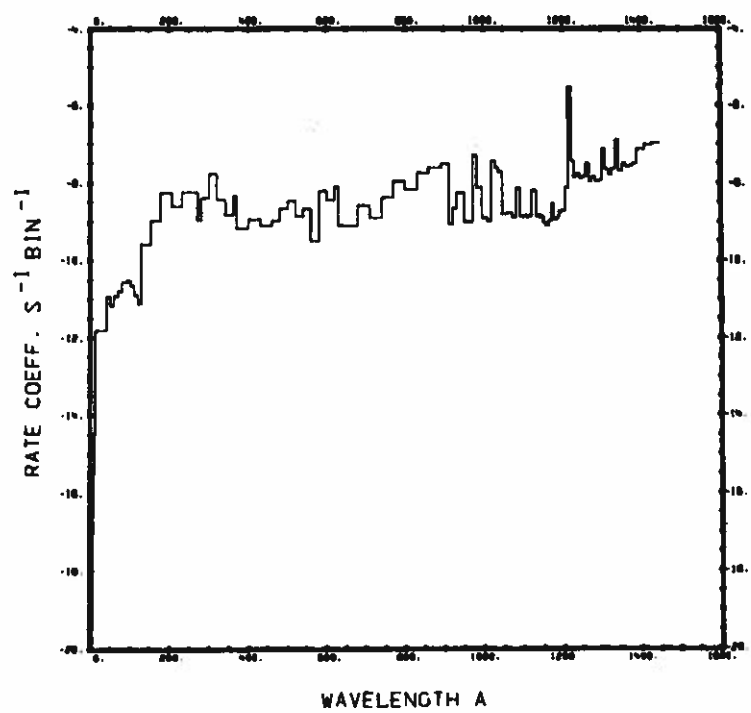


Fig. 5.
 $\text{C}(1\text{s}) + \nu \rightarrow \text{C}^+ + \text{e}.$

Atomic nitrogen, N

Cross section:

From $\lambda = 110 \text{ \AA}$ to threshold the cross section is calculated from fits made by Henry.²² At shorter wavelengths the cross section is based on fits made by Barfield et al.²³

Threshold:

$\lambda = 853.06 \text{ \AA}$ from Moore.¹⁹

Rate coefficient:

$N + v \rightarrow N^+ + e$: $1.85 \times 10^{-7} \text{ s}^{-1}$. This is in good agreement with $1.89 \times 10^{-7} \text{ s}^{-1}$ obtained by Siscoe and Mukherjee⁴ and $1.7 \times 10^{-7} \text{ s}^{-1}$ quoted by Axford.⁸

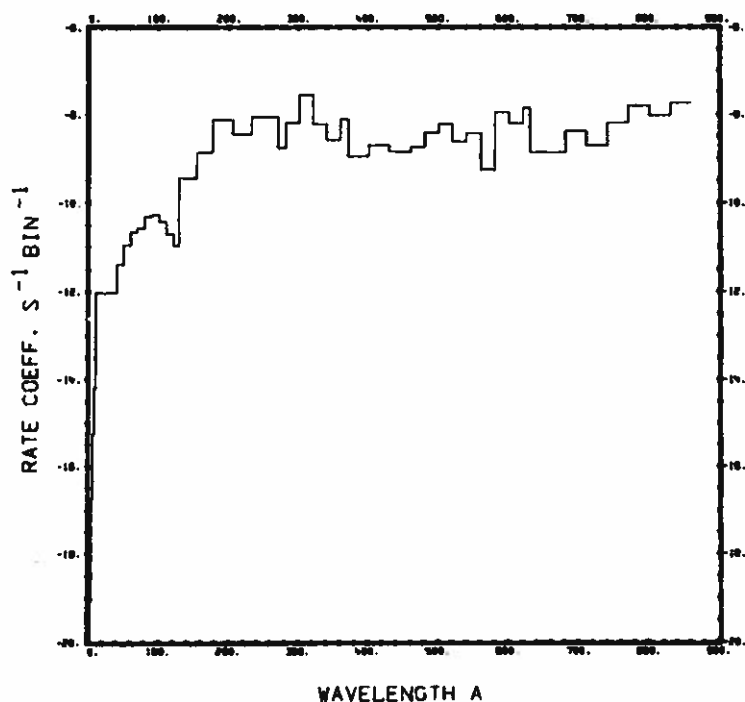


Fig. 6. $N + v \rightarrow N^+ + e$.

Atomic oxygen, $O(^3P)$, $O(^1D)$, $O(^1S)$

Cross sections:

From $\lambda = 600 \text{ \AA}$ to threshold the cross sections are calculated from fits made by Henry.²² At shorter wavelengths cross sections are based on fits made by Barfield et al.²³

Thresholds:

The threshold values are obtained from Moore¹⁹ for

$$O(^3P) : \lambda = 910.44 \text{ \AA}$$

$$O(^1D) : \lambda = 827.9 \text{ \AA}$$

$$O(^1S) : \lambda = 844.6 \text{ \AA}$$

Rate coefficients:

$$O(^3P) + v \rightarrow O^+ + e : 2.12 \times 10^{-7} \text{ s}^{-1}$$

$$O(^1D) + v \rightarrow O^+ + e : 1.82 \times 10^{-7} \text{ s}^{-1}$$

$$O(^1S) + v \rightarrow O^+ + e : 1.96 \times 10^{-7} \text{ s}^{-1}$$

The rates obtained by Siscoe and Mukherjee⁴ ($2.49 \times 10^{-7} \text{ s}^{-1}$) and by Axford⁸ ($2.5 \times 10^{-7} \text{ s}^{-1}$) are 17% higher than our value for $O(^3P)$, the rate obtained by Baurer and Bortner¹⁰ ($2.83 \times 10^{-7} \text{ s}^{-1}$) is 33% higher than ours, while the value computed by McElroy et al.⁷ ($6.3 \times 10^{-7} \text{ s}^{-1}$, when corrected to Earth orbit), is much too high. (The value they quote for Mars orbit is $2.7 \times 10^{-7} \text{ s}^{-1}$).

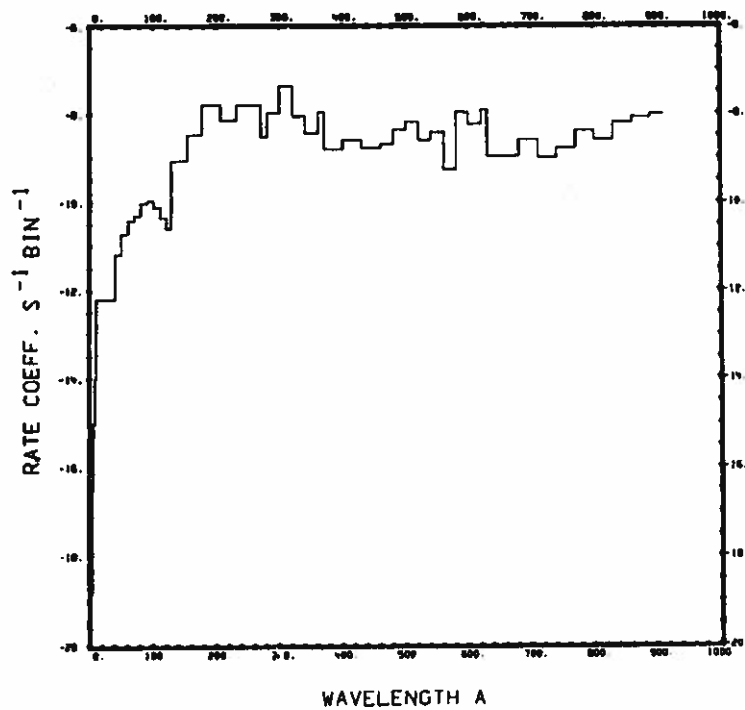


Fig. 7.
 $O(^3P) + \nu \rightarrow O^+ + e.$

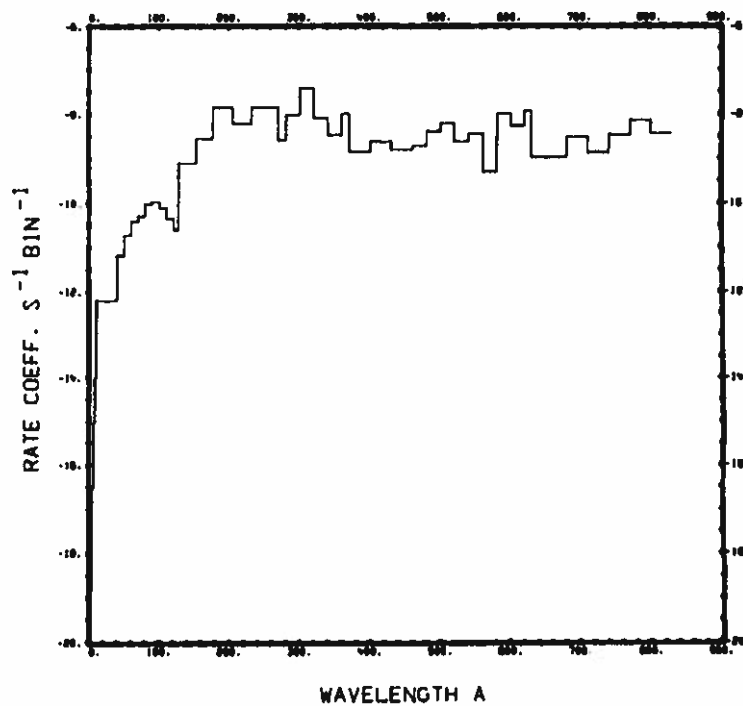


Fig. 8.
 $O(^1D) + \nu \rightarrow O^+ + e.$

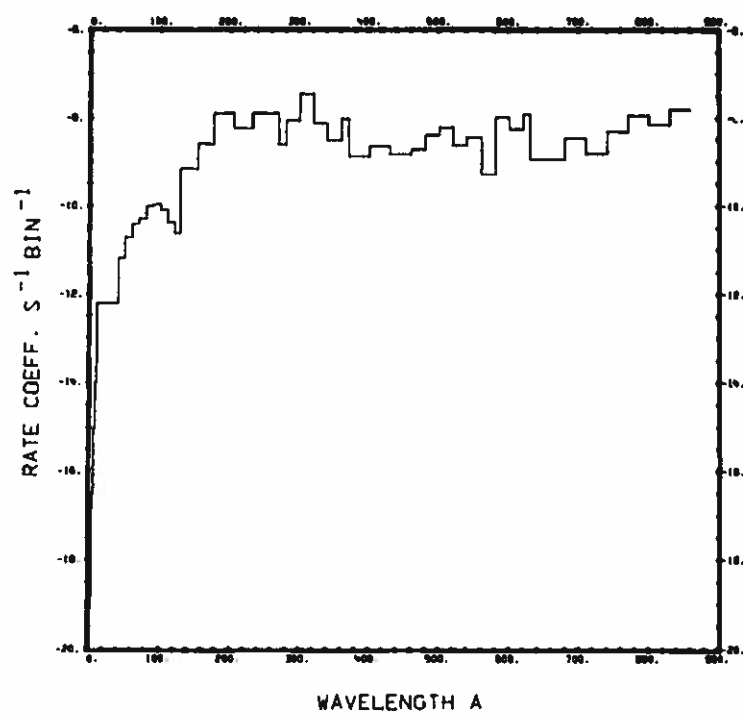


Fig. 9.
 $\text{O}(^1\text{S}) + \nu \rightarrow \text{O}^+ + \text{e}.$

Molecular hydrogen, H₂

Cross section:

In the range from $\lambda = 1 \text{ \AA}$ to 200 \AA the molecular cross section is approximated by twice the cross section of atomic hydrogen. From $\lambda = 209.3 \text{ \AA}$ to 452.2 \AA we used values measured by Samson and Cairns.²⁴ Between $\lambda = 500 \text{ \AA}$ and 970 \AA the cross section was measured by Cook and Metzger.²⁵ A value at 584 \AA is taken from Brolley et al.²⁶

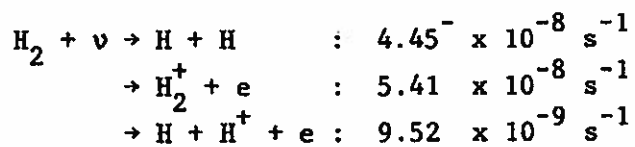
Branching ratios:

The branching ratio for ionization and dissociation is determined from the data of Cook and Metzger,²⁵ for dissociative ionization it is taken from Browning and Fryar.²⁷

Thresholds:

For dissociation the $v = 0, J = 0$ threshold was determined by Herzberg and Monfils²⁸ at $\lambda = 844.79 \text{ \AA}$. Rotational predissociation extends the threshold to longer wavelengths depending on the degree of thermal excitation. The ionization threshold was determined by Beutler and Jünger²⁹ for $J = 0$ to $J = 0$ at $\lambda = 803.67 \text{ \AA}$. The threshold for photodissociative ionization according to Browning and Fryar²⁷ is at $\lambda = 685.8 \text{ \AA}$.

Rate coefficients:



Our combined rate for ionization and dissociative ionization $6.36 \times 10^{-8} \text{ s}^{-1}$ is smaller than the ionization rate of $8.4 \times 10^{-8} \text{ s}^{-1}$ obtained by Siscoe and Mukherjee.⁴

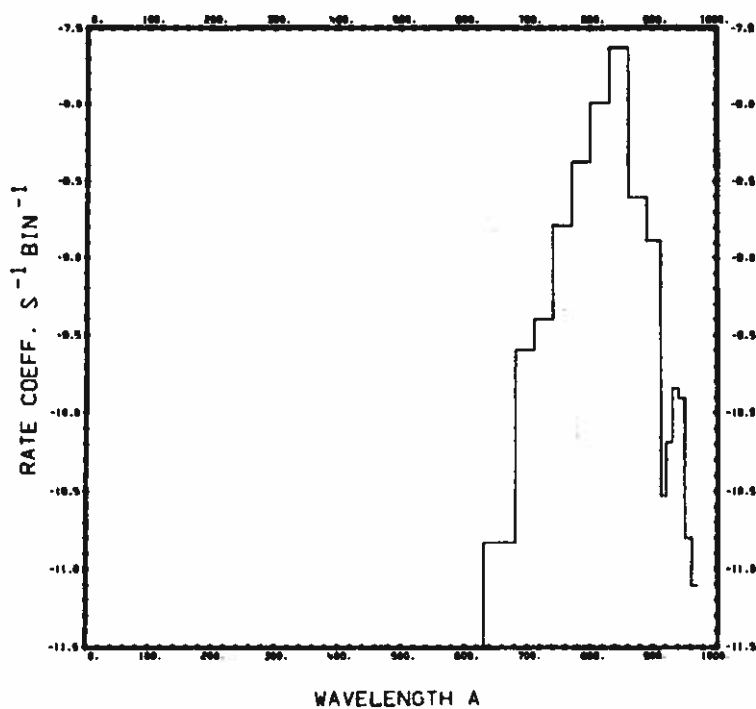


Fig. 10.
 $\text{H}_2 + \nu \rightarrow \text{H} + \text{H}.$

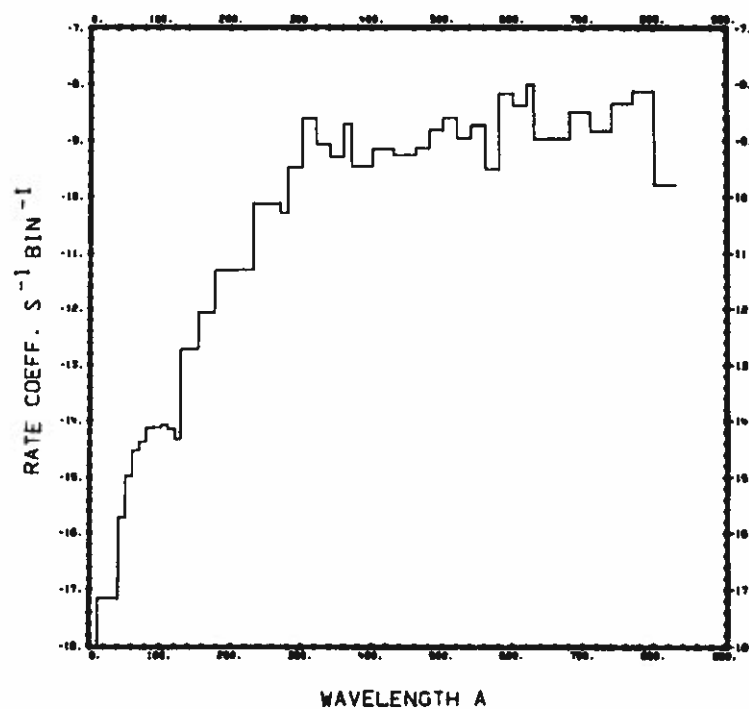


Fig. 11.
 $\text{H}_2 + \nu \rightarrow \text{H}_2^+ + \text{e}.$

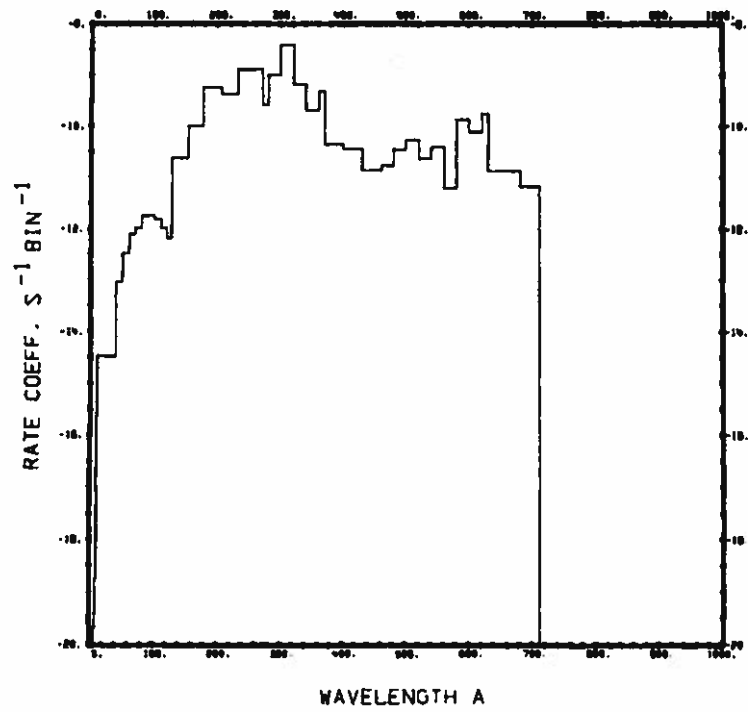


Fig. 12.
 $\text{H}_2 + \nu \rightarrow \text{H} + \text{H}^+ + \text{e}.$

Methylidene, CH

Cross section:

Between $\lambda = 12 \text{ \AA}$ and 617 \AA the cross section comes from calculations by Walker and Kelly,³⁰ and between $\lambda = 827 \text{ \AA}$ and 1170 \AA it comes from calculations by Barsuhn and Nesbet.³¹ In the region $\lambda = 1170 \text{ \AA}$ to 1240 \AA a continuum cross section was assumed as suggested by Bates and Spitzer.³² The cross section from 1240 \AA to 3573 \AA was obtained from the oscillator strength data of Linevsky³³ and Fink and Welge.³⁴

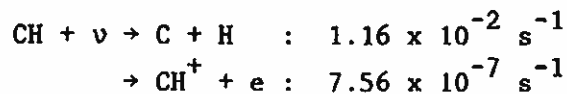
Branching ratio:

The branching ratio for dissociation and ionization was obtained from the calculations of Barsuhn and Nesbet.³¹

Thresholds:

The threshold for dissociation, based on the predissociation limit, is given by Herzberg and Johns³⁵ as $\lambda = 3589.9 \text{ \AA}$. One of the dissociation continua given by Bates and Spitzer³² is at $\lambda = 1240 \text{ \AA}$. The ionization limit determined by Barsuhn and Nesbet³¹ is at $\lambda = 1170 \text{ \AA}$.

Rate coefficients:



The dissociation is dominated by predissociation around $\lambda = 1343 \text{ \AA}$. Our dissociation rate is almost twice that obtained by Wyckoff and Wehinger³⁶ ($6.4 \times 10^{-3} \text{ s}^{-1}$), while our ionization rate agrees well with their value of $7.9 \times 10^{-7} \text{ s}^{-1}$.

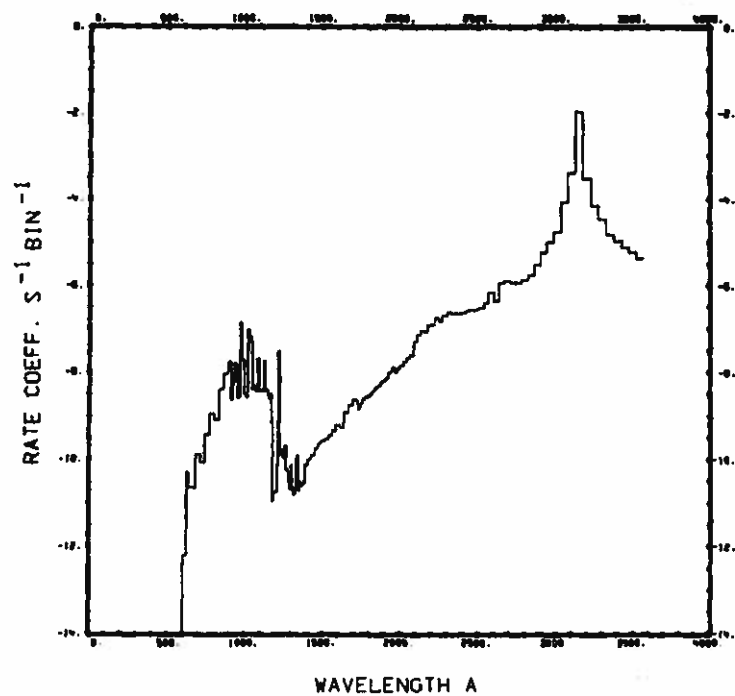


Fig. 13.
 $\text{CH} + \nu \rightarrow \text{C} + \text{H}_\gamma$

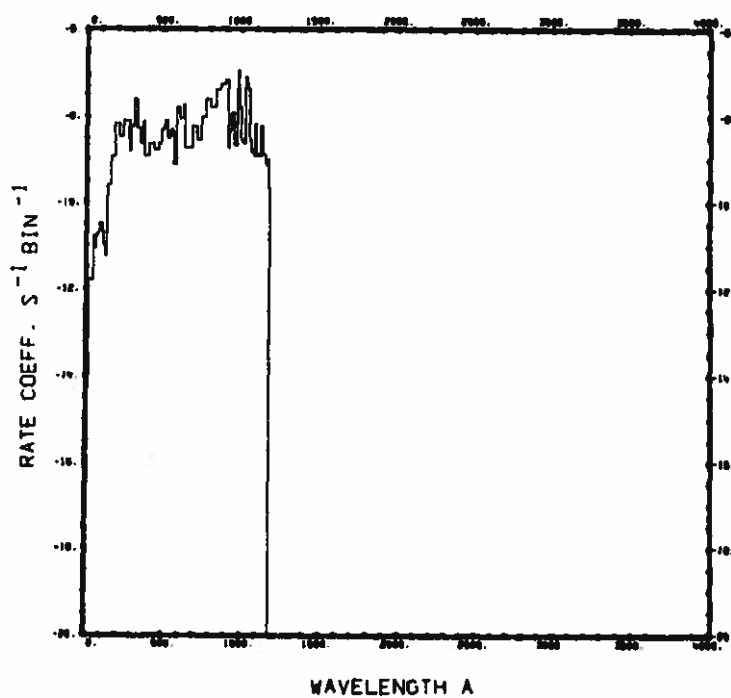


Fig. 14.
 $\text{CH} + \nu \rightarrow \text{CH}^+ + \text{e}$

Carbon monoxide, $\text{CO}(X^1\Sigma^+)$, $\text{CO}(a^3\Pi)$

Cross sections:

From $\lambda = 2 \text{ \AA}$ to 303.8 \AA cross sections from many sources, averaged by Henry and McElroy,³⁷ were used. From $\lambda = 303.8 \text{ \AA}$ to 1037.6 \AA the cross section was taken from Cairns and Samson,³⁸ and supplemented with values from Cook et al.³⁹ in the wavelength region 600 \AA to 1002.5 \AA . No dissociation or ionization cross sections for any of the three metastable triplet states $a^3\Pi$, $a'^3\Sigma^+$ and $d^3\Delta_i$ are available. But since the potential curve for the lowest of these, the $a^3\Pi$, is very similar to that of the ground state $X^1\Sigma^+$ (see Hall et al.⁴⁰), Collins⁴¹ suggested scaling the ground state cross sections with respect to $1/\lambda$ such that the thresholds are shifted by 6.00 eV to longer wavelengths. The 6.00 eV shift corresponds to the energy difference between $a^3\Pi$ and $X^1\Sigma^+$ states.

Branching ratios:

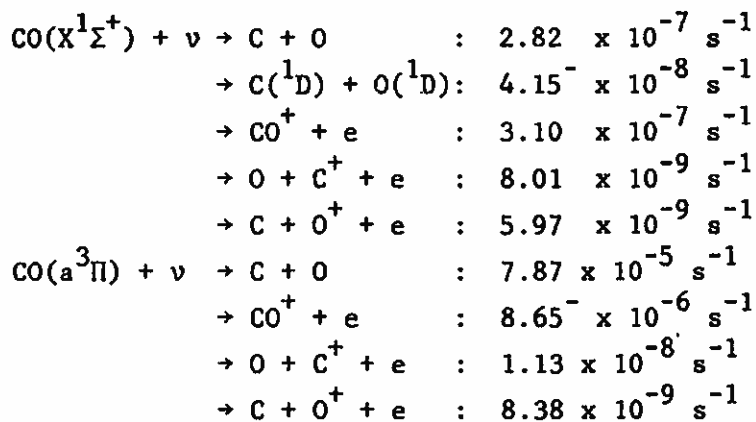
The branching ratio between dissociation and all ionization processes was determined from the data of Cairns and Samson.³⁸ Since no branching ratios are available for dissociation into the 1S and 1D metastable states of C and O, we followed the suggestion of McElroy and McConnell⁶ that all such dissociations end up in $\text{C}(^1D)$ and $\text{O}(^1D)$ and estimated the branching ratio from the data of Cook et al.³⁹ The branching ratios for ionization and dissociative ionizations was taken from Kronebusch and Berkowitz.⁴²

Thresholds:

The threshold for dissociation of $\text{CO}(X^1\Sigma^+)$ into the ground states of C and O is at $\lambda = 1117.8 \text{ \AA}$ as given by Krupenie⁴³ and into the metastable states $\text{C}(^1D)$ and $\text{O}(^1D)$ it is at $\lambda = 863.4 \text{ \AA}$ as tabulated by Cook et al.³⁹. The ionization threshold, also from Krupenie, is $\lambda = 884.79 \text{ \AA}$. For dissociative ionization into $\text{O} + \text{C}^+ + e$ the threshold is $\lambda = 554.7 \text{ \AA}$ and into $\text{C} + \text{O}^+ + e$ it is $\lambda = 501.8 \text{ \AA}$. Both values are from Kronebusch and Berkowitz.⁴²

For $\text{CO}(a^3\Pi)$ dissociation, $\lambda = 2431.8 \text{ \AA}$ and for ionization $\lambda = 1549.1 \text{ \AA}$; both from Krupenie.⁴³ The dissociative ionization thresholds have been obtained by subtracting 6.00 eV from the corresponding ground state values; for $\text{O} + \text{C}^+ + e$ the threshold is then at $\lambda = 758.3 \text{ \AA}$ and for $\text{C} + \text{O}^+ + e$ it is $\lambda = 662.7 \text{ \AA}$.

Rate coefficients:



McElroy and McConnell⁶ obtain $6.0 \times 10^{-7} \text{ s}^{-1}$ for the first dissociation branch (after correcting to Earth orbit), which is about twice our value and $5.8 \times 10^{-8} \text{ s}^{-1}$ for the second dissociation branch. On the other hand, Wyckoff and Wehinger³⁶ calculated $1.9 \times 10^{-7} \text{ s}^{-1}$ for the total dissociation rate, or about 40% less than our value ($3.23 \times 10^{-7} \text{ s}^{-1}$). Our combined rate for ionization and dissociative ionization out of the ground state ($3.24 \times 10^{-7} \text{ s}^{-1}$) is somewhat larger than the value obtained by Wyckoff and Wehinger³⁶ ($2.7 \times 10^{-7} \text{ s}^{-1}$), but smaller than the ionization rates obtained by Siscoe and Mukherjee⁴ ($7.81 \times 10^{-7} \text{ s}^{-1}$) or by McElroy et al.⁷ ($1.0 \times 10^{-6} \text{ s}^{-1}$ when corrected to Earth orbit; they quote $4.4 \times 10^{-7} \text{ s}^{-1}$ at Mars orbit). For the dissociative ionization branch that leads to $\text{C} + \text{O}^+ + \text{e}$, McElroy and McConnell⁶ give $1.6 \times 10^{-8} \text{ s}^{-1}$, when corrected to Earth orbit; 2.7 times larger than our value. (They give $6.9 \times 10^{-9} \text{ s}^{-1}$ at Mars orbit). The rate coefficients for the metastable state of CO should be considered to be estimates only.

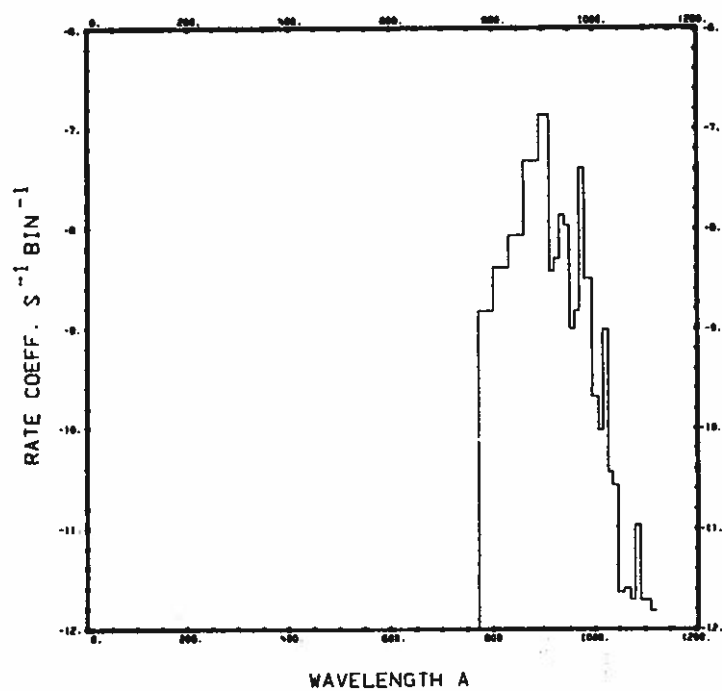


Fig. 15.
 $\text{CO}(X^1\Sigma^+) + \nu \rightarrow \text{C} + \text{O}.$

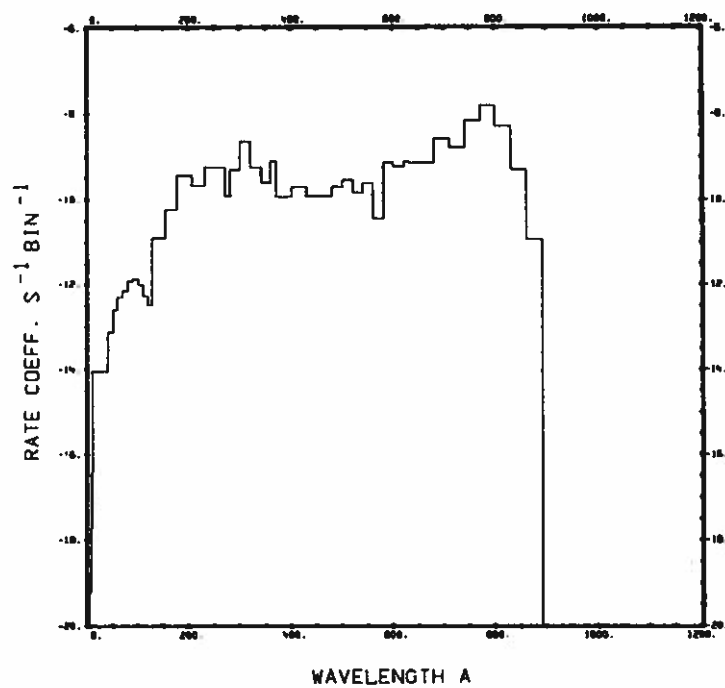


Fig. 16.
 $\text{CO}(X^1\Sigma^+) + \nu \rightarrow \text{C}(^1\text{D}) + \text{O}(^1\text{D}).$

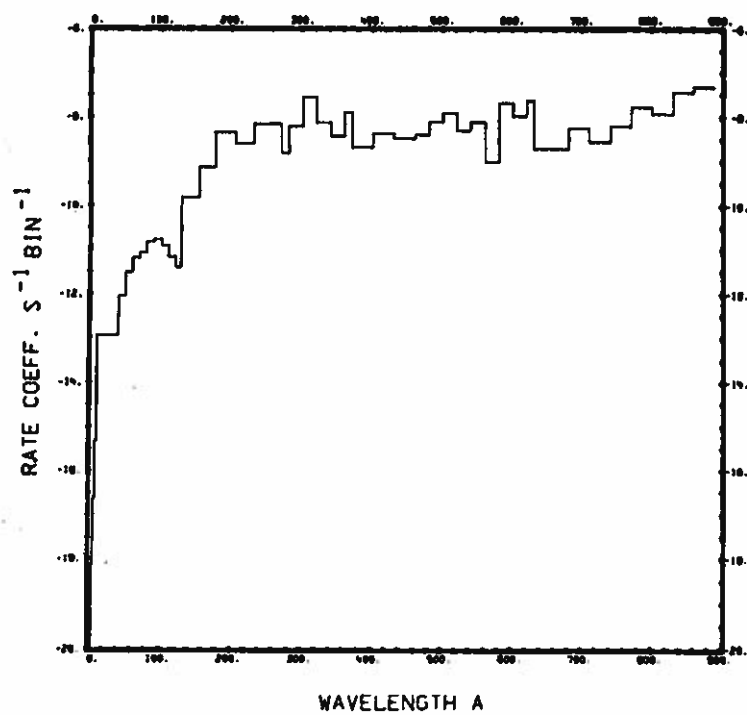


Fig. 17.
 $\text{CO}(X^1\Sigma^+) + \nu \rightarrow \text{CO}^+ + e.$

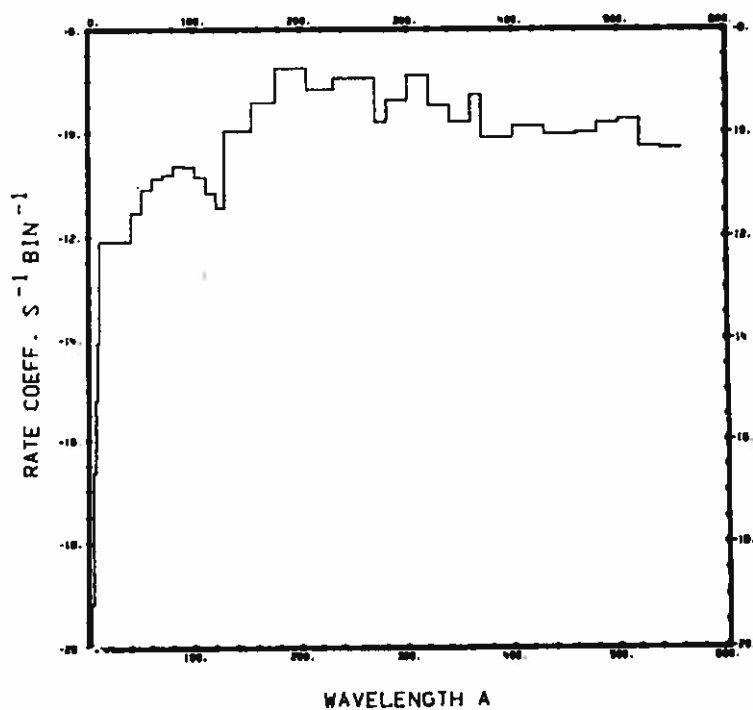


Fig. 18.
 $\text{CO}(X^1\Sigma^+) + \nu \rightarrow \text{O} + \text{C}^+ + e.$

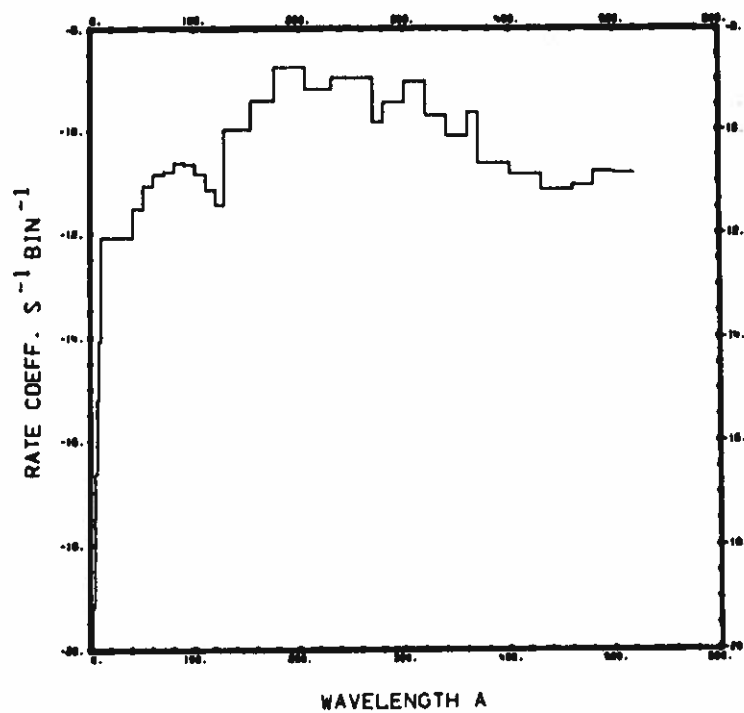


Fig. 19.
 $\text{CO}(X^1\Sigma^+) + \nu \rightarrow \text{C} + \text{O}^+ + \text{e}.$

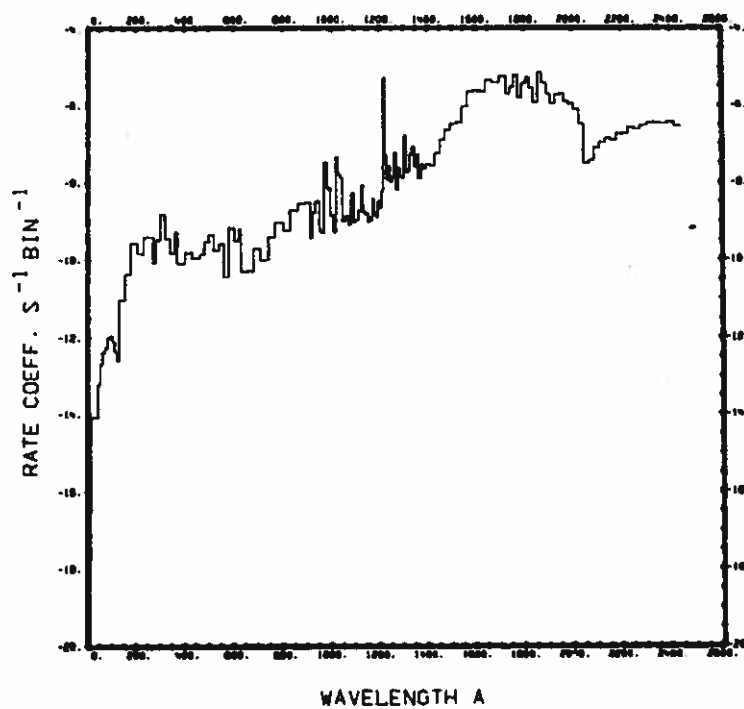


Fig. 20.
 $\text{CO}(a^3\Pi) + \nu \rightarrow \text{C} + \text{O}.$

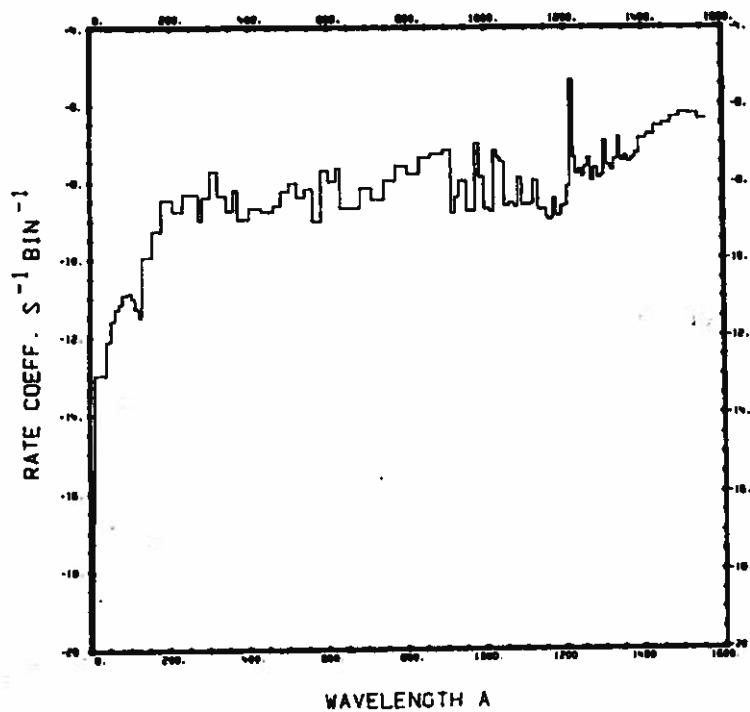


Fig. 21.
 $\text{CO}(a^3\Pi) + \nu \rightarrow \text{CO}^+ + e.$

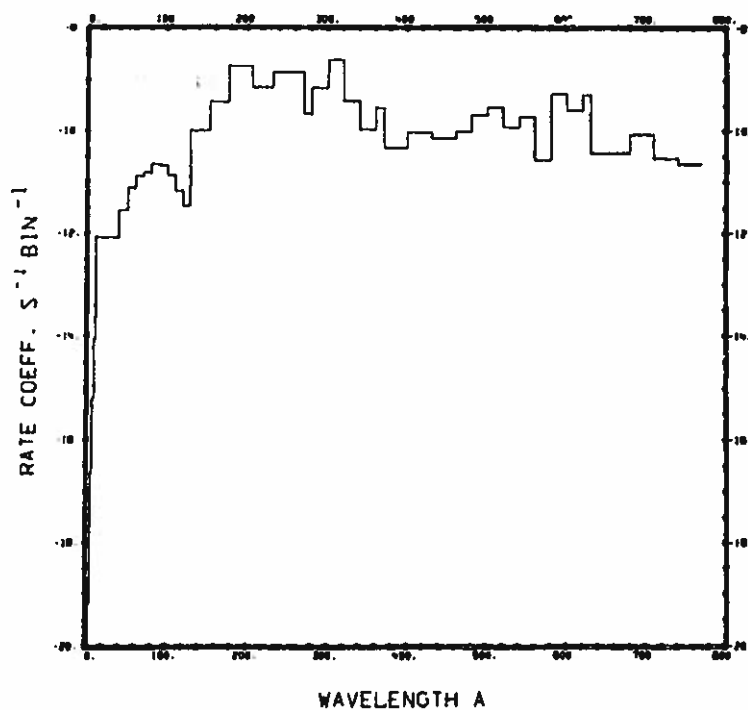


Fig. 22.
 $\text{CO}(a^3\Pi) + \nu \rightarrow \text{O} + \text{C}^+ + e.$

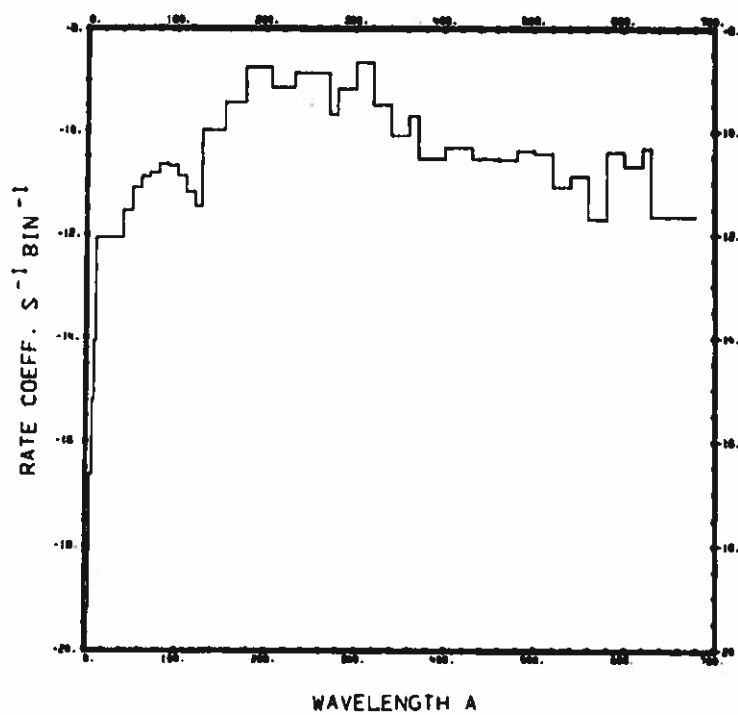


Fig. 23.
 $\text{CO}(a^3\Pi) + \nu \rightarrow \text{C} + \text{O}^+ + e^-$

Molecular nitrogen, N₂

Cross section:

From $\lambda = 9.9 \text{ \AA}$ to 247.2 \AA cross sections from various sources have been summarized by Huffman.⁴⁴ In the range from 303.8 \AA to 1037.6 \AA the cross section was taken from Samson and Cairns⁴⁵ and was supplemented with data from Cook and Metzger⁴⁶ in the range 600 \AA to 978 \AA and from Huffman et al.⁴⁷ in the range 798 \AA to 1000 \AA . A very broad and strong absorption line of N₂ at 972.5 \AA overlaps the solar Lyman γ emission line. The measured cross section of the N₂ line varies widely: Clark⁴⁸ gives $\sigma = 1.45 \times 10^{-16} \text{ cm}^2$, Watanabe and Marmo⁴⁹ give $\sigma = 1.12 \times 10^{-17} \text{ cm}^2$, Itamoto and McAllister⁵⁰ give $\sigma = 3.72 \times 10^{-16} \text{ cm}^2$ (these values quoted by Huffman et al.⁴⁷), Huffman et al.⁴⁷ report $\sigma = 3.02 \times 10^{-16} \text{ cm}^2$, Cook and Metzger⁴⁶ give $\sigma = 1.94 \times 10^{-16} \text{ cm}^2$, Samson and Cairns⁴⁵ measured $\sigma = 3.56 \times 10^{-16} \text{ cm}^2$, Huffman⁴⁴ reported $\sigma = 3.70 \times 10^{-16} \text{ cm}^2$, Geiger and Schröder⁵¹ give $\sigma = 1.51 \times 10^{-16} \text{ cm}^2$, and Gürtler et al.⁵² measured $\sigma = 3.57 \times 10^{-16} \text{ cm}^2$. The average is $\sigma = 2.51 \times 10^{-16} \text{ cm}^2$, which is the value that was adopted here. The line corresponds to the $b^1\Pi_u - X^1\Sigma_g^+$, $v' = 3$ transition (see Gürtler et al.⁵²). Cook and Metzger⁴⁶ had identified the line as the $v' = 2$ transition. According to Lofthus and Krupenie⁵³ these levels are pre-dissociating.

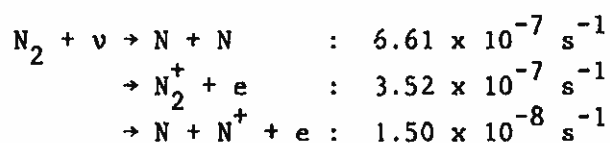
Branching ratios:

The branching ratio for dissociation and ionization are based on the data obtained by Huffman,⁴⁴ Samson and Cairns,⁴⁵ and Cook and Metzger.⁴⁶ The branching ratio for dissociative ionization is taken from Kronebusch and Berkowitz.⁴²

Thresholds:

The threshold for dissociation as given by Herzberg⁵⁴ is $\lambda = 1021.4 \text{ \AA}$. Lofthus and Krupenie⁵³ give the ionization threshold $\lambda = 796 \text{ \AA}$ and Kronebusch and Berkowitz⁴² give the threshold for dissociative ionization $\lambda = 510.4 \text{ \AA}$.

Rate coefficients:



The rate coefficient for dissociation is dominated by the predissociation line at $\lambda = 972.5 \text{ \AA}$. Thus this rate coefficient will be drastically reduced if the N_2 molecule's radial velocity with respect to the sun Doppler shifts the predissociation line out of coincidence with the solar Lyman γ emission line.

Between the extreme values of the cross sections for the N_2 line (see above) the rate coefficient varies from $8.53 \times 10^{-7} \text{ s}^{-1}$ to $2.80 \times 10^{-7} \text{ s}^{-1}$ assuming zero Doppler shift. Our combined rate for ionization and dissociative ionization $3.67 \times 10^{-7} \text{ s}^{-1}$ is about 80% larger than the value reported by McElroy et al.⁷ ($2.0 \times 10^{-7} \text{ s}^{-1}$, after correcting to Earth orbit), but it is comparable to $3.47 \times 10^{-7} \text{ s}^{-1}$ quoted by Siscoe and Mukherjee.⁴ Baurer and Bortner¹⁰ quote $4.22 \times 10^{-7} \text{ s}^{-1}$. The rate coefficients obtained by Wyckoff and Wehinger³⁶ for dissociation ($1.8 \times 10^{-7} \text{ s}^{-1}$) and for ionization ($1.3 \times 10^{-7} \text{ s}^{-1}$) are much smaller than our values. The ionization rate coefficient is sensitive to the cross section around $\lambda = 300 \text{ \AA}$, where data are sparse.

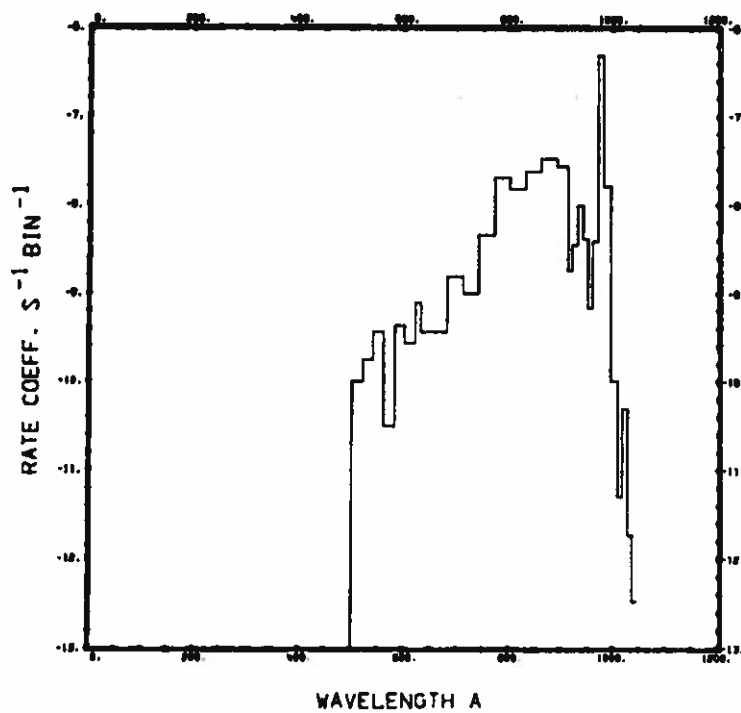


Fig. 24.
 $N_2 + \nu \rightarrow N + N.$

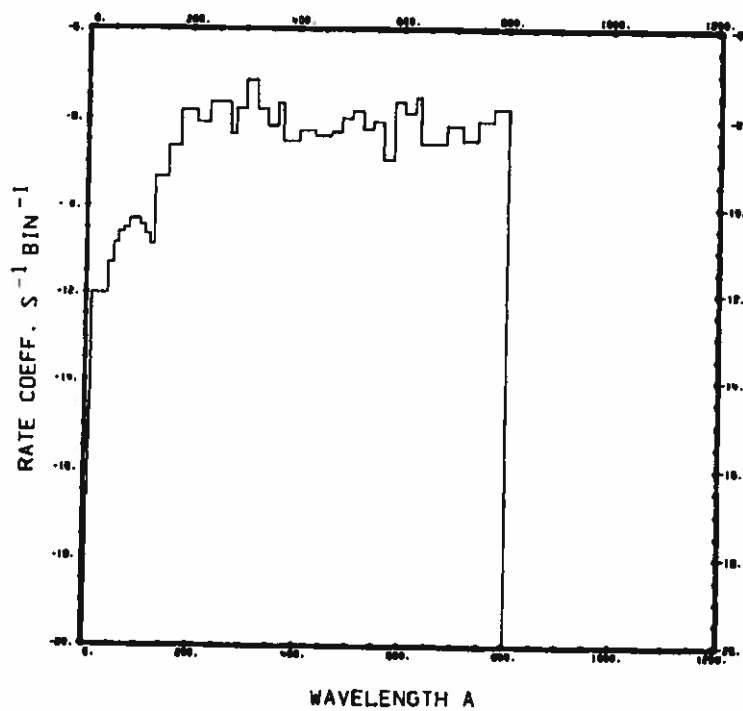


Fig. 25.
 $N_2 + \nu \rightarrow N_2^+ + e.$

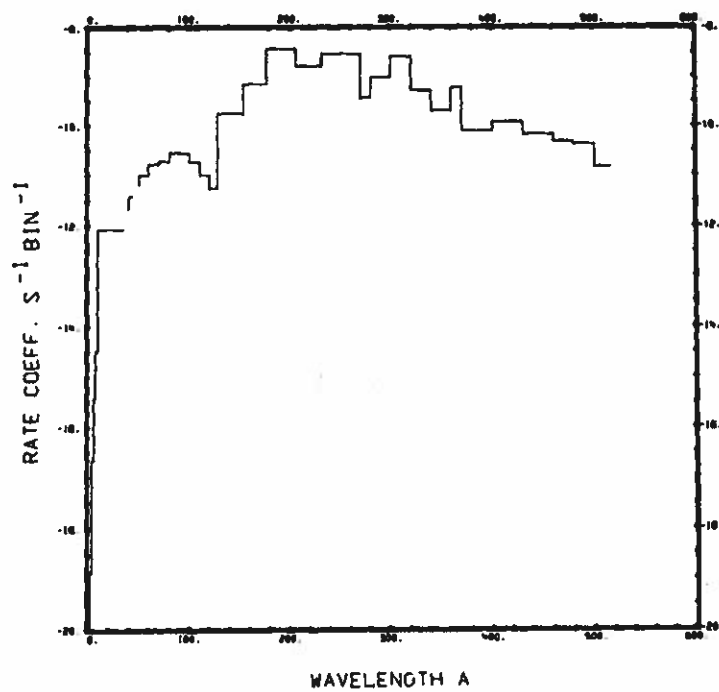


Fig. 26.
 $N_2 + \nu + N + N^+ + e.$

Nitric oxide, NO

Cross section:

From $\lambda = 1$ to 180 \AA the cross section is synthesized from the atomic cross sections of N and O. Between $\lambda = 180 \text{ \AA}$ and 580 \AA the cross section data from Lee et al.⁵⁵ were used. In the range 580 \AA to 1350 \AA the cross section comes from Watanabe et al.⁵⁶ and between $\lambda = 1350 \text{ \AA}$ and 2271 \AA it comes from Marmo.⁵⁷

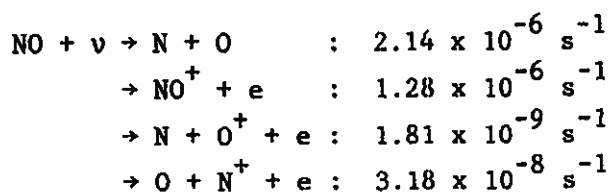
Branching ratios:

The data for the branching between dissociation and all ionization processes come from Watanabe et al.⁵⁶ The branching ratios for photodissociative ionization are given by Kronebusch and Berkowitz.⁴²

Thresholds:

Marmo⁵⁷ and McNesby and Okabe⁵⁸ give the threshold for dissociation at $\lambda = 1910 \text{ \AA}$. The threshold for ionization is given by Watanabe et al.⁵⁶ as $\lambda = 1340 \text{ \AA}$. The thresholds for dissociative ionization into $\text{N} + \text{O}^+$ and $\text{N}^+ + \text{O}$ are $\lambda = 616.2 \text{ \AA}$ and $\lambda = 589.3 \text{ \AA}$, respectively.

Rate coefficients:



Our rate for dissociation is smaller than the value quoted by Baurer and Bortner¹⁰ ($6.10 \times 10^{-6} \text{ s}^{-1}$). Our rate for all ionization processes ($1.31 \times 10^{-6} \text{ s}^{-1}$) is in very good agreement with the value obtained by Siscoe and Mukherjee⁴ ($1.348 \times 10^{-6} \text{ s}^{-1}$) but is about double the value quoted by Baurer and Bortner¹⁰ ($6.24 \times 10^{-7} \text{ s}^{-1}$).

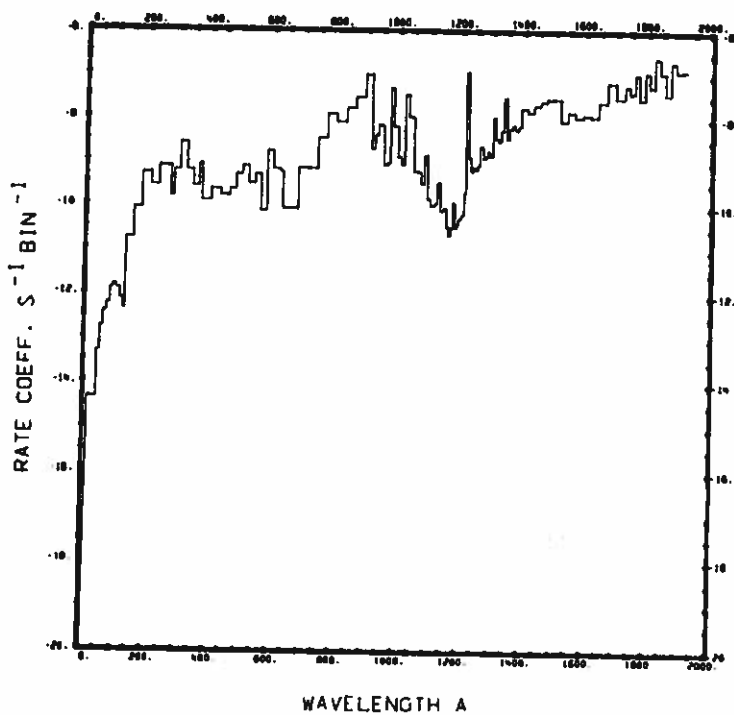


Fig. 27.
 $\text{NO} + \nu \rightarrow \text{N} + \text{O}.$

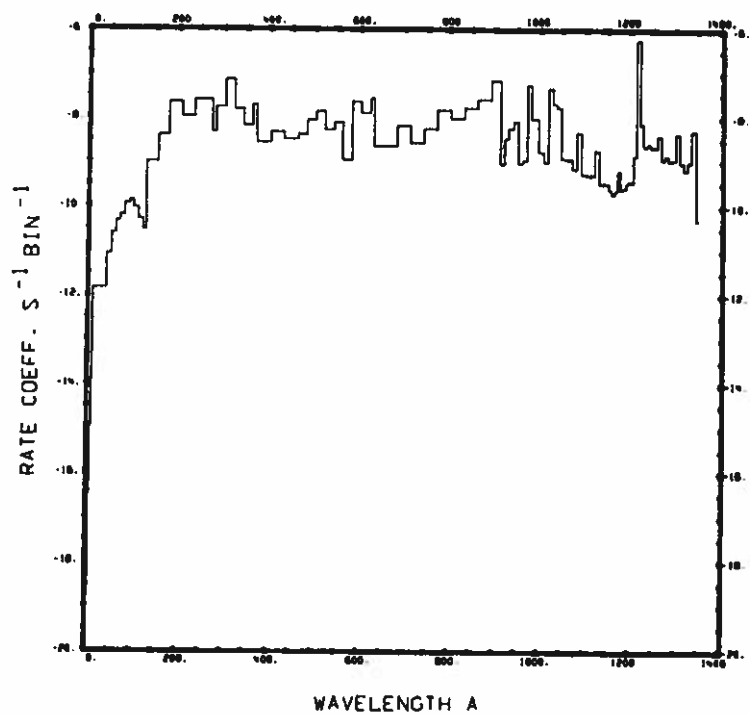


Fig. 28.
 $\text{NO} + \nu \rightarrow \text{NO}^+ + e.$

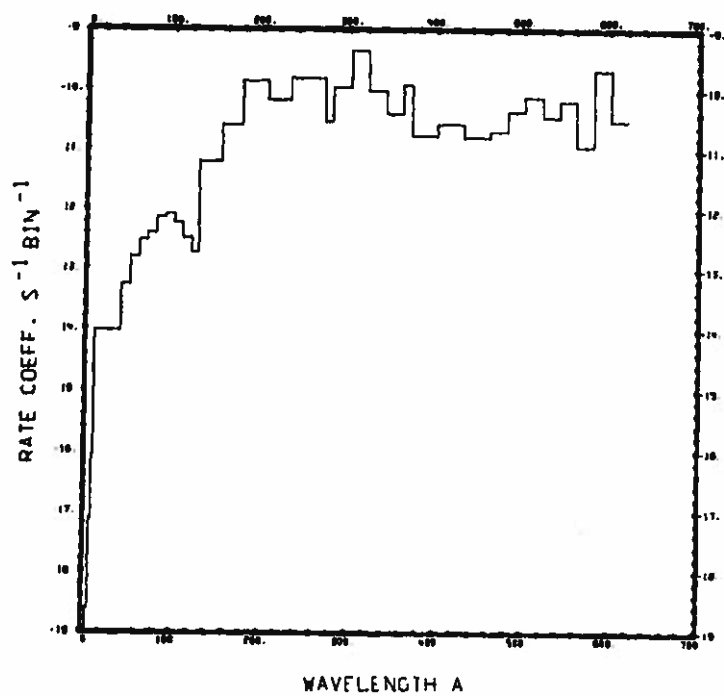


Fig. 29.
 $\text{NO} + \nu \rightarrow \text{N} + \text{O}^+ + \text{e}.$

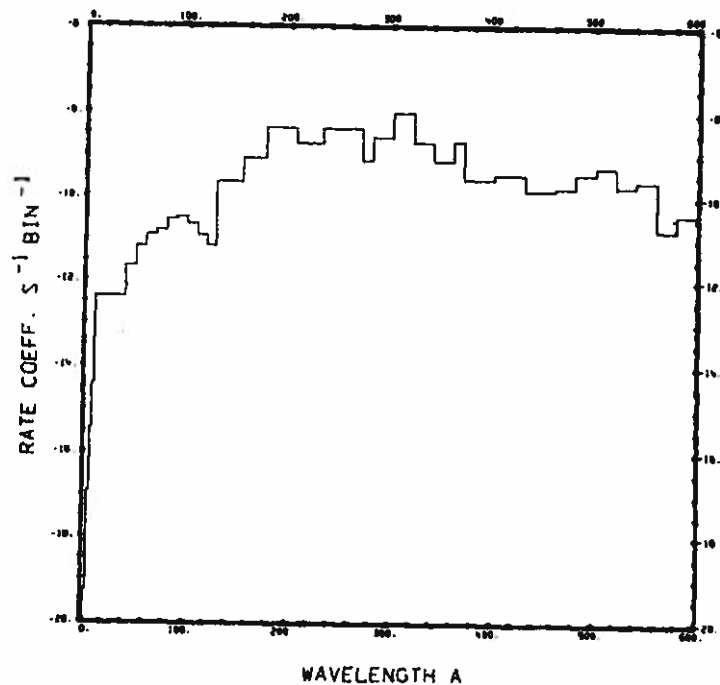


Fig. 30.
 $\text{NO} + \nu \rightarrow \text{O} + \text{N}^+ + \text{e}.$

Molecular oxygen, O₂

Cross section:

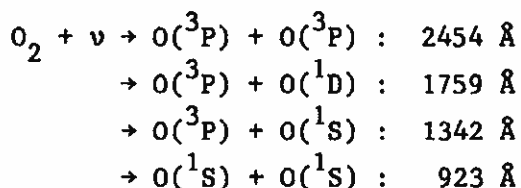
From $\lambda = 1 \text{ \AA}$ to 295 \AA the cross section is based on fits made by Barfield et al.²³ for atomic oxygen multiplied by two; it is supplemented by values taken from Huffman.⁹ Between $\lambda = 209.3 \text{ \AA}$ and 1037.6 \AA data are taken from Samson and Cairns^{24,45} and are supplemented with the cross section from Cook and Metzger⁴⁶ in the interval $\lambda = 600 \text{ \AA}$ to 912 \AA . Data are also taken from Matsunaga and Watanabe⁵⁹ in the range from 580 \AA to 1077 \AA . Between 1062 \AA and 1751 \AA the data from Watanabe⁶⁰ are used. From 1163 \AA to 2424.5 \AA a cross section was used that had been compiled by Ackerman¹⁴ and Ackerman et al.⁶¹ from many sources.

Branching ratios:

Branching ratios for the sum of processes leading to dissociation and the sum of processes leading to ionization are obtained from data of Huffman,⁴⁴ Samson and Cairns,⁴⁵ Cook and Metzger⁴⁶ and Matsunaga and Watanabe.⁵⁹ Dissociation into $O(^3P) + O(^3P)$, $O(^3P) + O(^1D)$ and $O(^1S) + O(^1S)$ is given by branching ratios of Lee et al.,⁶² Hudson,⁶³ Ackerman et al.⁶¹ and Ditchburn and Young.⁶⁴ Photodissociative ionization branching ratios are obtained from Comes et al.,⁶⁵ Weissler et al.,⁶⁶ and Kronebusch and Berkowitz.⁴²

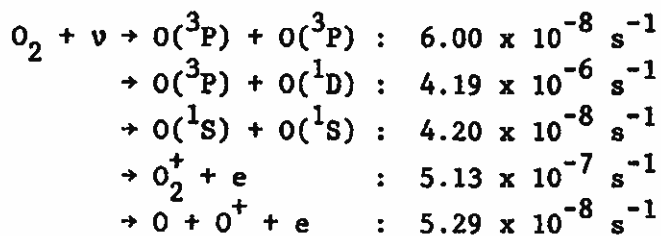
Thresholds:

Some important threshold wavelengths for dissociation as given by McNesby and Okabe⁵⁸ are:

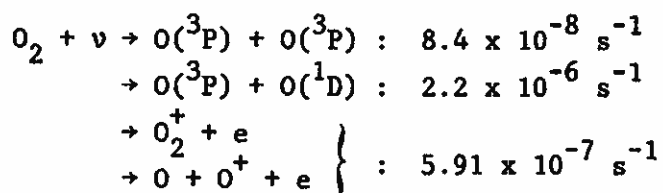


Huffman⁹ quotes 1027.8 \AA for the ionization threshold. Threshold for dissociative ionization is at 585 \AA , given by Kronebusch and Berkowitz.⁴²

Rate coefficients:



for comparison, the rates quoted by Baurer and Bortner¹⁰ are:



McElroy and Hunten⁵ give $1.3 \times 10^{-9} \text{ s}^{-1}$ for the first dissociation branch and $6.0 \times 10^{-6} \text{ s}^{-1}$ for the second dissociation branch (after correcting to Earth orbit).

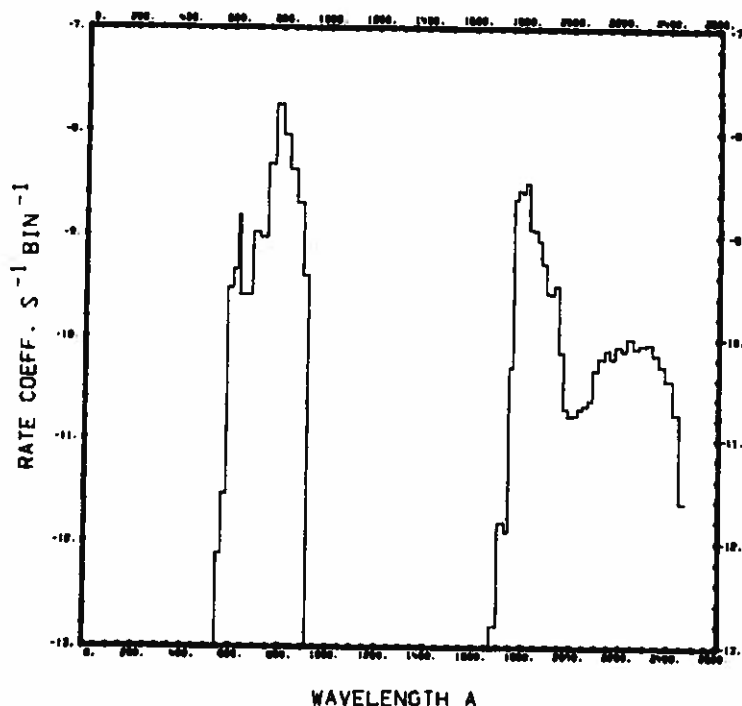


Fig. 31. $\text{O}_2 + \nu \rightarrow \text{O}(^3\text{P}) + \text{O}(^3\text{P})$.

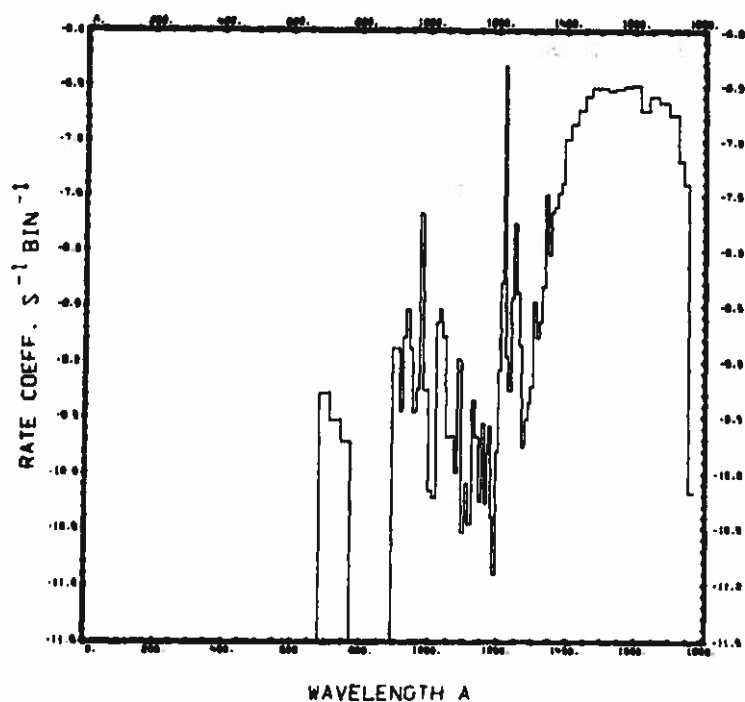


Fig. 32.
 $O_2 + \nu \rightarrow O(^3P) + O(^1D)$.

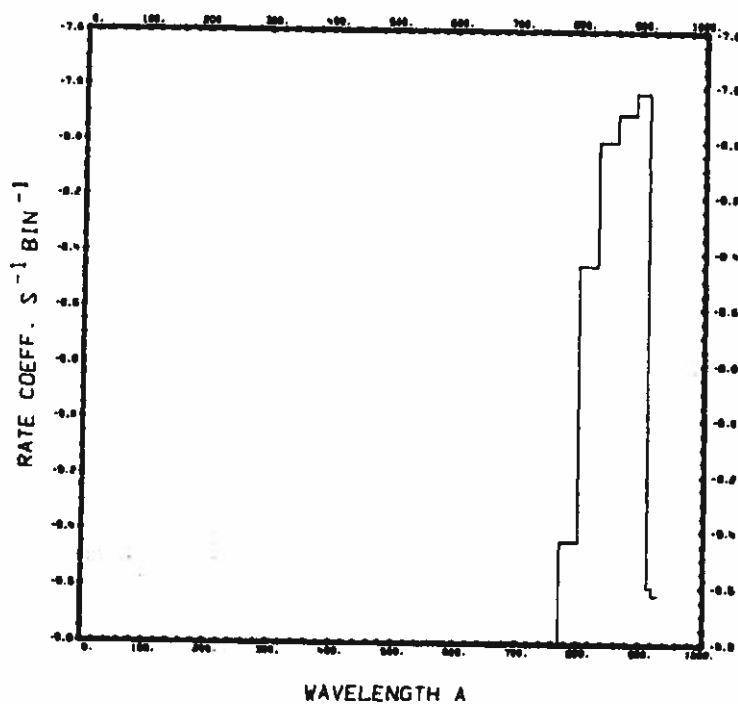


Fig. 33.
 $O_2 + \nu \rightarrow O(^1S) + O(^1S)$.

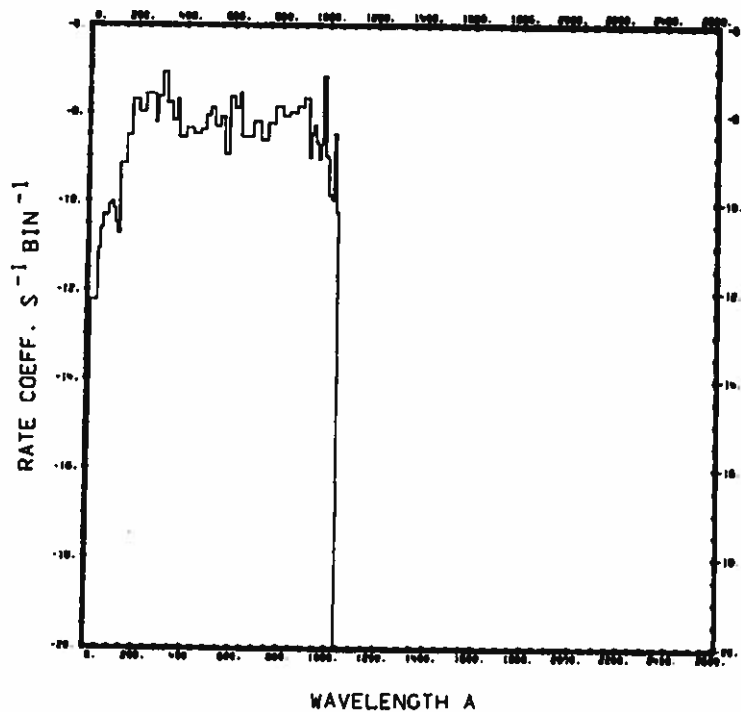


Fig. 34.
 $\text{O}_2 + \nu \rightarrow \text{O}_2^+ + \text{e}$.

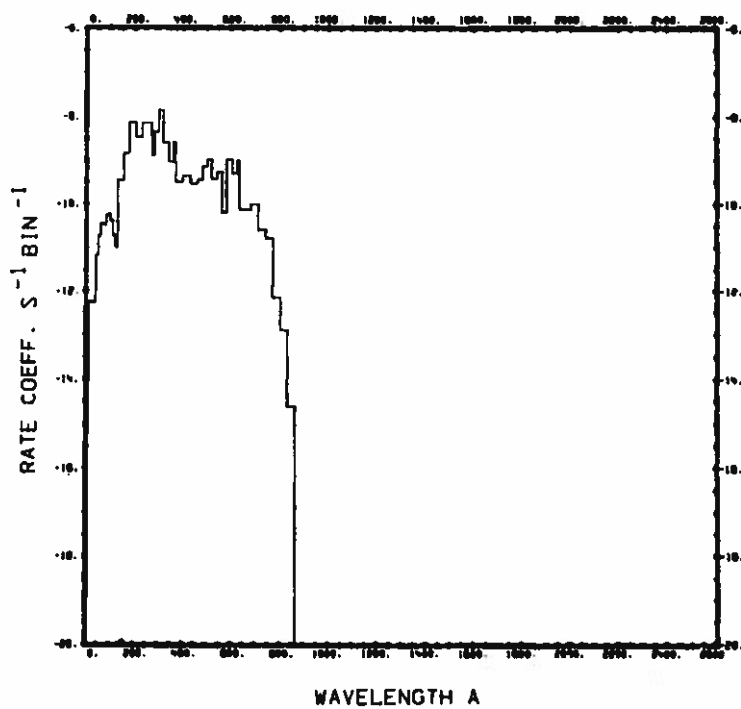


Fig. 35.
 $\text{O}_2 + \nu \rightarrow \text{O} + \text{O}^+ + \text{e}$.

Water, H₂O

Cross section:

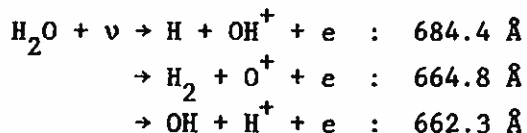
From $\lambda = 1 \text{ \AA}$ to 100 \AA the molecular cross section has been approximated by the sum of the atomic cross sections. Between 180 \AA and 720 \AA , cross section data were taken from Phillips et al.,⁶⁷ supplemented with data from Dibeler et al.⁶⁸ From $\lambda = 700 \text{ \AA}$ to 980.8 \AA the cross section was determined by Katayama et al.⁶⁹ In the range $\lambda = 850 \text{ \AA}$ to 1110 \AA the measurements made by Watanabe and Jursa⁷⁰ were incorporated. Between $\lambda = 1060 \text{ \AA}$ and 1860 \AA data are based on measurements made by Watanabe and Zelikoff.⁷¹

Branching ratios:

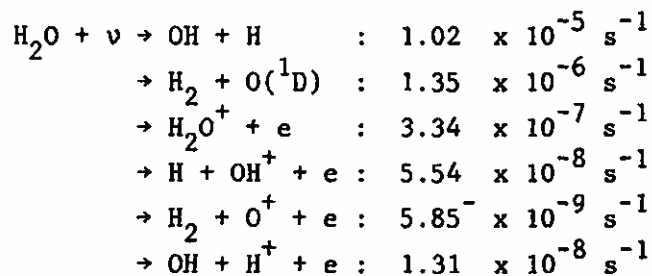
The branching ratio for dissociation and ionization is obtained from the papers of Katayama et al.⁶⁹ and Watanabe and Jursa.⁷⁰ Branching ratios for dissociative ionization are obtained from Dibeler et al.⁶⁸ and from Kronebusch and Berkowitz.⁴²

Thresholds:

The dissociation into $\text{H} + \text{OH}$ has a threshold at $\lambda = 1860 \text{ \AA}$ as determined by Watanabe and Zelikoff,⁷¹ while the threshold for dissociation into $\text{H}_2 + \text{O}(^1\text{D})$ is at $\lambda = 1450 \text{ \AA}$ as assumed from discussions given by McNesby et al.⁷² The ionization threshold of $\lambda = 984 \text{ \AA}$ reported by Katayama et al.⁶⁹ is in good agreement with values measured by Dibeler et al.⁶⁸ and Watanabe and Jursa.⁷⁰ Thresholds for dissociative ionization as reported by Kronebusch and Berkowitz⁴² are



Rate coefficients:



The dissociation rate of $1.16 \times 10^{-5} \text{ s}^{-1}$ is in good agreement with the rates predicted by Potter and del Duca¹ ($1.38 \times 10^{-5} \text{ s}^{-1}$) and by Wyckoff and Wehinger³⁶ ($1.1 \times 10^{-5} \text{ s}^{-1}$), but it is larger than the rate given by Baurer and Bortner¹⁰ ($8.3 \times 10^{-6} \text{ s}^{-1}$) and is much smaller than the value quoted by Jackson^{2,3} ($5 \times 10^{-5} \text{ s}^{-1}$). Our combined ionization rate coefficient $4.08 \times 10^{-7} \text{ s}^{-1}$ is also in good agreement with the rate given by Wyckoff and Wehinger³⁶ ($4.4 \times 10^{-7} \text{ s}^{-1}$) but is smaller than the rate quoted by Siscoe and Mukherjee⁴ ($6.24 \times 10^{-7} \text{ s}^{-1}$). Our total photo rate coefficient for destruction of H_2O is $1.20 \times 10^{-5} \text{ s}^{-1}$. This is in good agreement with the rate given by Wyckoff and Wehinger³⁶ ($1.1 \times 10^{-5} \text{ s}^{-1}$) and the approximate rate obtained by Bertaux et al.²¹ ($9.3 \times 10^{-6} \text{ s}^{-1}$).

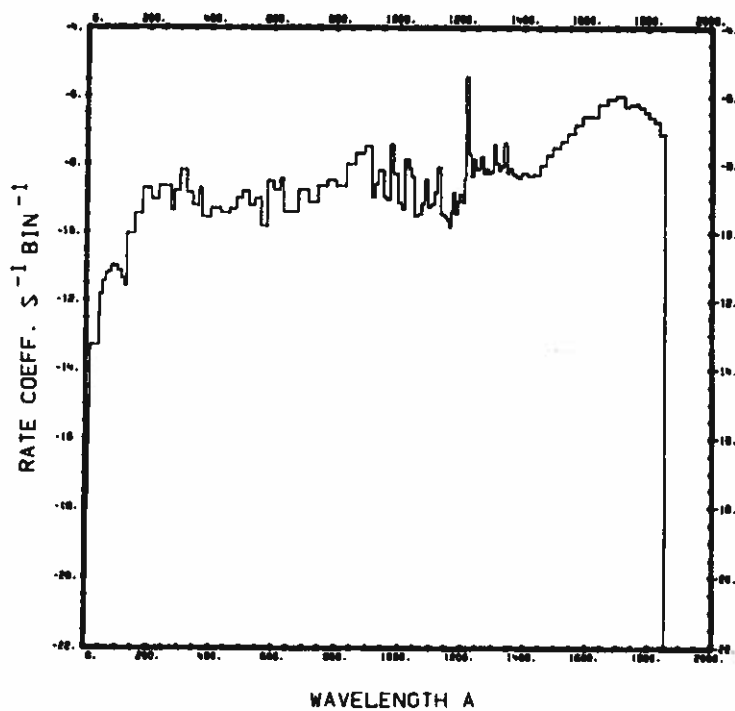


Fig. 36.
 $\text{H}_2\text{O} + \nu \rightarrow \text{OH} + \text{H}_{\frac{1}{2}}$

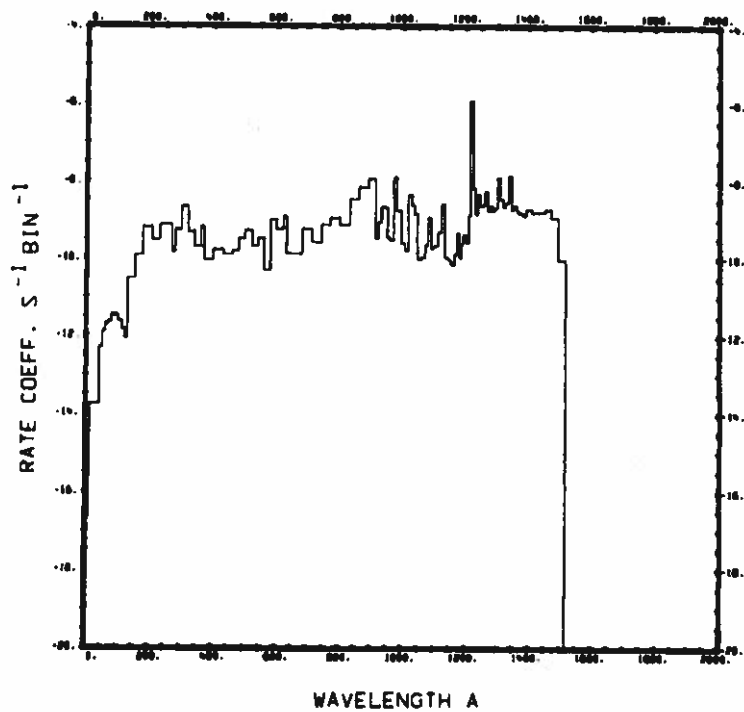


Fig. 37.
 $\text{H}_2\text{O} + \nu \rightarrow \text{H}_2 + \text{O}(^1\text{D})$

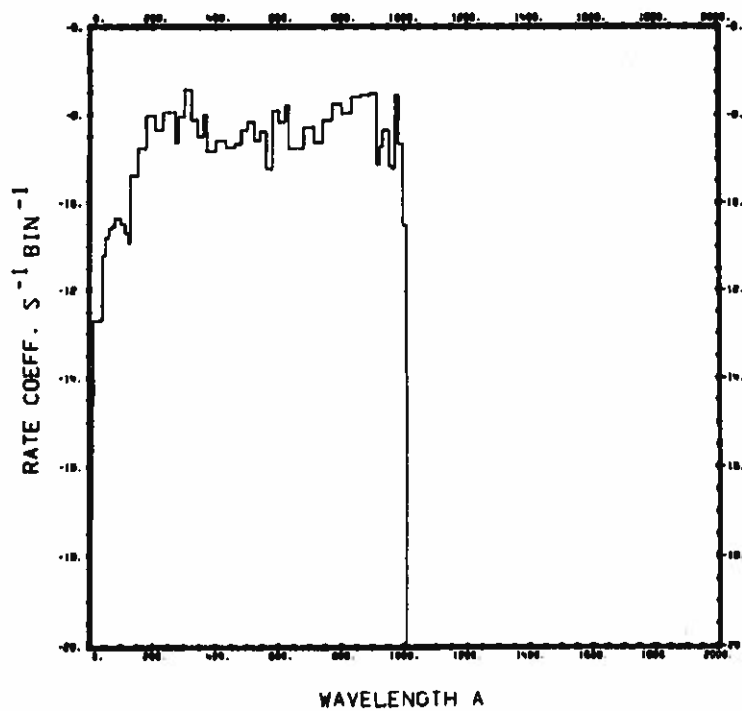


Fig. 38.
 $H_2O + \nu \rightarrow H_2O^+ + e.$

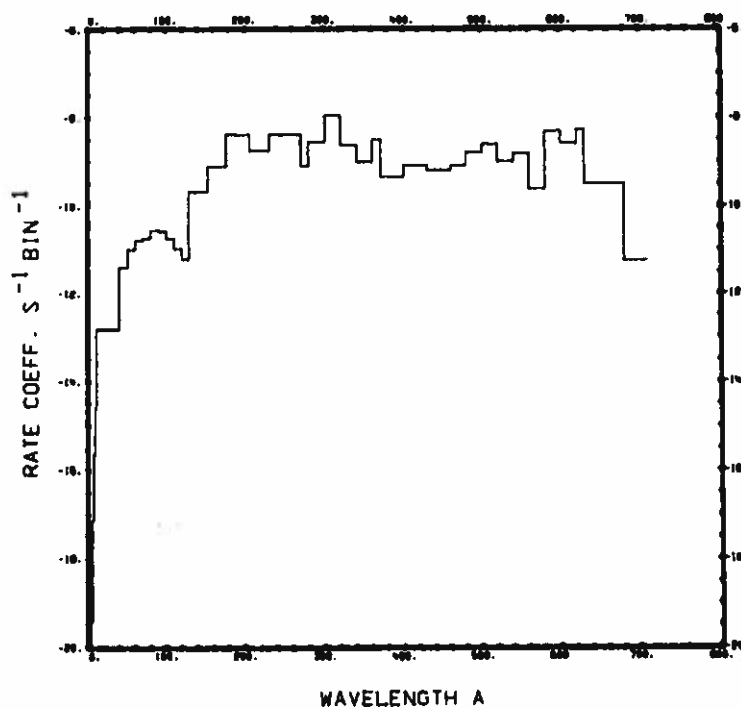


Fig. 39.
 $H_2O + \nu \rightarrow H + OH^+ + e.$

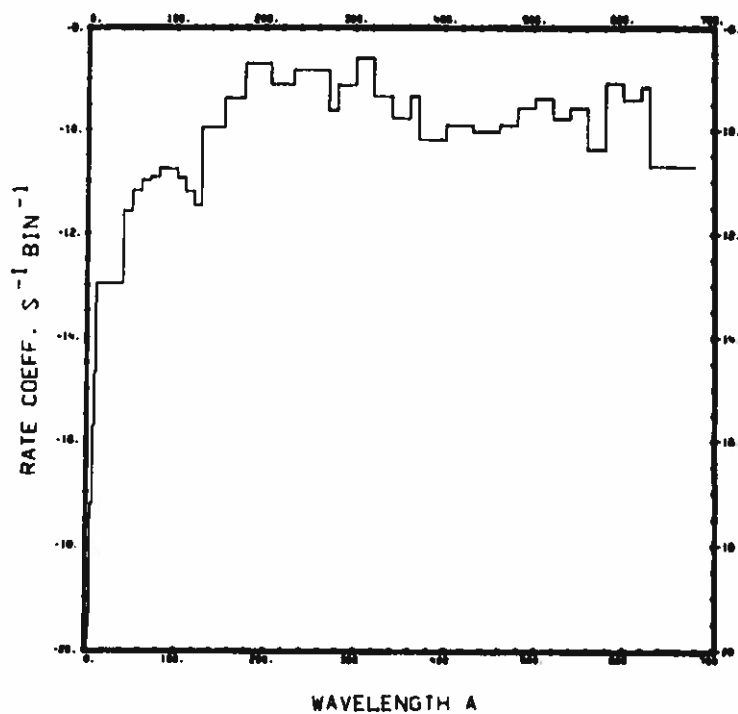


Fig. 40.
 $\text{H}_2\text{O} + \nu \rightarrow \text{H}_2 + \text{O}^+ + \text{e}.$

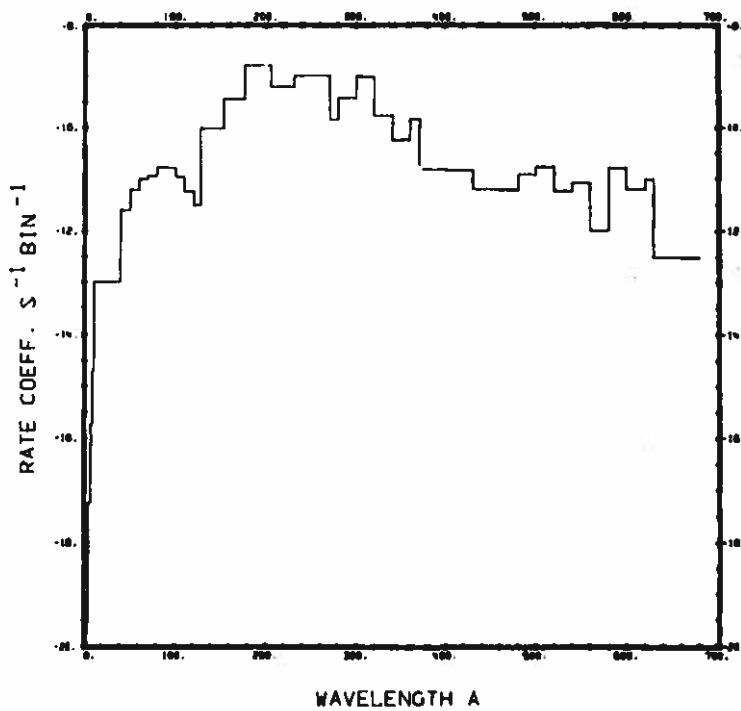


Fig. 41.
 $\text{H}_2\text{O} + \nu \rightarrow \text{OH} + \text{H}^+ + \text{e}.$

Hydrogen cyanide, HCN

Cross section:

Between $\lambda = 1 \text{ \AA}$ and 900 \AA the molecular cross section is synthesized from the atomic cross sections of H, C and N. From $\lambda = 1050 \text{ \AA}$ to 1950 \AA the cross section was measured by West.⁷³

Branching ratios:

Since no branching ratios are available, it is assumed that the entire rate corresponds to dissociation.

Threshold:

Threshold is assumed to be at 1950 \AA .

Rate coefficient:

$$\text{HCN} + \nu \rightarrow \text{H} + \text{CN} : 1.30 \times 10^{-5} \text{ s}^{-1}$$

This agrees with the rate obtained by Jackson^{2,3} ($1.1 \times 10^{-5} \text{ s}^{-1}$) who used the same cross section data for $\lambda > 1050 \text{ \AA}$. The rate coefficient is completely dominated by the solar Lyman α contribution.

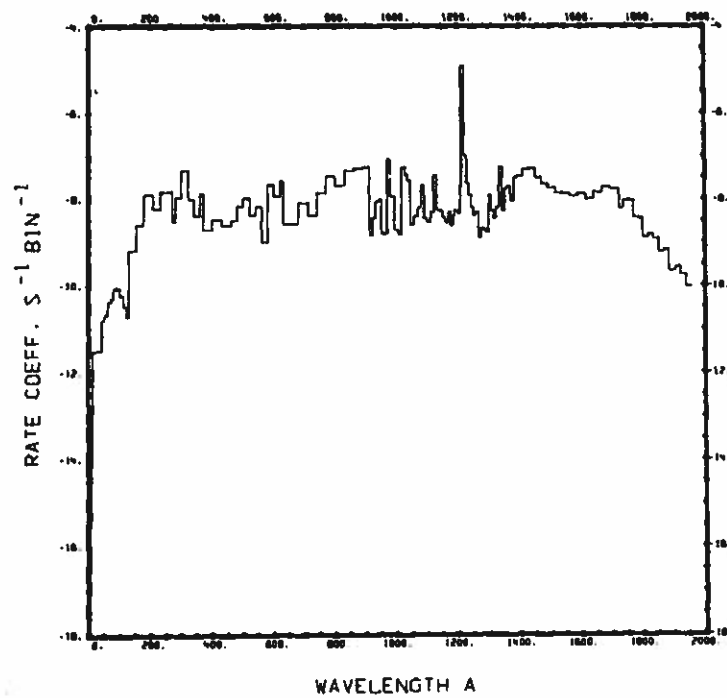


Fig. 42.
 $\text{HCN} + \nu \rightarrow \text{H} + \text{CN}$.

Carbon dioxide, CO₂

Cross section:

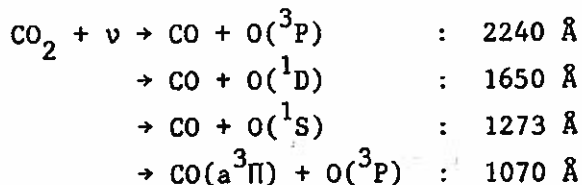
From $\lambda = 2 \text{ \AA}$ to 270 \AA the cross section compiled by Henry and McElroy³⁷ was used. Between 303.7 \AA and 555.26 \AA the cross section comes from the measurements made by Cairns and Samson.³⁸ The range from 580 \AA to 1670 \AA is covered by the data from Nakata et al.⁷⁴ From $\lambda = 1670 \text{ \AA}$ to 1990 \AA the compiled cross section from Huffman⁹ was used.

Branching ratios:

The branching ratio for all ionization processes versus all dissociation processes was obtained from the data of Nakata et al.⁷⁴ The dissociation branching ratio for production of CO in the $X^1\Sigma^+$ or in the $a^3\Pi$ states from $\lambda = 851 \text{ \AA}$ to 1090 \AA was determined from the data of Lawrence.⁷⁵ The structural features of this data are in excellent agreement with the total absorption coefficients of Nakata et al.⁷⁴ Ionization and dissociative ionization branching ratios are given by Kronebusch and Berkowitz.⁴²

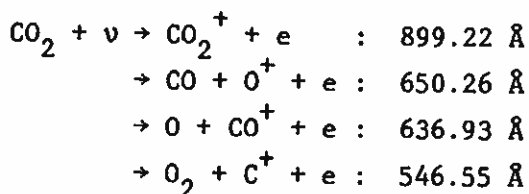
Thresholds:

Some important threshold values for dissociation are given by McNesby and Okabe.⁵⁸

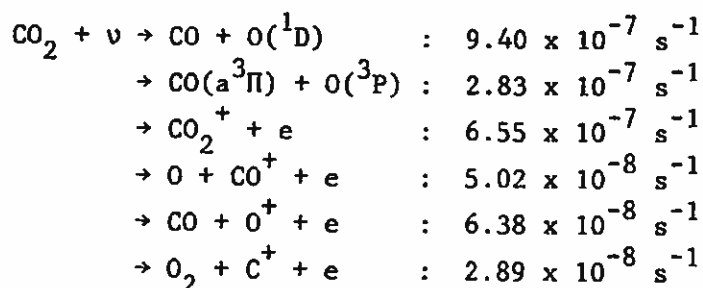


Here CO without further notation stands for the ground state. The first of these dissociations is spin forbidden, the cross section between $\lambda = 1650 \text{ \AA}$ and 2240 \AA is very small, and apparently too small to be measured between $\lambda = 1990 \text{ \AA}$ and 2240 \AA . Therefore, the effective threshold for the rate coefficients reported here is 1990 \AA .

Thresholds for ionization are given by Kronebusch and Berkowitz.⁴²



Rate coefficients:



Dissociation into the ground state of CO is accompanied by formation of atomic oxygen in the ${}^1\text{D}$ state with small amounts in the ${}^3\text{P}$ and ${}^1\text{S}$ states which have not been separated in the above results. Our value for this process is a factor of ten larger than the one quoted by Baurer and Bortner¹⁰ ($9.4 \times 10^{-8} \text{ s}^{-1}$). For the $\text{O}({}^3\text{P})$ branch they obtain $1.1 \times 10^{-8} \text{ s}^{-1}$. McElroy and Hunten⁵ obtain $1.5 \times 10^{-6} \text{ s}^{-1}$ for the $\text{O}({}^1\text{D})$ branch and $2.8 \times 10^{-8} \text{ s}^{-1}$ for the $\text{O}({}^3\text{P})$ branch (after correcting to Earth orbit). Their small rate for the $\text{O}({}^3\text{P})$ branch appears to come from the small cross section ($\sim 10^{-20} \text{ cm}^2$) between $\lambda = 1650 \text{ \AA}$ and 1990 \AA and not from the branch yielding $\text{CO}({}^3\Pi) + \text{O}({}^3\text{P})$. Our rate coefficient for all ionization processes is $7.98 \times 10^{-7} \text{ s}^{-1}$. This is half way between the rates given by Siscoe and Mukherjee⁴ ($1.038 \times 10^{-6} \text{ s}^{-1}$) and McElroy et al.⁷ ($5.6 \times 10^{-7} \text{ s}^{-1}$, after correcting to Earth orbit).

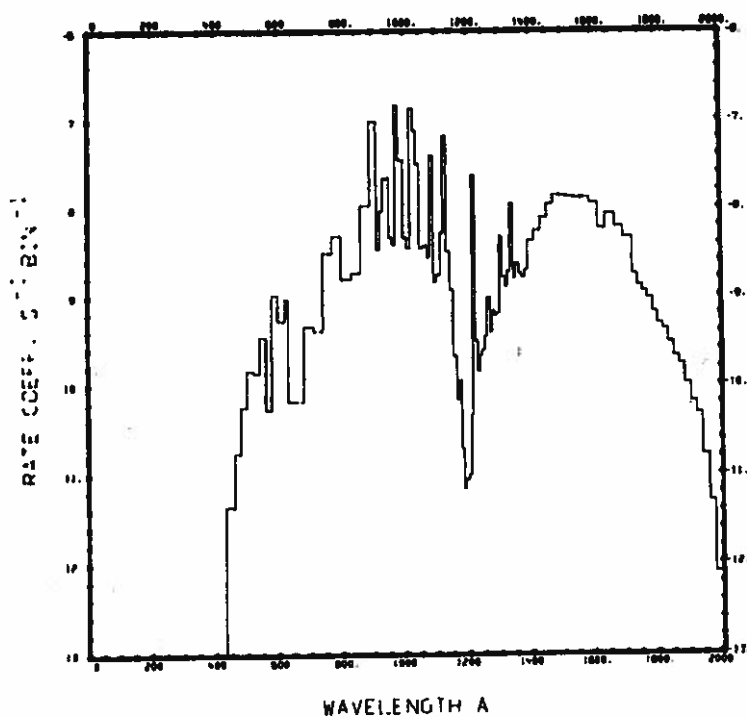
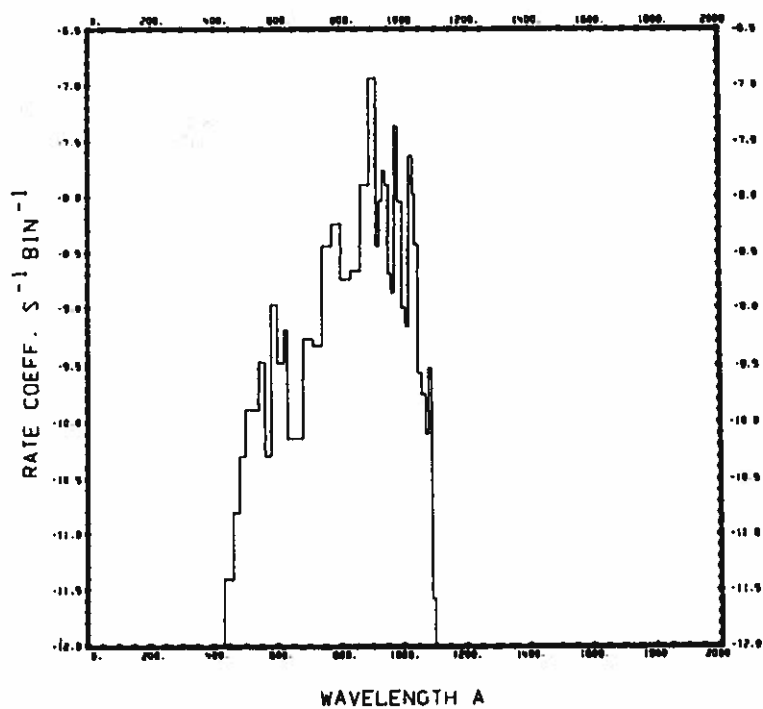


Fig. 43
 $\text{CO}_2 + v \rightarrow \text{CO} + \text{O}(^1\text{D})$.

Fig. 44.
 $\text{CO}_2 + v \rightarrow \text{CO}(a^3\Pi) + \text{O}(^3\text{P})$.



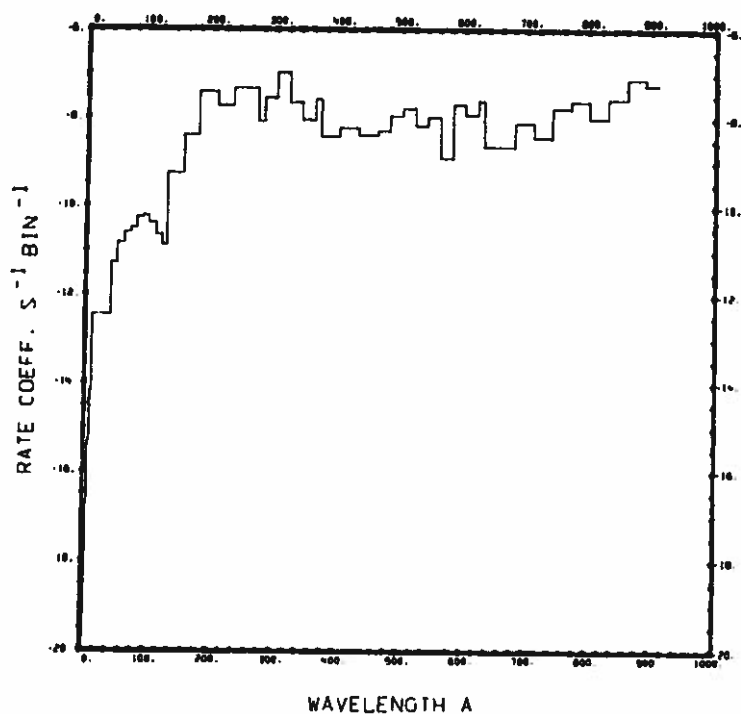


Fig. 45.
 $\text{CO}_2 + \nu \rightarrow \text{CO}_2^+ + e.$

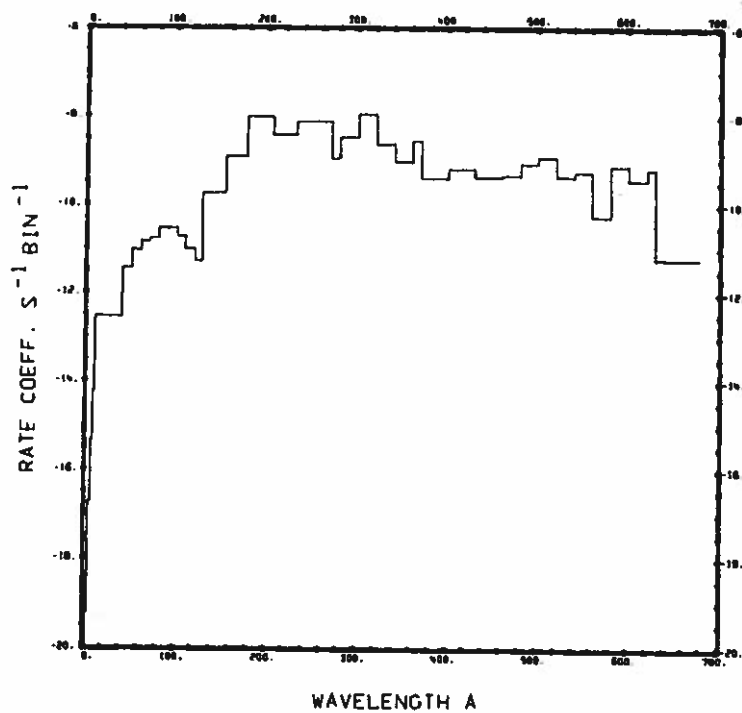


Fig. 46.
 $\text{CO}_2 + \nu \rightarrow \text{O} + \text{CO}^+ + e.$

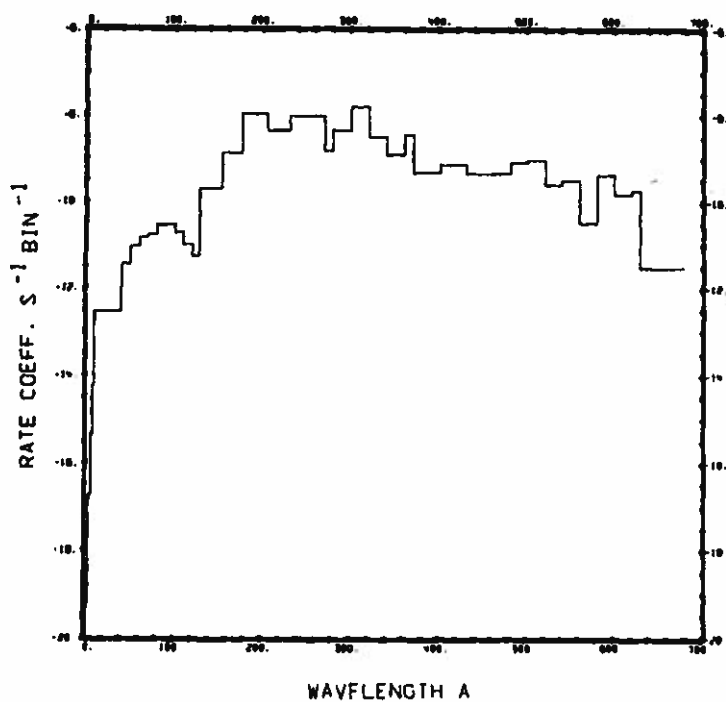


Fig. 47.
 $\text{CO}_2 + \nu \rightarrow \text{CO} + \text{O}^+ + \text{e}.$

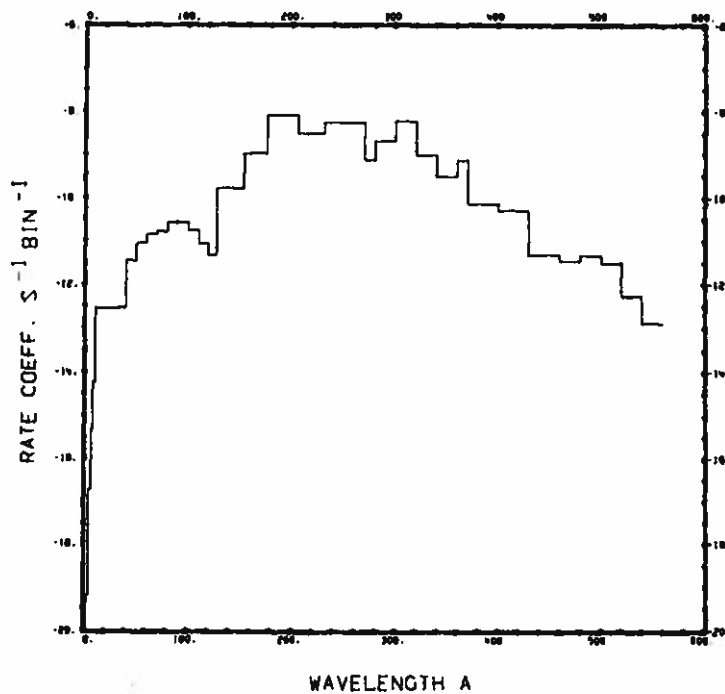


Fig. 48.
 $\text{CO}_2 + \nu \rightarrow \text{O}_2 + \text{C}^+ + \text{e}.$

Ammonia, NH_3

Cross section:

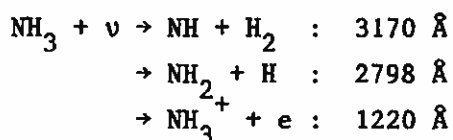
From $\lambda = 1 \text{ \AA}$ to 350 \AA cross sections for the atomic constituents were summed to approximate the cross section of the molecule. In the range $\lambda = 374.1 \text{ \AA}$ to 1306 \AA the measured cross section of Sun and Weissler⁷⁶ was used. In the interval $\lambda = 580 \text{ \AA}$ to 1650 \AA the cross section was taken from Watanabe and Sood.⁷⁷ From $\lambda = 1650 \text{ \AA}$ to 2170 \AA the cross section comes from Watanabe⁷⁸ and in the range $\lambda = 2140 \text{ \AA}$ to 2330 \AA it comes from Thompson et al.⁷⁹

Branching ratios:

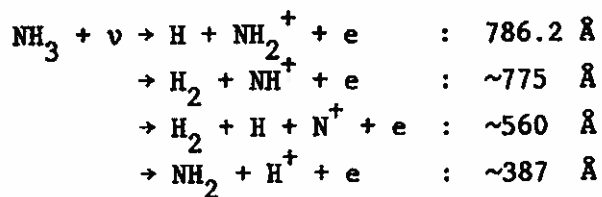
The branching between ionization and dissociation processes was obtained from the work of Watanabe and Sood⁷⁷ and from Dibeler et al.⁶⁸ Branching ratios for the various dissociation products are obtained from McNesby et al.⁷² and Groth et al.⁸⁰ Dissociative ionization branching ratios are taken from Dibeler et al.⁶⁸ and Kronebusch and Berkowitz.⁴²

Thresholds:

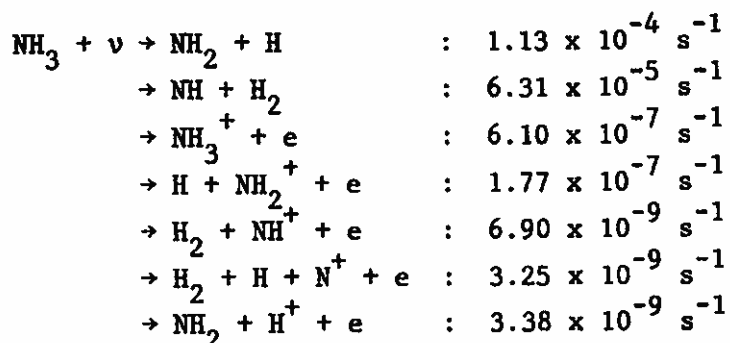
Threshold values for dissociation and ionization are given by Okabe and Lenzi.⁸¹



These thresholds are for dissociation into the ground states of NH and NH_2 for which the cross sections are very small. Cross sections are much larger for transitions into excited states (these have been taken into account in the calculation of the rate coefficients). For dissociative ionization thresholds are not well known except for the products $\text{H} + \text{NH}_2^+ + e$. Kronebusch and Berkowitz⁴² give



Rate coefficients:



Our total rate coefficient ($1.77 \times 10^{-4} \text{ s}^{-1}$) is between the values obtained by Potter and del Duca¹ ($6.8 \times 10^{-5} \text{ s}^{-1}$) and by Jackson^{2,3} ($4.8 \times 10^{-4} \text{ s}^{-1}$).

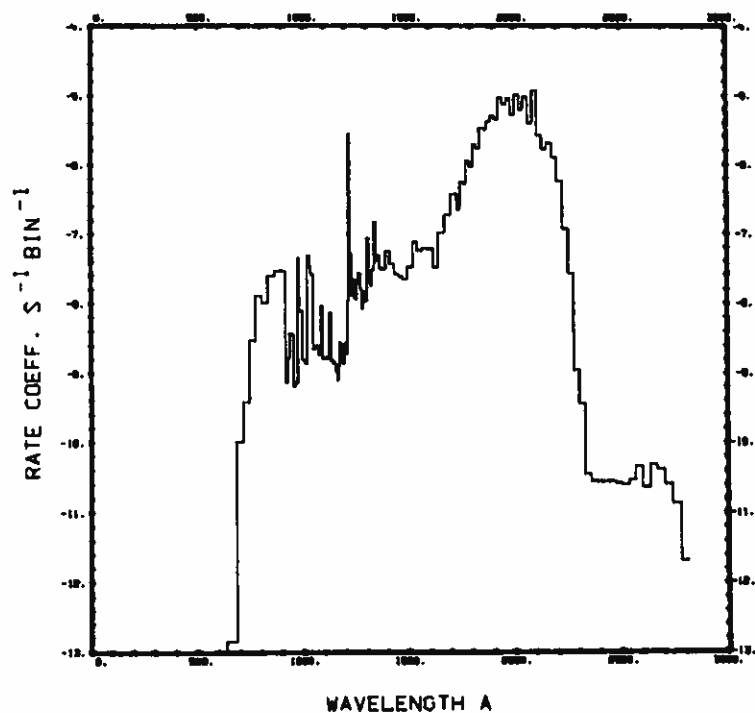


Fig. 49. $\text{NH}_3 + \nu \rightarrow \text{NH}_2 + \text{H}$.

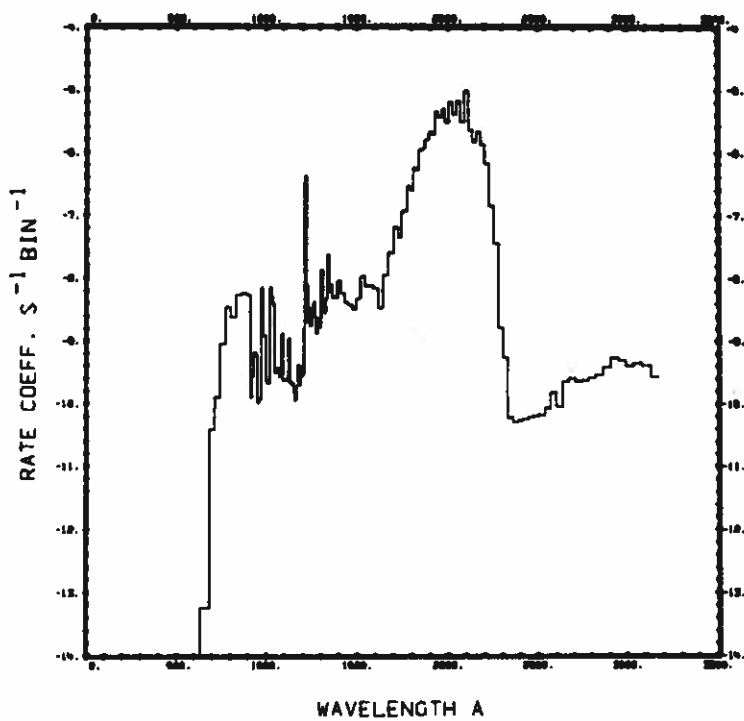


Fig. 50.
 $\text{NH}_3 + \nu \rightarrow \text{NH} + \text{H}_2$.

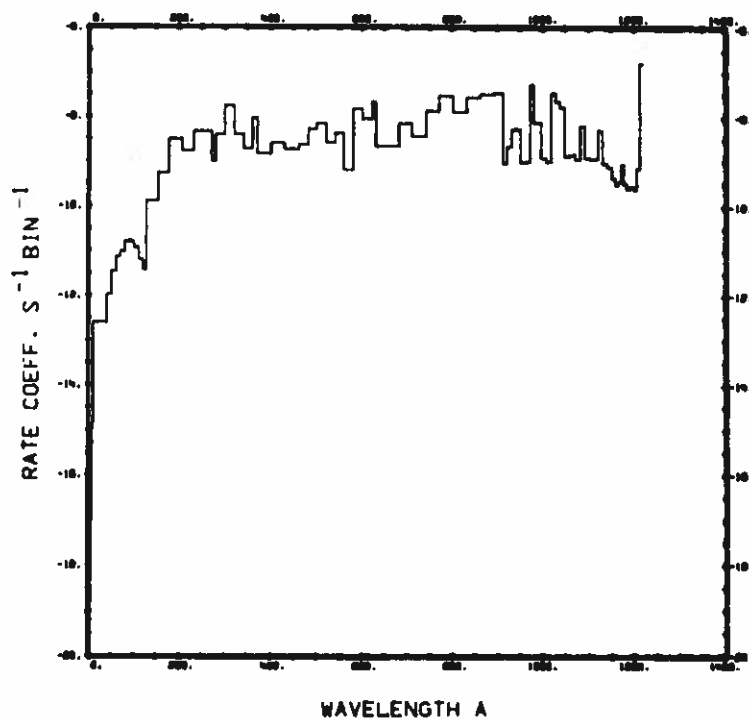


Fig. 51.
 $\text{NH}_3 + \nu \rightarrow \text{NH}_3^+ + e$.

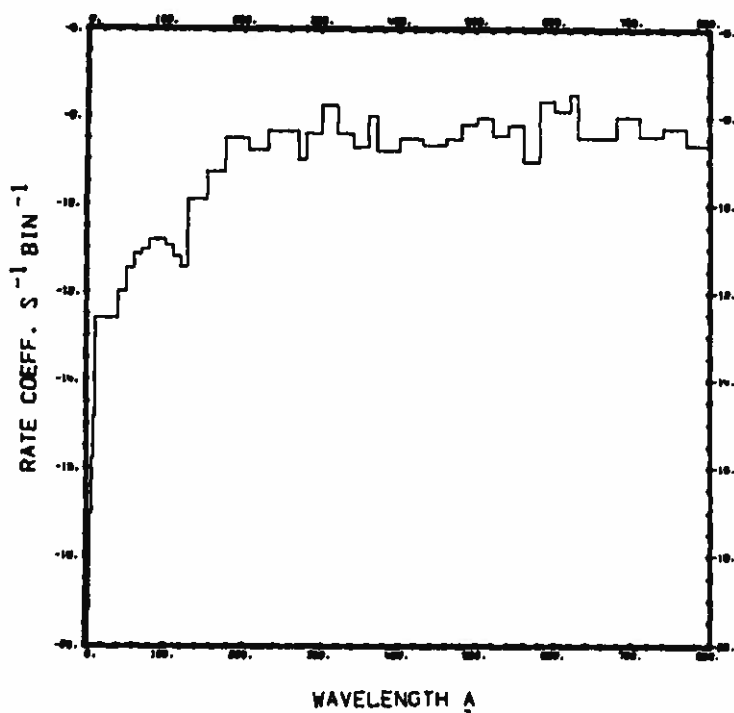


Fig. 52.
 $\text{NH}_3 + \nu \rightarrow \text{H} + \text{NH}_2^+ + \text{e}.$

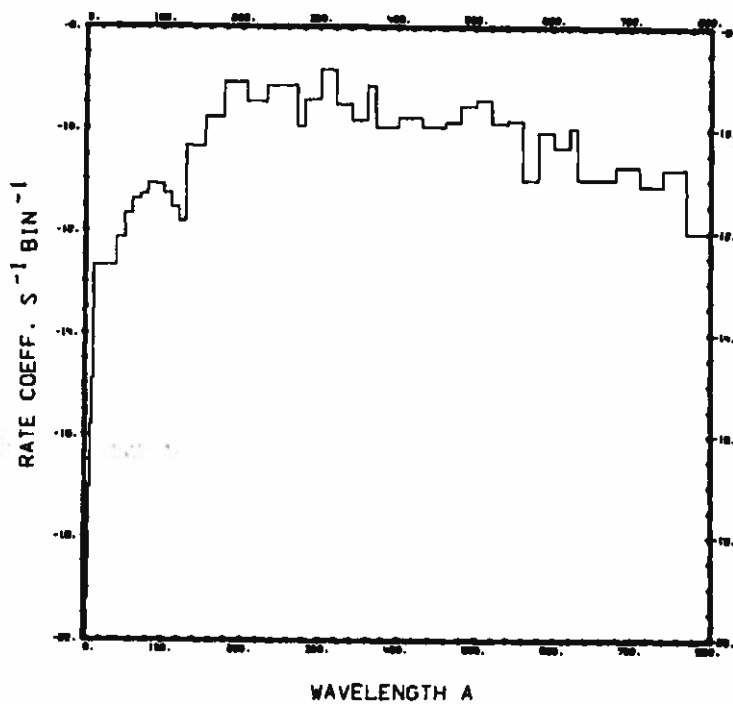


Fig. 53.
 $\text{NH}_3 + \nu \rightarrow \text{H}_2 + \text{NH}^+ + \text{e}.$

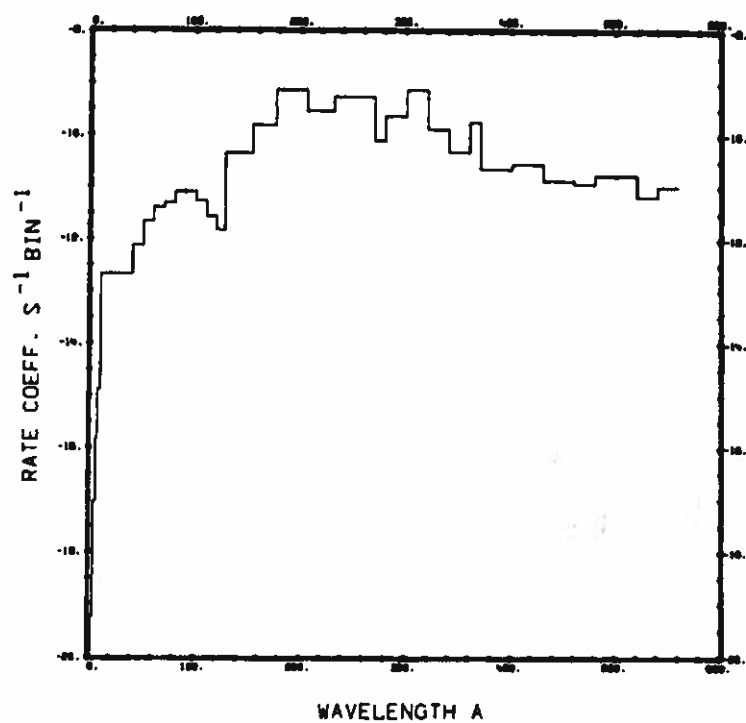


Fig. 54
 $\text{NH}_3 + \nu \rightarrow \text{H}_2 + \text{H} + \text{N}^+ + \text{e}.$

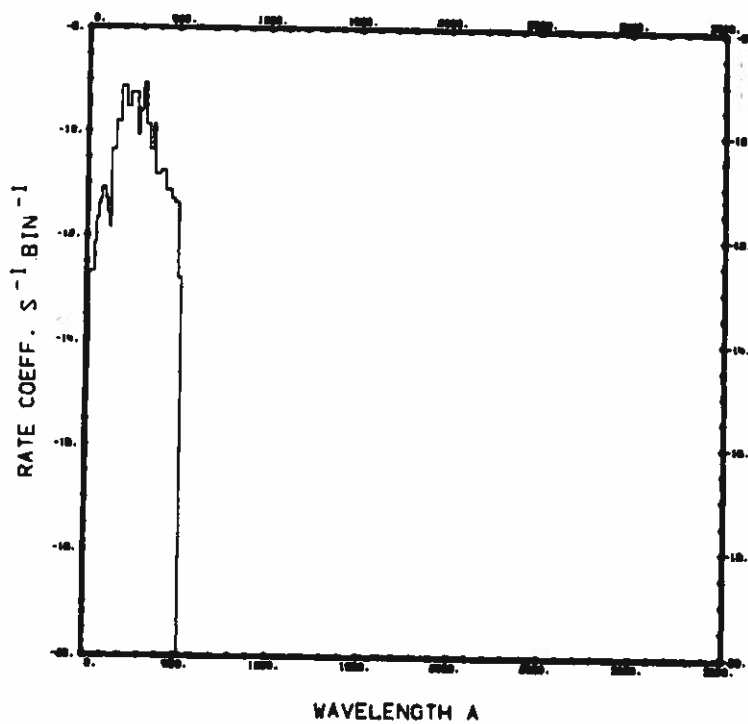


Fig. 55.
 $\text{NH}_3 + \nu \rightarrow \text{NH}_2 + \text{H}^+ + \text{e}.$

Acetylene, C₂H₂

Cross Section:

In the range $\lambda = 1 \text{ \AA}$ to 500 \AA the sum of the cross sections of the atomic constituents approximate the molecular cross section. From $\lambda = 600 \text{ \AA}$ to 1000 \AA the cross section measured by Metzger and Cook⁸² was used. Values between 1050 \AA and 2011 \AA come from measurements made by Nakayama and Watanabe.⁸³

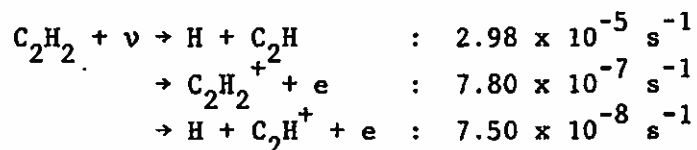
Branching ratios:

The branching ratio between dissociation and all ionization processes from $\lambda = 600 \text{ \AA}$ to 1000 \AA is taken from Schoen,⁸⁴ and in the range from $\lambda = 1050 \text{ \AA}$ to the ionization threshold it is taken from Nakayama and Watanabe.⁸³ For dissociative ionization the branching is obtained from Schoen's data.

Thresholds:

For the pure dissociation the threshold given by Okabe⁸⁵ is 2306 \AA . The threshold for pure ionization is at $\lambda = 1086 \text{ \AA}$ as given by Herzberg.⁸⁶ The first threshold for dissociative ionization was determined by Metzger and Cook,⁸² it is at $\lambda = 697 \text{ \AA}$.

Rate coefficients:



Our combined rate coefficient for these processes is $3.07 \times 10^{-5} \text{ s}^{-1}$ and falls between the values obtained by Potter and del Duca¹ ($6.5 \times 10^{-6} \text{ s}^{-1}$) and by Jackson^{2,3} ($1.7 \times 10^{-4} \text{ s}^{-1}$).

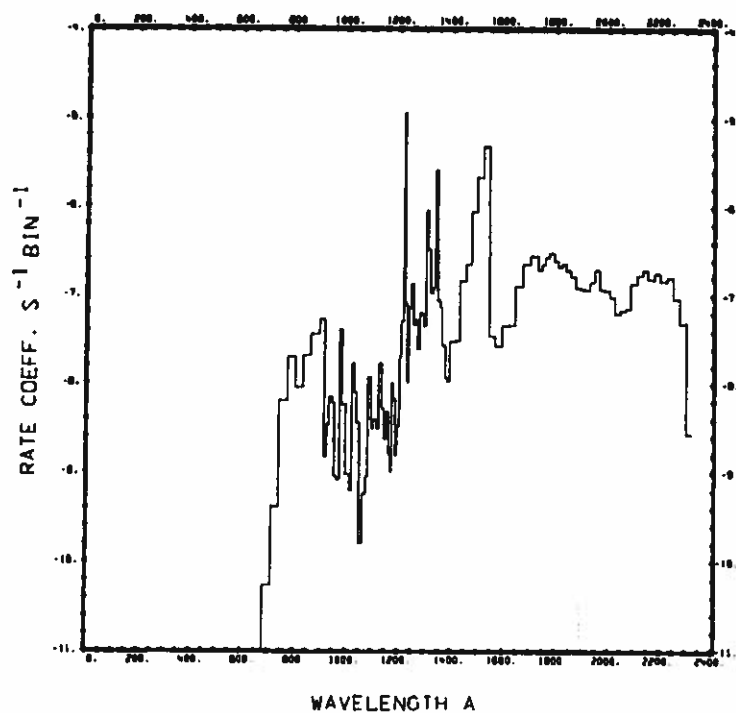


Fig. 56.
 $\text{C}_2\text{H}_2 + \nu \rightarrow \text{H} + \text{C}_2\text{H}.$

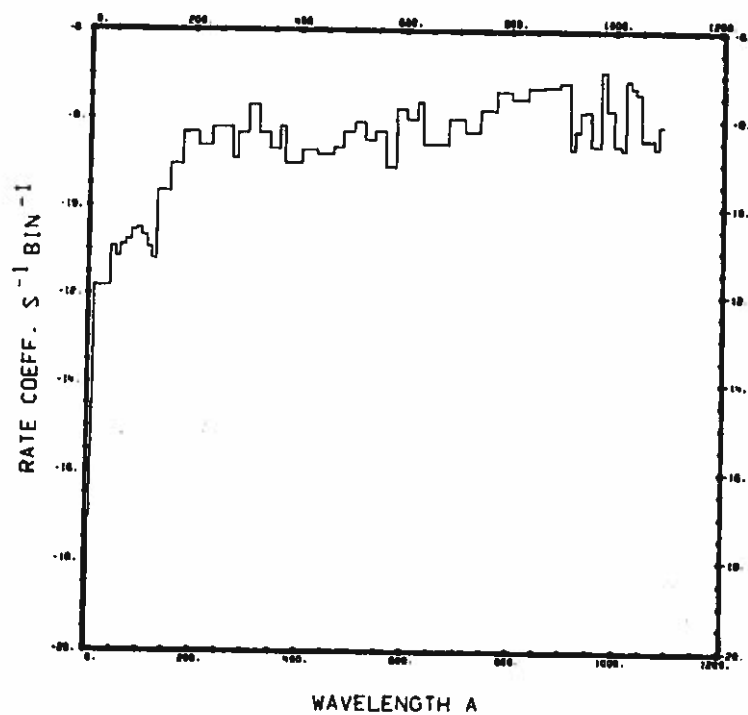


Fig. 57.
 $\text{C}_2\text{H}_2 + \nu \rightarrow \text{C}_2\text{H}_2^+ + \text{e}.$

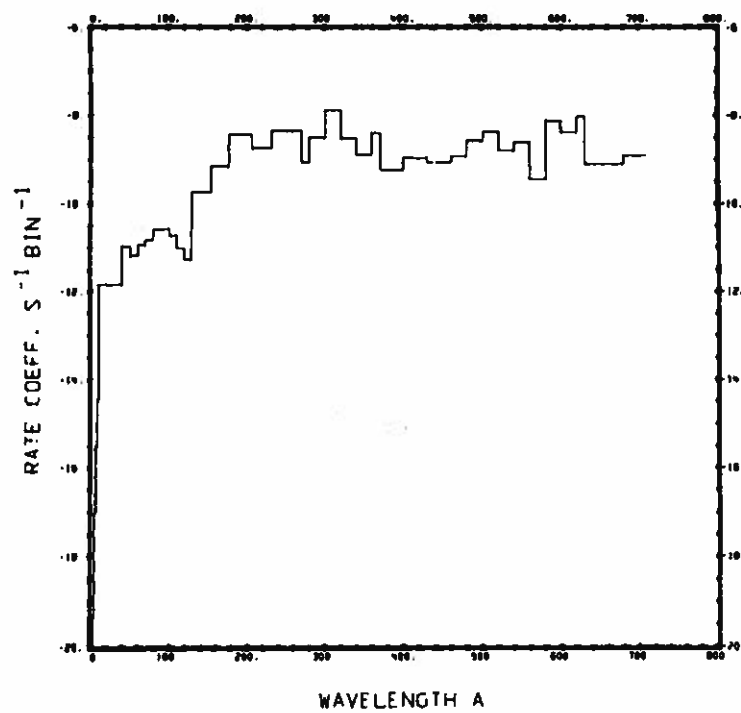
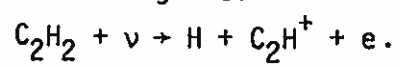


Fig. 58.



Formaldehyde, H₂CO

Cross section:

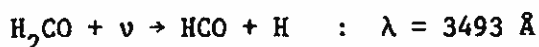
From $\lambda = 1 \text{ \AA}$ to 500 \AA the molecular cross section is synthesized from the cross sections of the atomic constituents. Between $\lambda = 600 \text{ \AA}$ and 1760 \AA the cross section reported by Mentall, et al.⁸⁷ was used. The values of Gentieu and Mentall⁸⁸ were employed in the range $\lambda = 1760 \text{ \AA}$ to 1850 \AA . The cross section between $\lambda = 2000 \text{ \AA}$ and 3740 \AA comes from Calvert and Pitts.⁸⁹

Branching ratios:

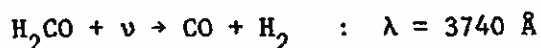
For dissociation forming $\text{CO} + \text{H}_2$ and $\text{HCO} + \text{H}$, the branching ratio in the range $\lambda = 2991 \text{ \AA}$ to 3392 \AA comes from Clark et al.;⁹⁰ a few values are also given by Calvert and Pitts.⁸⁹ The branching ratio for dissociation into $\text{CO} + \text{H} + \text{H}$ is from Mentall et al.⁸⁷ in the range $\lambda = 600 \text{ \AA}$ to 1141.6 \AA and from Stief et al.⁹¹ at 1236 \AA and 1470 \AA . Branching ratios for ionization and dissociative ionization are from Guyon et al.⁹² in the wavelength range 680 \AA to 1043 \AA and from Mentall et al.⁸⁷ between $\lambda = 600 \text{ \AA}$ and 1141.6 \AA .

Thresholds:

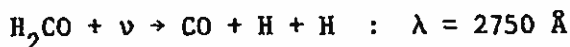
Dissociation thresholds are



from Glicker and Stief,⁹³

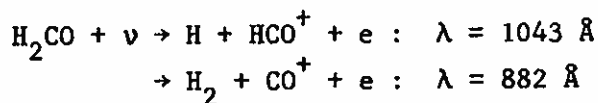


from Calvert and Pitts,⁸⁹



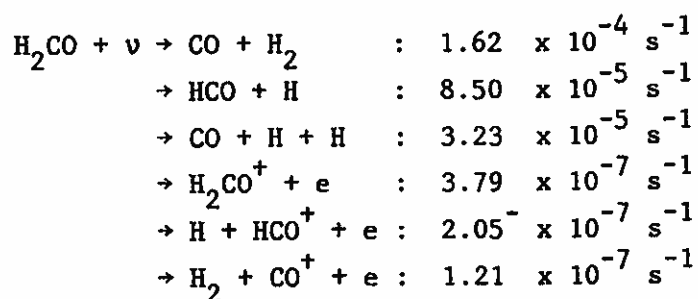
from Clark et al.⁹⁰

The ionization threshold at $\lambda = 1141.6 \text{ \AA}$ and the dissociative ionization thresholds



were determined by Guyon et al.⁹²

Rate coefficients:



Baurer and Bortner¹⁰ quote $1.5 \times 10^{-4} \text{ s}^{-1}$ for the first dissociation branch and $1.1 \times 10^{-4} \text{ s}^{-1}$ for the second branch. They don't mention the third branch. Their total dissociation rate coefficient ($2.6 \times 10^{-4} \text{ s}^{-1}$) is in good agreement with the sum of our three dissociation rates ($2.79 \times 10^{-4} \text{ s}^{-1}$).

Our total rate coefficient ($2.80 \times 10^{-4} \text{ s}^{-1}$) falls between the two values obtained by Jackson^{2,3} ($5.3 \times 10^{-4} \text{ s}^{-1}$ and $1.8 \times 10^{-4} \text{ s}^{-1}$).

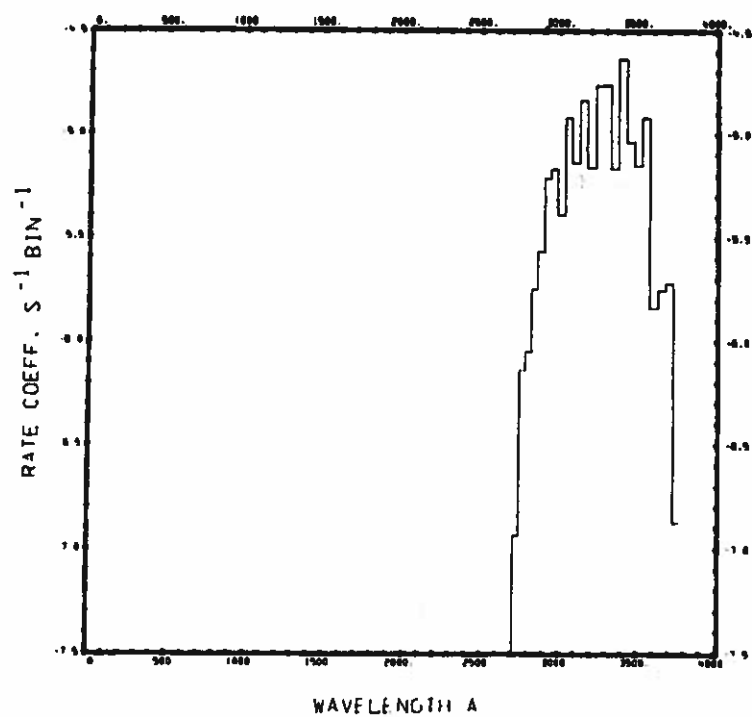


Fig. 59.
 $\text{H}_2\text{CO} + \nu \rightarrow \text{CO} + \text{H}_2$.

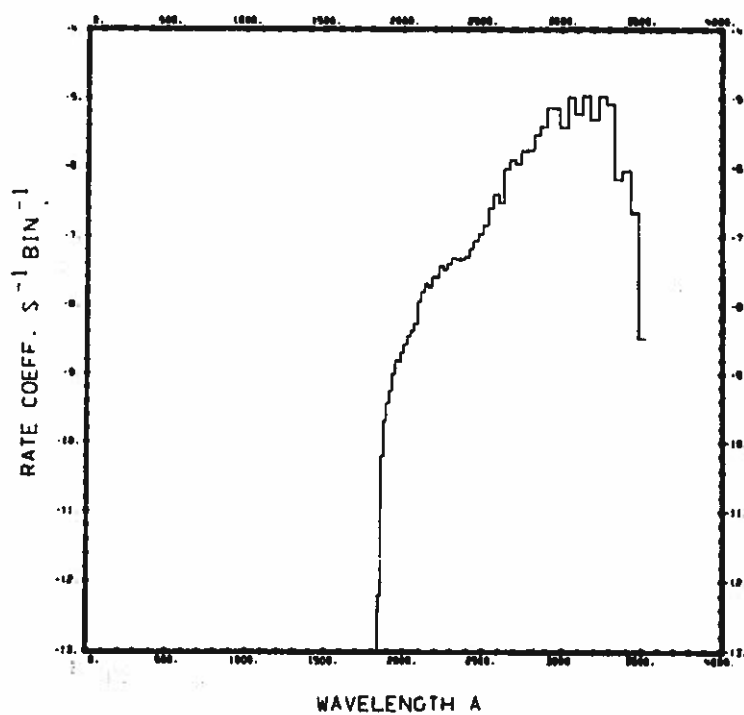


Fig. 60.
 $\text{H}_2\text{CO} + \nu \rightarrow \text{HCO} + \text{H}$.

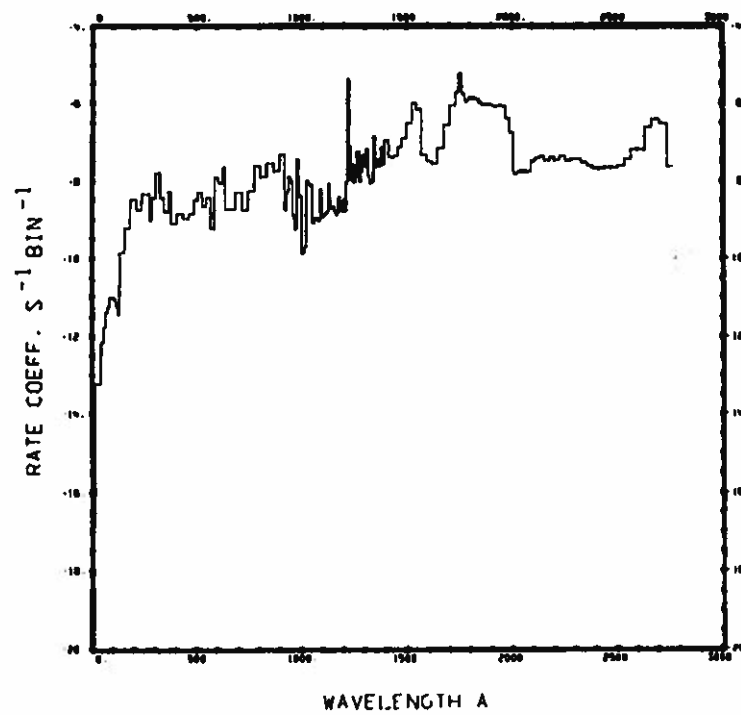


Fig. 61.
 $\text{H}_2\text{CO} + \nu \rightarrow \text{CO} + \text{H} + \text{H}.$

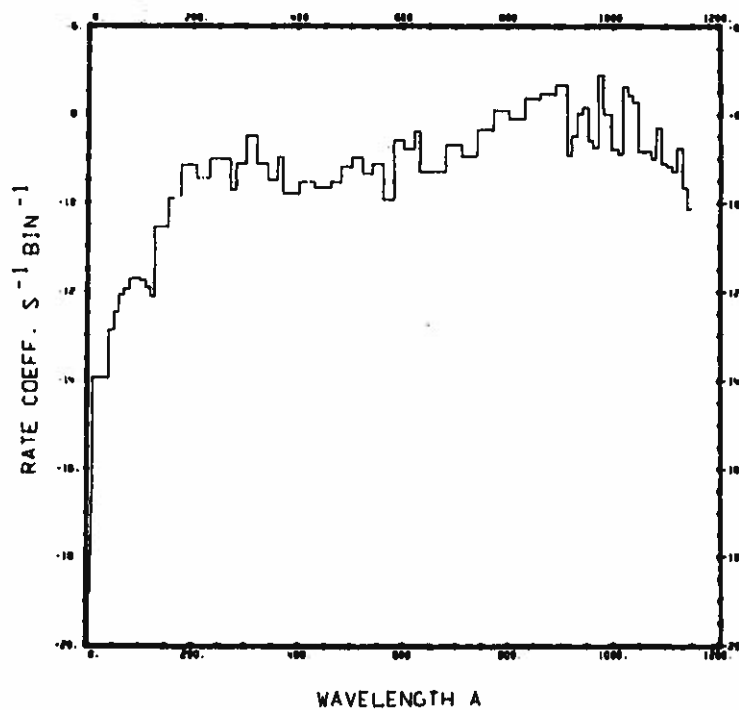


Fig. 62.
 $\text{H}_2\text{CO} + \nu \rightarrow \text{H}_2\text{CO}^+ + \text{e}.$

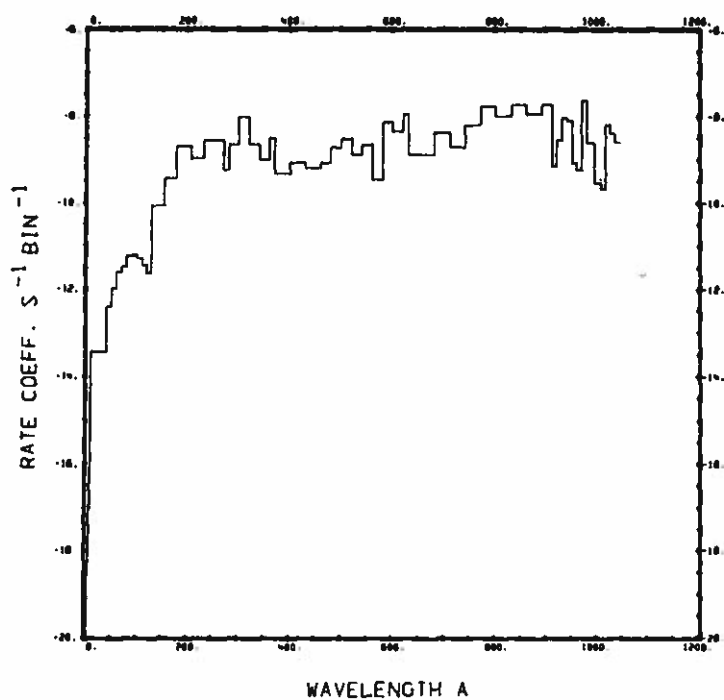


Fig. 63.
 $\text{H}_2\text{CO} + \nu \rightarrow \text{H} + \text{HCO}^+ + \text{e}.$

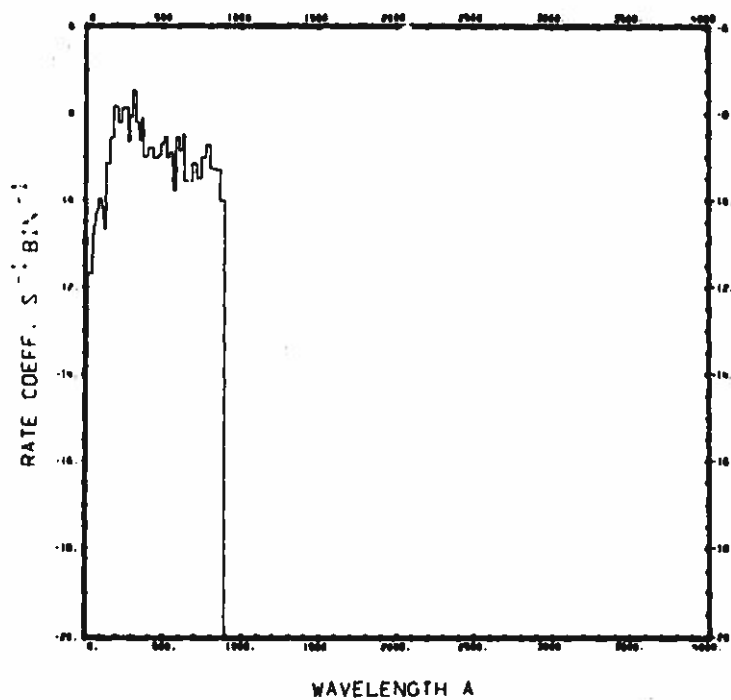


Fig. 64.
 $\text{H}_2\text{CO} + \nu \rightarrow \text{H}_2 + \text{CO}^+ + \text{e}.$

Methane, CH₄

Cross section:

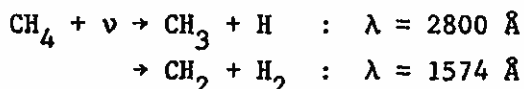
From $\lambda = 23.6 \text{ \AA}$ to 250 \AA the data of Lukirskii et al.⁹⁴ were used. The cross section measured by Ditchburn⁹⁵ was used in the range from 278 \AA to 1513 \AA . These data were supplemented by those of Sun and Weissler⁷⁶ from 951.9 \AA to 1306 \AA . The cross section at 1850 \AA was measured by Thompson et al.⁷⁹

Branching ratios:

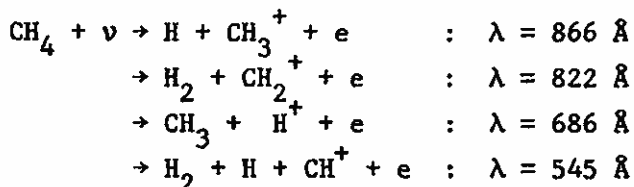
The branching ratio for the formation of $\text{CH} + \text{H}_2 + \text{H}$ is from Gorden and Ausloos.⁹⁶ Ditchburn⁹⁵ and Sun and Weissler⁷⁶ supplied the data for dissociation to $\text{CH}_3 + \text{H}$ and $\text{CH}_2 + \text{H}_2$. Data from Gorden and Ausloos⁹⁶ and Stief et al.⁹¹ were also used for the branching ratio to form $\text{CH}_2 + \text{H}_2$. All branching ratios for ionization and dissociative ionization were taken from Kronebusch and Berkowitz.⁴²

Thresholds:

The threshold wavelengths for dissociation



are given by Ditchburn,⁹⁵ while the estimated threshold $\lambda = 1360 \text{ \AA}$, to form $\text{CH} + \text{H}_2 + \text{H}$, comes from Gorden and Ausloos.⁹⁶ The simple ionization threshold is given by Ditchburn⁹⁵ to be 945 \AA . Approximate dissociative ionization thresholds are given by Kronebusch and Berkowitz⁴²



Rate coefficients:

$\text{CH}_4 + \nu \rightarrow \text{CH}_3 + \text{H}$:	$1.01 \times 10^{-6} \text{ s}^{-1}$
$\rightarrow \text{CH}_2 + \text{H}_2$:	$5.61 \times 10^{-6} \text{ s}^{-1}$
$\rightarrow \text{CH} + \text{H}_2 + \text{H}$:	$5.00 \times 10^{-7} \text{ s}^{-1}$
$\rightarrow \text{CH}_4^+ + e$:	$3.60 \times 10^{-7} \text{ s}^{-1}$
$\rightarrow \text{H} + \text{CH}_3^+ + e$:	$1.98 \times 10^{-7} \text{ s}^{-1}$
$\rightarrow \text{H}_2 + \text{CH}_2^+ + e$:	$2.09 \times 10^{-8} \text{ s}^{-1}$
$\rightarrow \text{CH}_3 + \text{H}^+ + e$:	$9.09 \times 10^{-9} \text{ s}^{-1}$
$\rightarrow \text{H}_2 + \text{H} + \text{CH}^+ + e$:	$4.16 \times 10^{-9} \text{ s}^{-1}$

Our rate coefficient for all ionizing processes ($5.92 \times 10^{-7} \text{ s}^{-1}$) is somewhat smaller than the ionization rate coefficient quoted by Siscoe and Mukherjee⁴ ($8.74 \times 10^{-7} \text{ s}^{-1}$). Our total rate coefficient ($7.71 \times 10^{-6} \text{ s}^{-1}$) is also somewhat smaller than the rate coefficients reported by Potter and del Duca¹ ($1.0 \times 10^{-5} \text{ s}^{-1}$) and by Jackson^{2,3} ($8.2 \times 10^{-6} \text{ s}^{-1}$). The dissociation rates are dominated by the hydrogen Ly α flux.

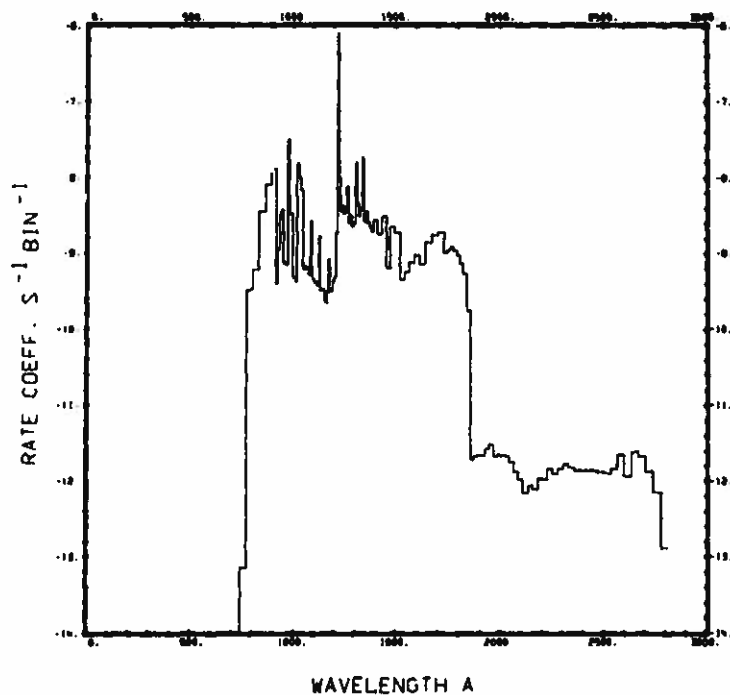


Fig. 65. $\text{CH}_4 + \nu \rightarrow \text{CH}_3 + \text{H}$.

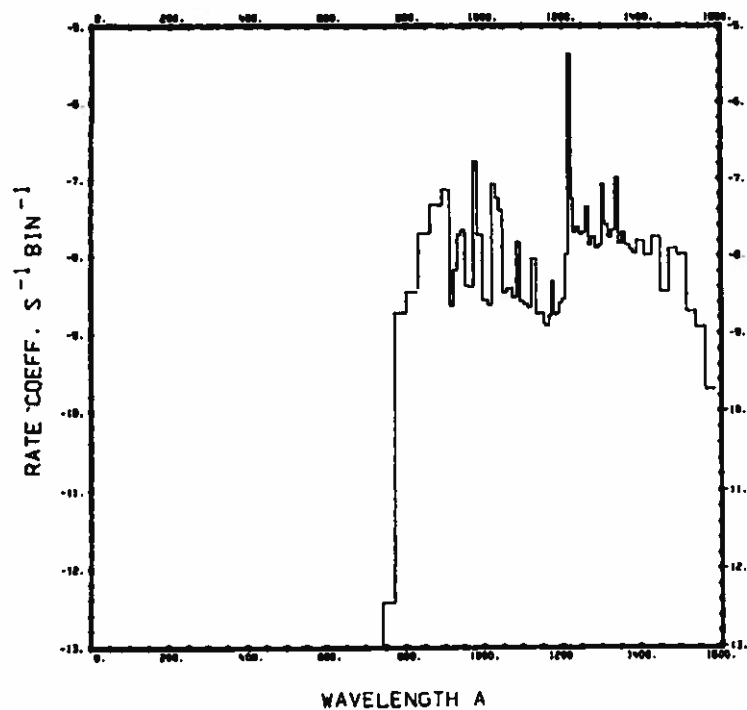


Fig. 66.
 $\text{CH}_4 + \nu \rightarrow \text{CH}_2 + \text{H}_2.$

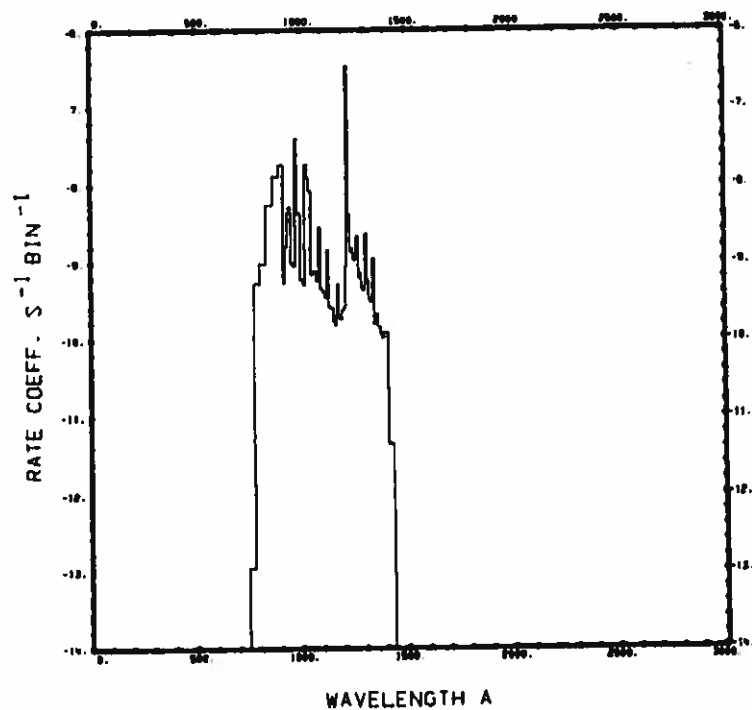


Fig. 67.
 $\text{CH}_4 + \nu \rightarrow \text{CH} + \text{H}_2 + \text{H}.$

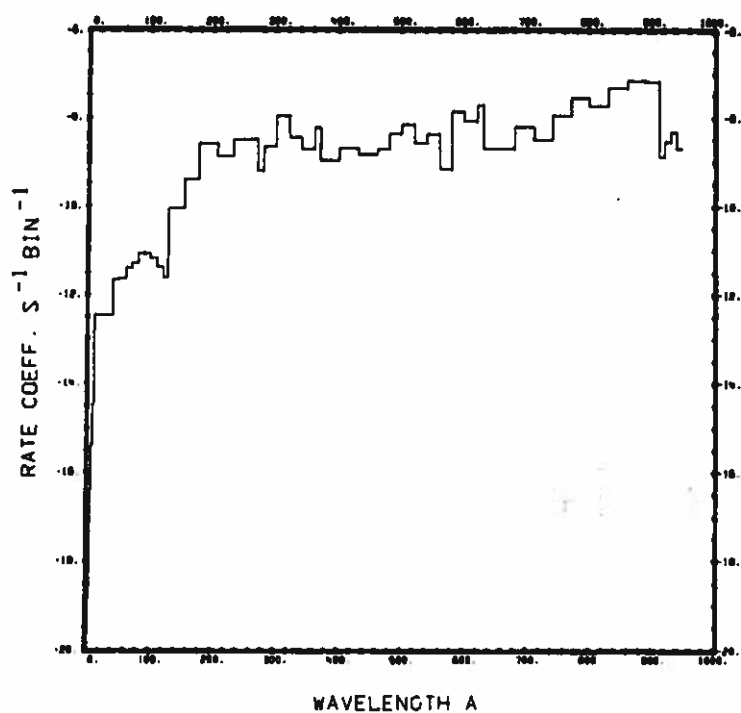


Fig. 68.
 $\text{CH}_4 + \nu \rightarrow \text{CH}_4^+ + \text{e}$.

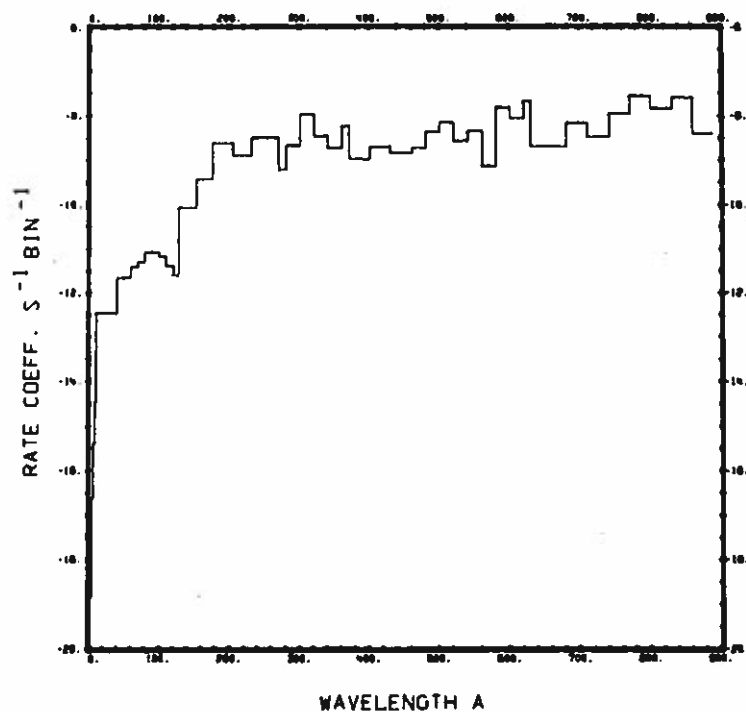


Fig. 69.
 $\text{CH}_4 + \nu \rightarrow \text{H} + \text{CH}_3^+ + \text{e}$.

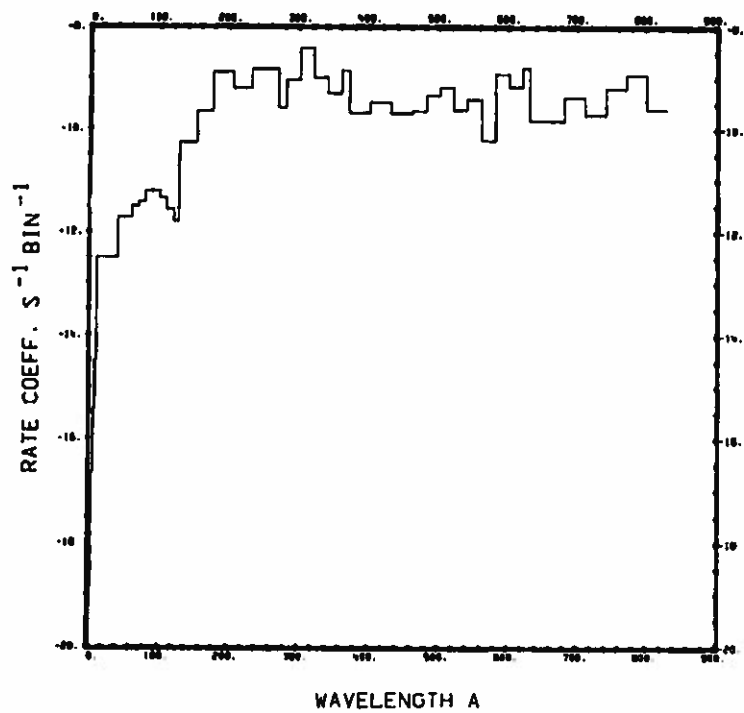


Fig. 70.
 $\text{CH}_4 + \nu \rightarrow \text{H}_2 + \text{CH}_2^+ + \text{e}$.

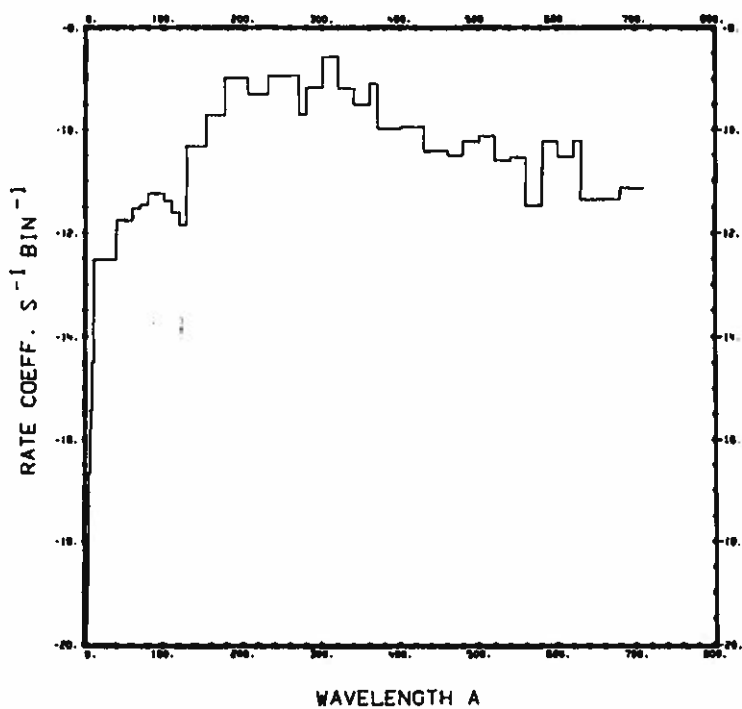


Fig. 71.
 $\text{CH}_4 + \nu \rightarrow \text{CH}_3 + \text{H}^+ + \text{e}$.

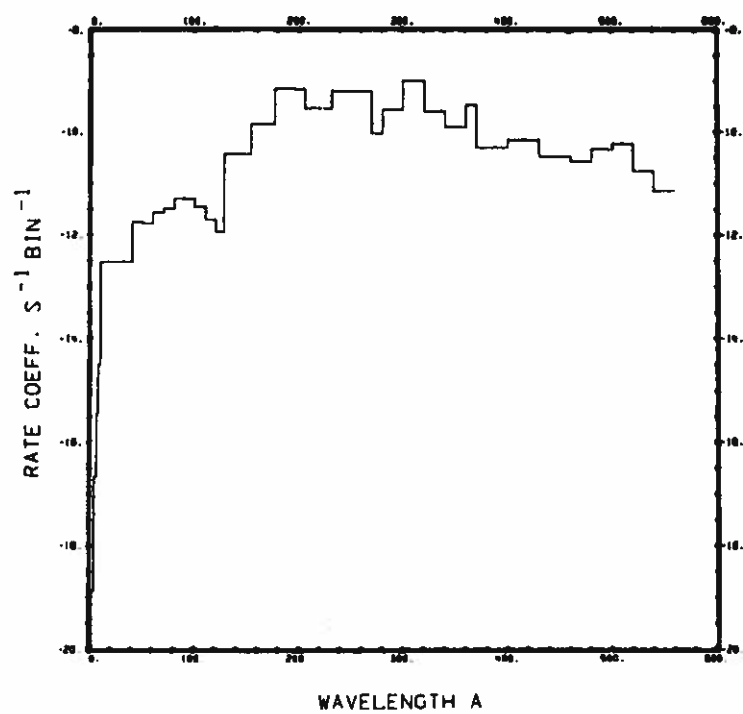
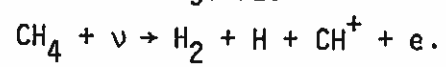


Fig. 72.



Formic Acid, HCOOH

Cross section:

The cross section from $\lambda = 1 \text{ \AA}$ to 600 \AA is synthesized from the cross sections of the atomic constituents. Between 600 \AA and 1100 \AA the cross section was estimated using the known cross section of H_2CO as a guide. From 1100 \AA to 2500 \AA the data from Barnes and Simpson⁹⁷ were used.

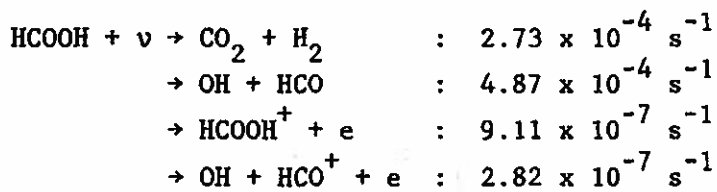
Branching ratios:

The branching ratio for dissociation into $\text{HCO} + \text{OH}$ and $\text{CO}_2 + \text{H}_2$ over a limited wavelength interval has been reported by Gorden and Ausloos.⁹⁸ All other branching ratios have been scaled to the formaldehyde data.

Thresholds:

The cross section data of Barnes and Simpson⁹⁷ decreases rapidly at 2500 \AA . Although this is not the dissociation limit, we assumed the threshold for both pure dissociation processes to be at $\lambda = 2500 \text{ \AA}$. The ionization threshold was measured by Bell et al.⁹⁹ to be $\lambda = 1094.4 \text{ \AA}$. Photodissociative ionization has a threshold at 902 \AA as listed by Field and Franklin.¹⁰⁰

Rate coefficients:



Our total rate coefficient ($7.62 \times 10^{-4} \text{ s}^{-1}$) is larger than the value obtained by Jackson^{2,3} ($1.4 \times 10^{-4} \text{ s}^{-1}$). Because the dissociation threshold is not well known and the branching is incomplete, the rate coefficients are only approximate.

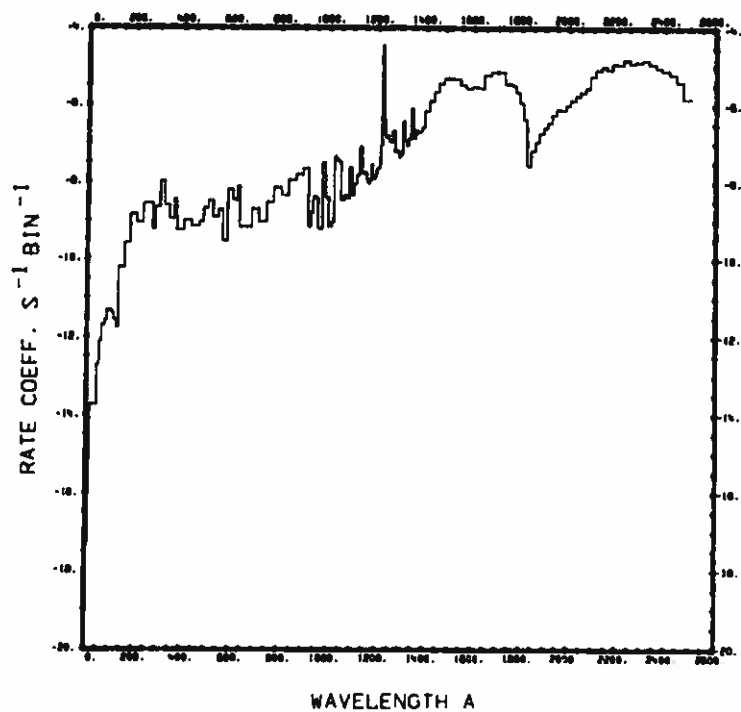


Fig. 73.
 $\text{HCOOH} + \nu \rightarrow \text{CO}_2 + \text{H}_2.$

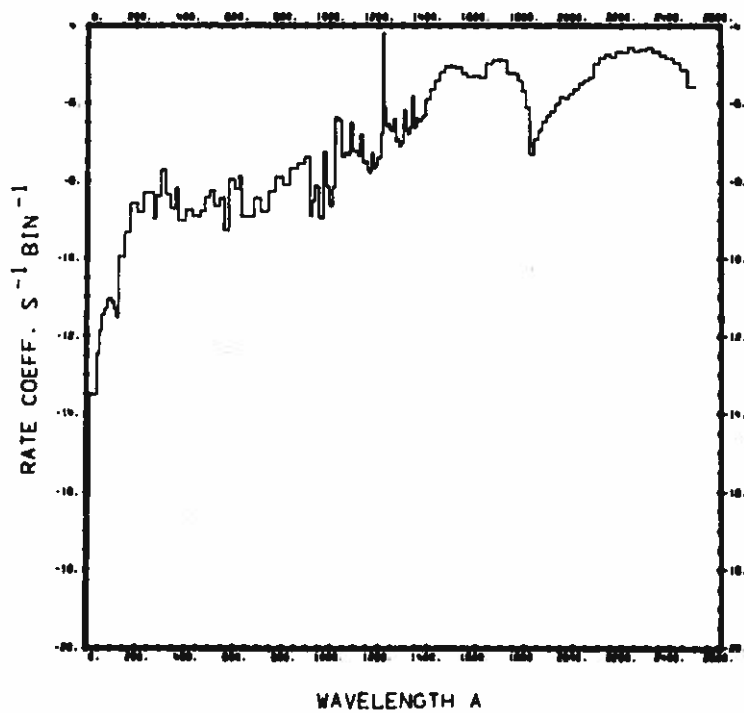


Fig. 74.
 $\text{HCOOH} + \nu \rightarrow \text{OH} + \text{HCO}.$

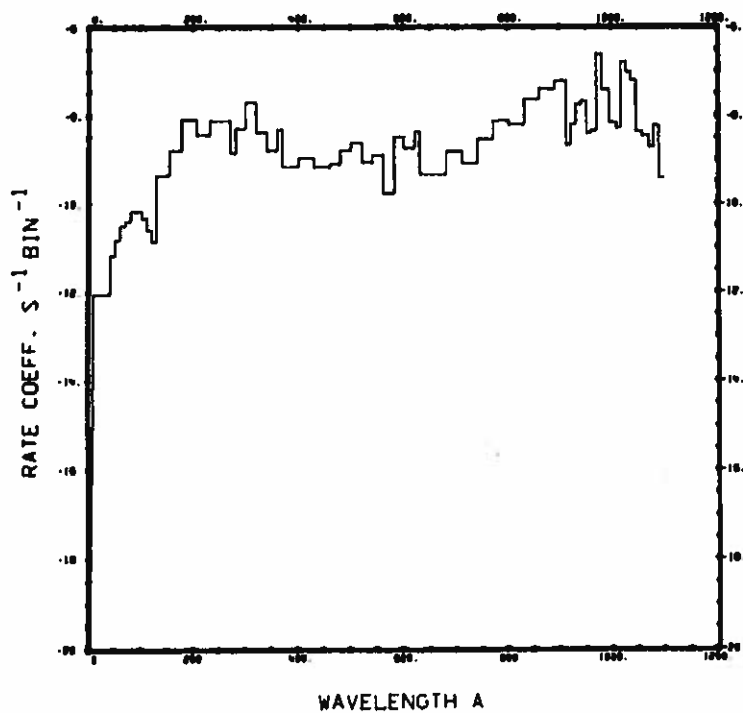


Fig. 75.
 $\text{HCOOH} + \nu \rightarrow \text{HCOOH}^+ + e.$

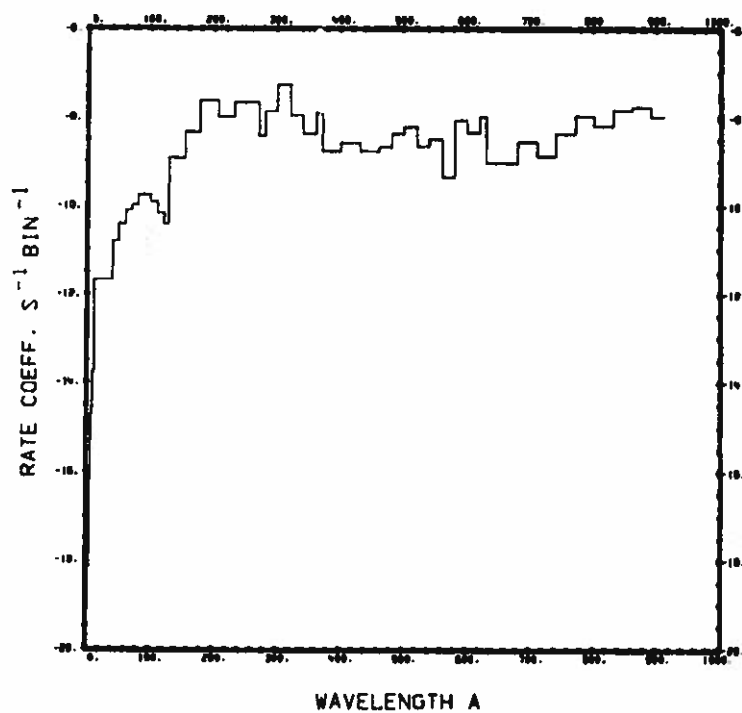


Fig. 76.
 $\text{HCOOH} + \nu \rightarrow \text{OH} + \text{HCO}^+ + e.$

Cyanoacetylene, HC₃N

Cross section:

In the range $\lambda = 1 \text{ \AA}$ to 800 \AA the cross section is synthesized from the cross sections of the atomic constituents. From $\lambda = 1058 \text{ \AA}$ to 1632 \AA data is taken from Connors et al.¹⁰¹

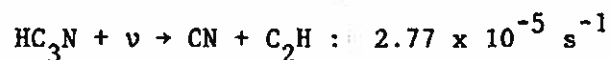
Branching ratios:

No branching ratios are available. It was assumed that only dissociation into CN + C₂H takes place.

Thresholds:

No data for the dissociation threshold was found; we assumed it to be at $\lambda = 1632 \text{ \AA}$.

Rate coefficients:



This is only a very approximate value. Our value is larger than the one found by Potter and del Duca¹ ($1.5 \times 10^{-5} \text{ s}^{-1}$), but smaller than that of Jackson^{2,3} ($7.6 \times 10^{-5} \text{ s}^{-1}$).

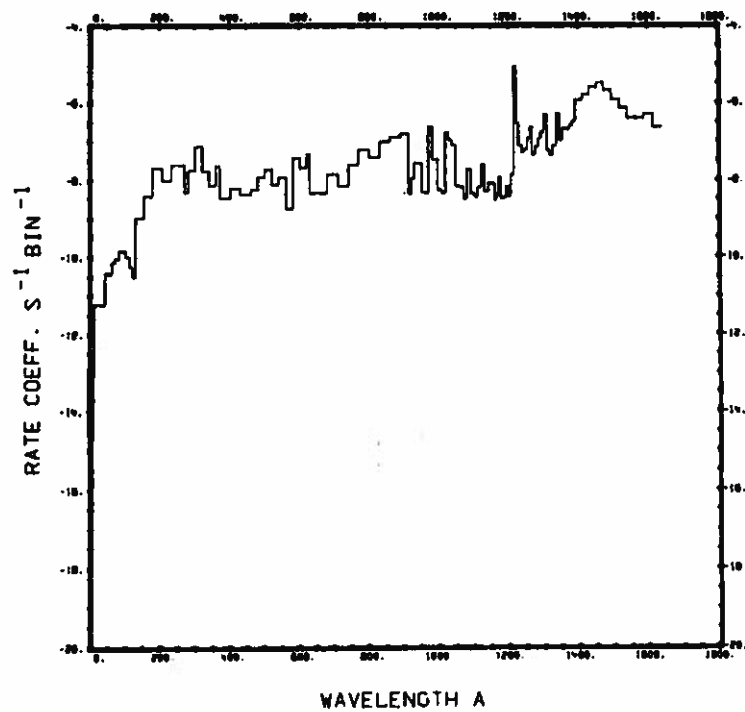
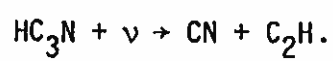


Fig. 77.



Ethylene, C_2H_4

Cross section:

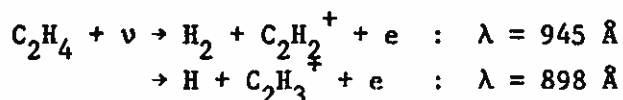
Between $\lambda = 180 \text{ \AA}$ and 700 \AA the measured cross section comes from Lee et al.⁵⁵ From $\lambda = 500 \text{ \AA}$ to $\lambda = 1200 \text{ \AA}$ the data is from Schoen⁸⁴ and in the range $\lambda = 1065 \text{ \AA}$ to 1973 \AA the cross section reported by Zelikoff and Watanabe¹⁰² was used.

Branching ratios:

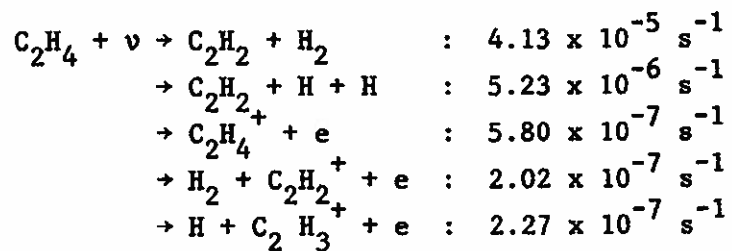
McNesby and Okabe⁵⁸ state that above $\lambda = 1236 \text{ \AA}$ only dissociation leading to $C_2H_2 + H_2$ occurs. Strobel¹⁰³ reports that dissociation leading to $C_2H_2 + H + H$ occurs with a probability of 65% at the Ly α line. We have assumed that below 1226 \AA $C_2H_2 + H + H$ makes up 65% of total dissociation and $C_2H_2 + H_2$ makes up 35%. Above 1226 \AA $C_2H_2 + H_2$ is the only branch. The branching ratios for ionization and dissociative ionization are from Schoen.⁸⁴ The branching ratio for dissociation was estimated.

Thresholds:

Wilkinson and Mulliken¹⁰⁴ suggest that the threshold for the dissociation continuum is at $\lambda = 1710 \text{ \AA}$ and that similar to the oxygen Schumann-Runge system predissociation bands on the long wavelength side converge to this limit. We have therefore assumed an effective threshold at $\lambda = 1973 \text{ \AA}$ (the 0,0 band is at $\lambda = 2026 \text{ \AA}$) for dissociation into $C_2H_2 + H_2$ and at $\lambda = 1226 \text{ \AA}$ for dissociation into $C_2H_2 + H + H$. The ionization threshold as determined by Zelikoff and Watanabe¹⁰² is at $\lambda = 1180 \text{ \AA}$. Thresholds for photodissociative ionization have been determined by Botter et al.¹⁰⁵



Rate coefficients:



Our total rate coefficient ($4.76 \times 10^{-5} \text{ s}^{-1}$) is smaller than the value obtained by Potter and del Duca¹ ($6.5 \times 10^{-5} \text{ s}^{-1}$); but considering the uncertainties about the threshold, this is good agreement.

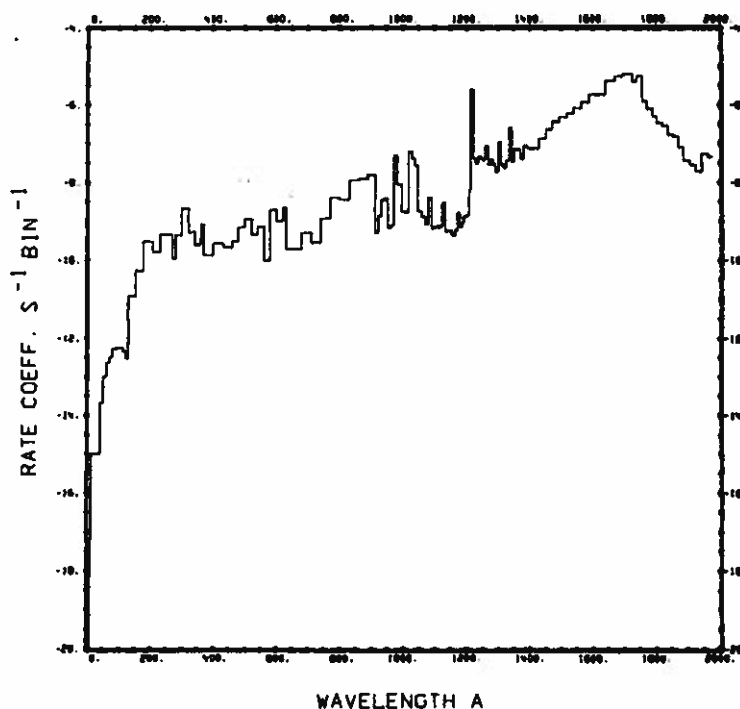


Fig. 78. $\text{C}_2\text{H}_4 + \nu \rightarrow \text{C}_2\text{H}_2 + \text{H}_2$.

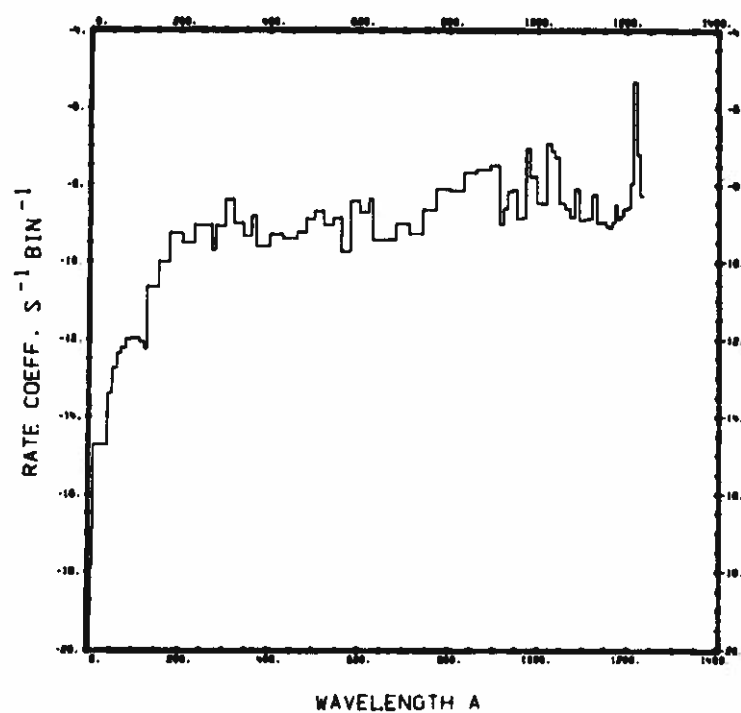


Fig. 79.
 $\text{C}_2\text{H}_4 + \nu \rightarrow \text{C}_2\text{H}_2 + \text{H} + \text{H}.$

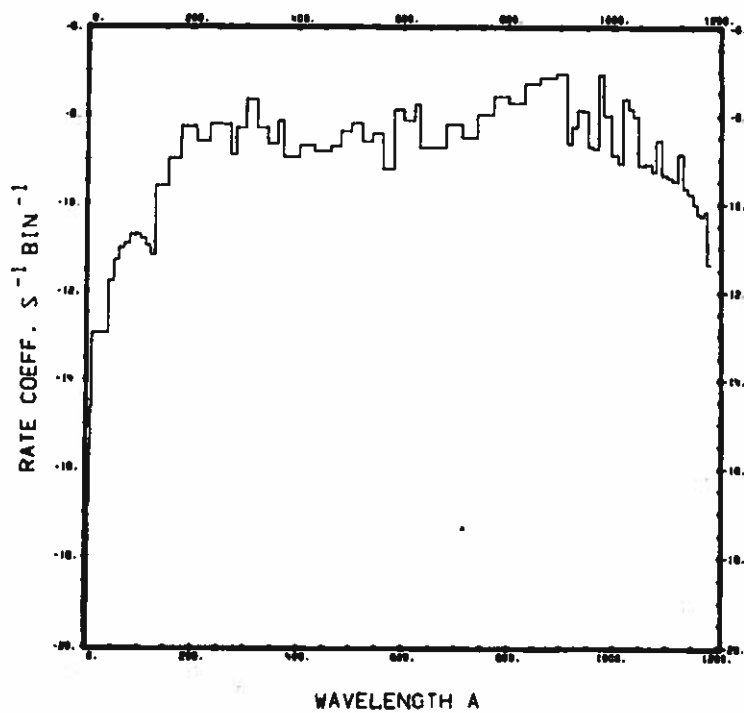


Fig. 80.
 $\text{C}_2\text{H}_4 + \nu \rightarrow \text{C}_2\text{H}_4^+ + \text{e}.$

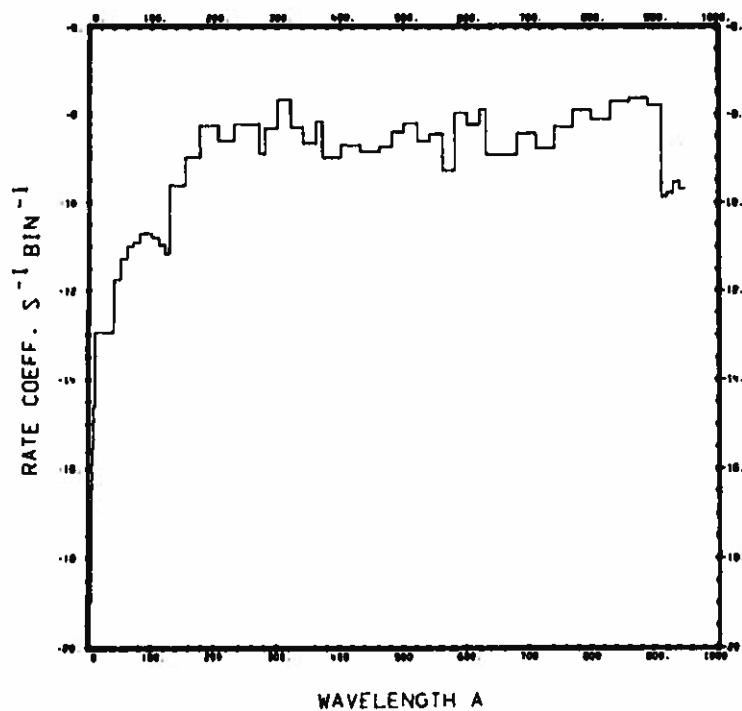


Fig. 81.
 $\text{C}_2\text{H}_4 + \nu \rightarrow \text{H}_2 + \text{C}_2\text{H}_2^+ + \text{e}$.

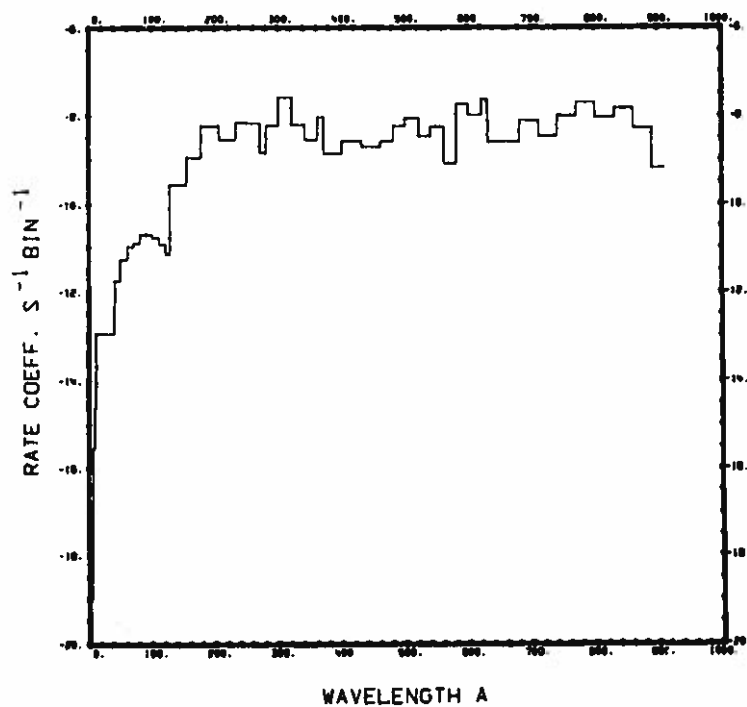


Fig. 82.
 $\text{C}_2\text{H}_4 + \nu \rightarrow \text{H} + \text{C}_2\text{H}_3^+ + \text{e}$.

Methanol, CH₃OH

Cross section:

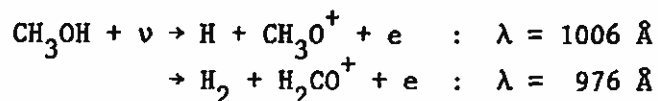
From $\lambda = 1 \text{ \AA}$ to 800 \AA the cross section is synthesized from its atomic constituents. Between 800 \AA and 1200 \AA data have been scaled from values of water. In the range from $\lambda = 1200 \text{ \AA}$ to 2053 \AA the data of Salahub and Sandorfy¹⁰⁶ are used.

Branching ratios:

The data of Porter and Noyes¹⁰⁷ indicate that the dissociation branch to $\text{OH} + \text{CH}_3$ contributes less than 5% of all photoprocesses. A 5% branching ratio was assumed for this process. All other branching ratios are guessed, the guesses are based on water data.

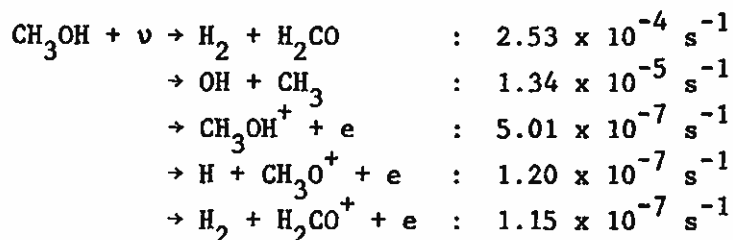
Thresholds:

Thresholds for dissociation are not available, but are probably at longer wavelengths than 2053 \AA , which is the value we assumed. The threshold for ionization $\lambda = 1143 \text{ \AA}$ is given by Salahub and Sandorfy;¹⁰⁶ while the threshold wavelengths for dissociative ionizations



are obtained from Field and Franklin.¹⁰⁰

Rate coefficients:



Our total rate coefficient ($2.67 \times 10^{-4} \text{ s}^{-1}$) is larger than the value given by Jackson^{2,3} ($4.7 \times 10^{-5} \text{ s}^{-1}$). The dissociation rates are dominated by $\text{Ly } \alpha$.

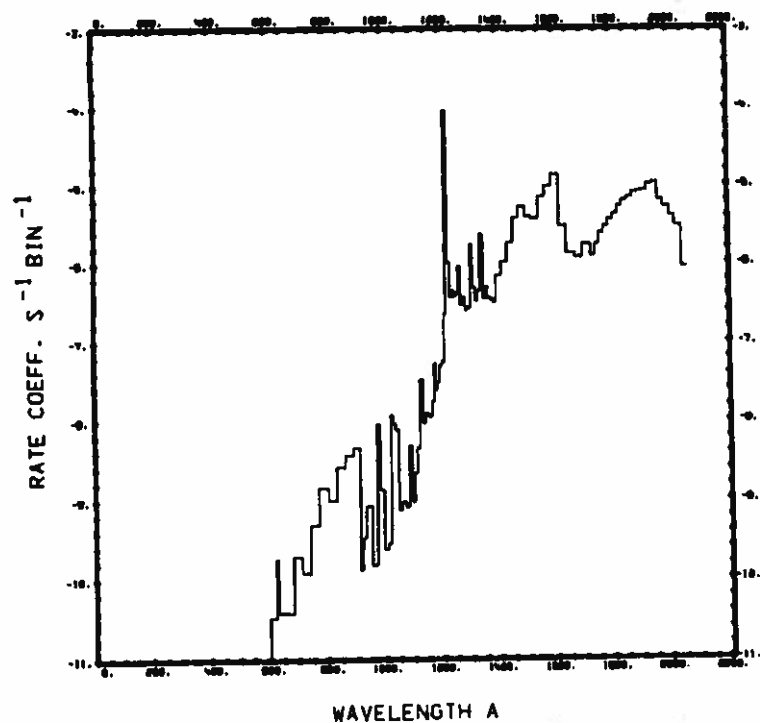


Fig. 83.
 $\text{CH}_3\text{OH} + \nu \rightarrow \text{H}_2 + \text{H}_2\text{CO}.$

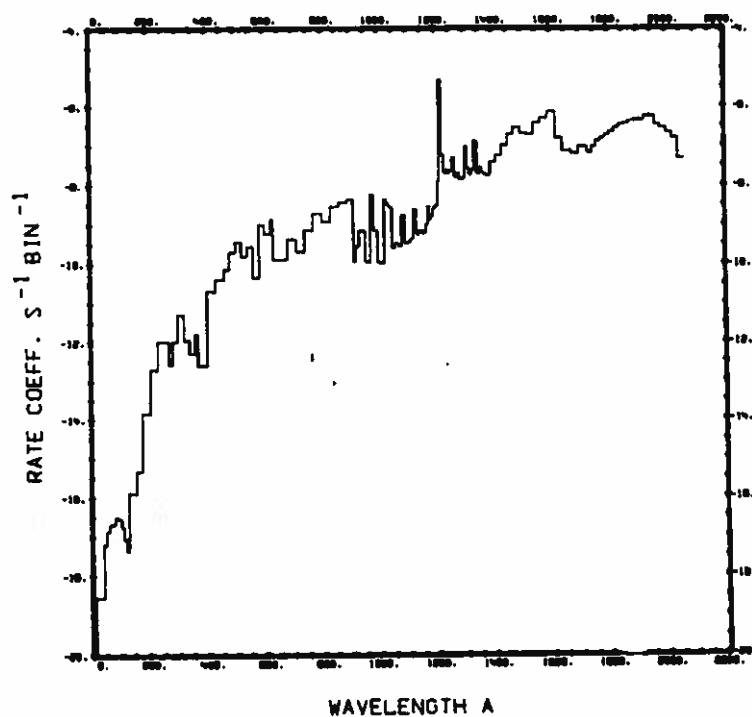


Fig. 84.
 $\text{CH}_3\text{OH} + \nu \rightarrow \text{OH} + \text{CH}_3.$

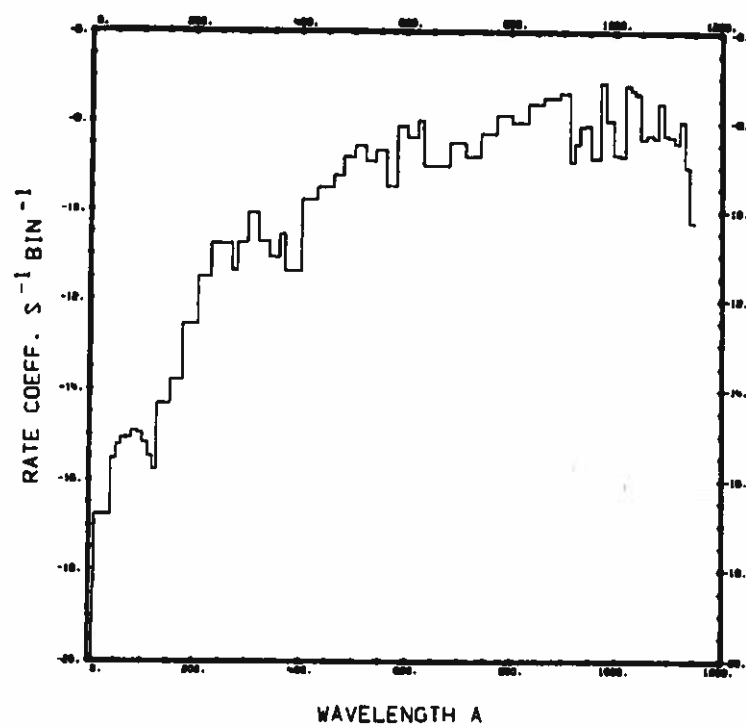


Fig. 85.
 $\text{CH}_3\text{OH} + \nu \rightarrow \text{CH}_3\text{OH}^+ + e_1$.

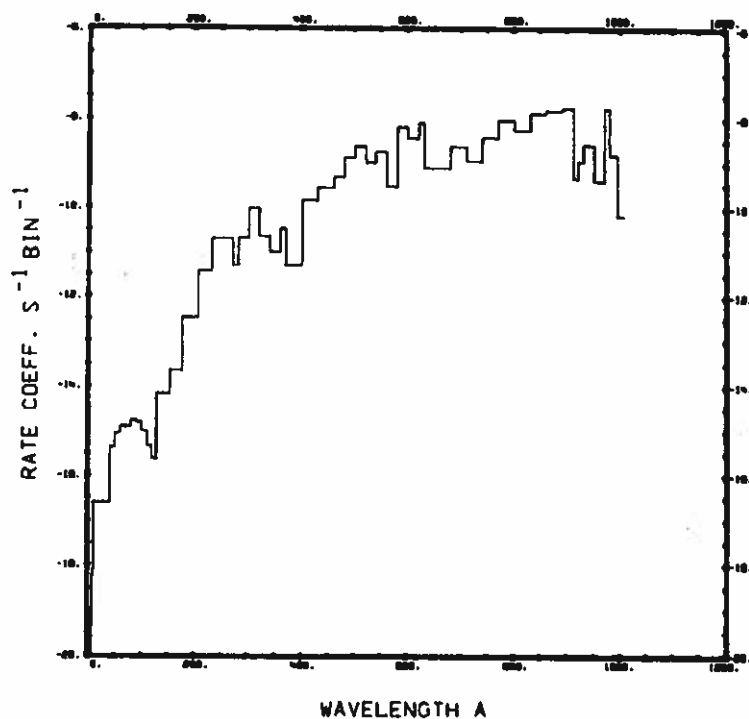


Fig. 86.
 $\text{CH}_3\text{OH} + \nu \rightarrow \text{H} + \text{CH}_3\text{O}^+ + e$.

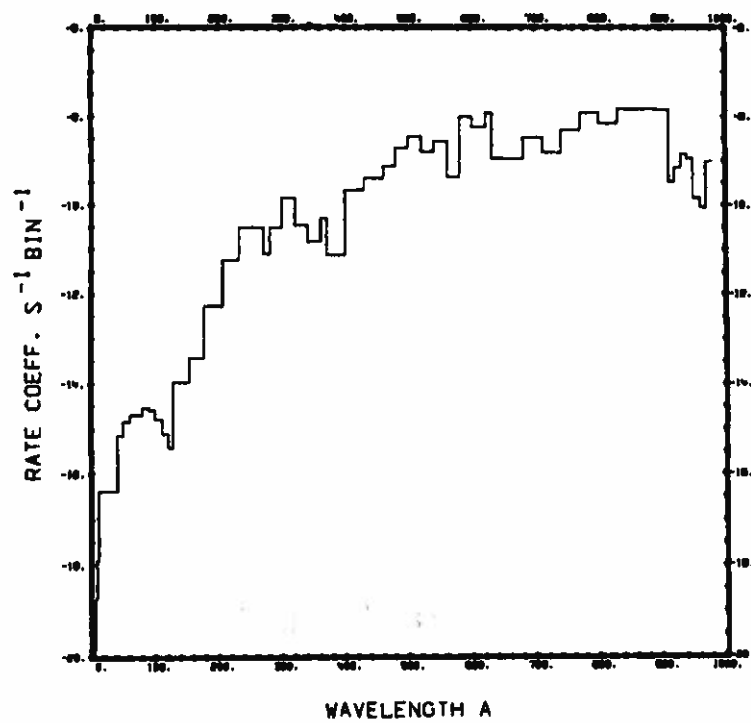
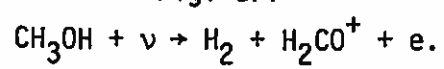


Fig. 87.



ACKNOWLEDGMENTS

We thank Dr. P. Giguere for helpful suggestions and for valuable comments in the reading of the manuscript.

REFERENCES

1. A. E. Potter and B. del Duca, "Lifetime in Space of Possible Parent Molecules of Cometary Radicals," *Icarus* 3, 103-108 (1964).
2. W. M. Jackson, "The Photochemical Formation of Cometary Radicals," *J. Photochem.* 5, 107-118 (1976).
3. W. M. Jackson, "Laboratory Observations of the Photochemistry of Parent Molecules: A Review," in *The Study of Comets*, B. Donn, M. Mumma, W. Jackson, M. A'Hearn, and R. Harrington, Eds., Proc. IAU Colloquium No. 25, Goddard Space Flight Center, Greenbelt, Md., October 28-November 1, 1974 (National Aeronautics and Space Administration, Washington, DC, 1976) NASA SP-393, Vol. 2, p. 679-702.
4. G. L. Siscoe and N. R. Mukherjee, "Upper Limits on the Lunar Atmosphere Determined from Solar-Wind Measurements," *J. Geophys. Res.* 77, 6042-6051 (1972).
5. M. B. McElroy and D. M. Hunten, "Photochemistry of CO₂ in the Atmosphere of Mars," *J. Geophys. Res. Space Phys.* 75, 1188-1201 (1970).
6. M. B. McElroy and J. C. McConnell, "Atomic Carbon in the Atmospheres of Mars and Venus," *J. Geophys. Res.* 76, 6674-6690 (1971).
7. M. B. McElroy, T. Y. Kong, and Y. L. Yung, "Composition and Structure of the Martian Upper Atmosphere: Analysis of Results from Viking," *Science* 194, 1295-1298 (1976).
8. W. I. Axford, "The Interaction of the Solar Wind with the Interstellar Medium," in *Solar Wind*, C. P. Sonett, P. J. Coleman, Jr., and J. M. Wilcox, Eds., Proc. NASA Conf., Asilomar Conf. Grounds, Pacific Grove, Cal., March 21-26, 1971 (National Aeronautics and Space Administration, Washington, D.C., 1972) NASA SP-308, p. 609-658.
9. R. E. Huffman, "Photochemical Processes: Cross Section Data," in *Defense Nuclear Agency Reaction Rate Handbook*, 2nd ed., M. H. Bortner and T. Baurer, Eds., DNA 1948H, Chapt. 12 (1971).
10. T. Baurer and M. H. Bortner, "Summary of Suggested Rate Constants," in *Defense Nuclear Agency Reaction Rate Handbook*, 2nd ed., M. H. Bortner and T. Baurer, Eds., DNA 1948H, Revision 7, Chapt. 24 (1978).
11. W. Swider, Jr., "Ionization Rates Due to the Attenuation of 1-100 Å Nonflare Solar X Rays in the Terrestrial Atmosphere," *Rev. Geophys.* 7, 573-594 (1969).
12. H. E. Hinteregger, "The Extreme Ultraviolet Solar Spectrum and its Variation during a Solar Cycle," *Ann. Geophys.* 26, 547-554 (1970).

13. L. A. Hall and H. E. Hinteregger, "Solar Radiation in the Extreme Ultraviolet and Its Variation with Solar Rotation," *J. Geophys. Res.* 75, 6959-6965 (1970).
14. M. Ackerman, "Ultraviolet Solar Radiation Related to Mesospheric Processes," in Mesospheric Models and Related Experiments, G. Fiocco, Ed., Proc. 4th ESRIN-ESLAB Symp., Frascati, Italy, July 6-10, 1970 (Reidel, Dordrecht-Holland, 1971), p. 149-159.
15. P. Simon, "Balloon Measurements of Solar Fluxes Between 1960 Å and 2300 Å," in Proceedings of the Third Conference on the Climatic Impact Assessment Program, A. J. Broderick and T. M. Hard, Eds., Proc. 3rd Conf. Climatic Impact Assessment Program, Transportation Syst. Cent., Kendall Square, Cambridge, Mass., February 26-March 1, 1974, Dept. Transportation report DOT-TSC-OST-74-15, p. 137-141.
16. M. Stobbe, "Zur Quantenmechanik Photoelektrischer Prozesse," *Ann. Physik*, Ser. 5, 7, 661-715 (1930).
17. F. Sauter, "Über den Atomaren Photoeffekt bei grosser Härte der anregenden Strahlung," *Ann. Physik*, Ser. 5, 9, 217-248 (1931).
18. H. A. Bethe and E. E. Salpeter, Quantum Mechanics of One- and Two-Electron Atoms, (Springer-Verlag, Berlin, Göttingen, Heidelberg, 1957) p. 315.
19. C. E. Moore, "Ionization Potentials and Ionization Limits Derived from the Analyses of Optical Spectra," *Nat. Stand. Ref. Data Ser.*, Nat. Bur. Stand. report NSRDS-NBS 34 (1970).
20. H. U. Keller, "Wasserstoff als Dissoziationsprodukt in Kometen," *Mitt. Astron. Ges.* 30, 143 (1971).
21. J. L. Bertaux, J. E. Blamont, and M. Festou, "Interpretation of Hydrogen Lyman-Alpha Observations of Comets Bennett and Encke," *Astron. Astrophys.* 25, 415-430 (1973).
22. R. J. W. Henry, "Photoionization Cross-Sections for Atoms and Ions of Carbon, Nitrogen, Oxygen, and Neon," *Astrophys. J.* 161, 1153-1155 (1970).
23. W. D. Barfield, G. D. Koontz, and W. F. Huebner, "Fits to New Calculations of Photoionization Cross Sections for Low-Z Elements," *J. Quant. Spectrosc. Radiat. Transfer* 12, 1409-1433 (1972).
24. J. A. R. Samson and R. B. Cairns, "Total Absorption Cross Sections of H₂, N₂ and O₂ in the Region 550-200 Å," *J. Opt. Soc. Am.* 55, 1035 (1965).
25. G. R. Cook and P. H. Metzger, "Photoionization and Absorption Cross Sections of H₂ and D₂ in the Vacuum Ultraviolet Region," *J. Opt. Soc. Am.* 54, 968-972 (1964).
26. J. E. Brolley, L. E. Porter, R. H. Sherman, J. K. Theobald, and J. C. Fong, "Photoabsorption Cross Sections of H₂, D₂, N₂, O₂, Ar, Kr, and Xe at the 584-Å Line of Neutral Helium," *J. Geophys. Res.* 78, 1627-1632 (1973).

27. R. Browning and J. Fryar, "Dissociative Photoionization of H_2 and D_2 through the $1s\sigma_g$ Ionic State," J. Phys. B: Atom. Molec. Phys. 6, 364-371 (1973).
28. G. Herzberg and A. Monfils, "The Dissociation Energies of the H_2 , HD, and D_2 Molecules," J. Mol. Spectrosc. 5, 482-498 (1960).
29. H. Beutler and H.-O. Jünger, "Über das Absorptionsspektrum des Wasserstoffs. III. Die Autoionisierung in Term $3p\pi\ ^1\Pi$ des H_2 und ihre Auswahlgesetze. Bestimmung der Ionisierungsenergie des H_2^u ," Z. Phys. 100, 80-94 (1936).
30. T. E. H. Walker and H. P. Kelly, "The Photoionization Cross Section for Diatomic CH," Chem. Phys. Letters 16, 511-514 (1972).
31. J. Barsuhn and R. K. Nesbet, "The Photoionization and Photodissociation of CH in the Vicinity of the Ionization Threshold," J. Chem. Phys. 68, 2783-2793 (1978).
32. D. R. Bates and L. Spitzer, Jr., "The Density of Molecules in Interstellar Space," Astrophys. J. 113, 441-463 (1951).
33. M. J. Linevsky, "Relative Oscillator Strengths of CH. The Heat of Dissociation of CH," J. Chem. Phys. 47, 3485-3490 (1967).
34. E. H. Fink and K. H. Welge, "Lifetime Measurements on $CH(A^2\Delta)$, $CH(B^2\Sigma^-)$, and $C_2(A_3\Pi_g)$ by the Phase-Shift Method," J. Chem. Phys. 46, 4315-4318 (1967).
35. G. Herzberg and J. W. C. Johns, "New Spectra of the CH Molecule," Astrophys. J. 158, 399-418 (1969).
36. S. Wyckoff and P. A. Wehinger, "Molecular Ions in Comet Tails," Astrophys. J. 204, 604-615 (1976).
37. R. J. W. Henry and M. B. McElroy, "Photoelectrons in Planetary Atmospheres," in The Atmospheres of Venus and Mars, J. C. Brandt and M. B. McElroy, Eds., (Gordon Breach Science Publishers, Inc., New York, London, Paris, 1968), p. 251-285.
38. R. B. Cairns and J. A. R. Samson, "Absorption and Photoionization Cross Sections of CO_2 , CO, Ar, and He at Intense Solar Emission Lines," J. Geophys. Res. 70, 99-104 (1965).
39. G. R. Cook, P. H. Metzger, and M. Ogawa, "Photoionization and Absorption Coefficients of CO in the 600 to 1000 Å Region," Can. J. Phys. 43, 1706-1722 (1965).
40. J. A. Hall, J. Schamps, J. M. Robbe, and H. Lefebvre-Brion, "Theoretical Study of the Perturbation Parameter in the $a^3\Pi$ and $A^1\Pi$ states of CO," J. Chem. Phys. 59, 3271-3283 (1973).
41. A. L. Collins, Los Alamos Scientific Laboratory, personal communication, 1978.

42. P. L. Kronebusch and J. Berkowitz, "Photodissociative Ionization in the 21-41 eV Region: O₂, N₂, CO, NO, CO₂, H₂O, NH₃ and CH₄," Int. J. Mass Spectrosc. Ion Phys. 22, 283-306 (1976).
43. P. H. Krupenie, "The Band Spectrum of Carbon Monoxide," Nat. Stand. Ref. Data Ser., Nat. Bur. Stand. report NSRDS-NBS 5 (1966).
44. R. E. Huffman, "Absorption Cross-Sections of Atmospheric Gases for Use in Aeronomy," Can. J. Chem. 47, 1823-1834 (1969).
45. J. A. R. Samson and R. B. Cairns, "Absorption and Photoionization Cross Sections of O₂ and N₂ at Intense Solar Emission Lines," J. Geophys. Res. 69, 4583-4590 (1964).
46. G. R. Cook and P. H. Metzger, "Photoionization and Absorption Cross Sections of O₂ and N₂ in the 600- to 1000-Å Region," J. Chem. Phys. 41, 321-336 (1964).
47. R. E. Huffman, Y. Tanaka, and J. C. Larrabee, "Absorption Coefficients of Nitrogen in the 1000-580 Å Wavelength Region," J. Chem. Phys. 39, 910-925 (1963).
48. K. C. Clark, "Ionospheric Absorption by N₂ and O₂ of Certain Extreme Ultraviolet Solar Wavelengths," Phys. Rev. 87, 271-276 (1952).
49. K. Watanabe and F. F. Marmo, "Photoionization and Total Absorption Cross Section of Gases. II. O₂ and N₂ in the Region 850-1500 Å," J. Chem. Phys. 25, 965-971 (1956).
50. F. K. Itamoto, Jr., and H. C. McAllister, "Absorption Coefficients of Nitrogen in the Region 850 to 1000 Å," Contribution No. 29, Scientific report No. 4, Hawaii Inst. Geophys., U. Hawaii, Honolulu (1961).
51. J. Geiger and B. Schröder, "Intensity Perturbations Due to Configuration Interaction Observed in the Electron Energy-Loss Spectrum of N₂," J. Chem. Phys. 50, 7-11 (1969).
52. P. Gürtler, V. Saile, and E. E. Koch, "High Resolution Absorption Spectrum of Nitrogen in the Vacuum Ultraviolet," Chem. Phys. Letters 48, 245-250 (1977).
53. A. Lofthus and P. H. Krupenie, "The Spectrum of Molecular Nitrogen," J. Phys. Chem. Ref. Data 6, 113-307 (1977).
54. G. Herzberg, Molecular Spectra and Molecular Structure, I. Spectra of Diatomic Molecules (D. Van Nostrand Co., Inc., Princeton, N.J., Toronto, London, New York, 1950).
55. L. C. Lee, R. W. Carlson, D. L. Judge, and M. Ogawa, "The Absorption Cross Sections of N₂, O₂, CO, NO, CO₂, N₂O, CH₄, C₂H₄, C₂H₆ and C₄H₁₀ from 180 to 700 Å," J. Quant. Spectrosc. Radiat. Transfer 13, 1023-1031 (1973).

56. K. Watanabe, F. M. Matsunaga, and H. Sakai, "Absorption Coefficient and Photoionization Yield of NO in the region 580-1350 Å," Appl. Opt. 6, 391-396 (1967).
57. F. F. Marmo, "Absorption Coefficients of Nitrogen Oxide in the Vacuum Ultraviolet," J. Opt. Soc. Am. 43, 1186-1190 (1953).
58. J. R. McNesby and H. Okabe, "Vacuum Ultraviolet Photochemistry," Adv. Photochem. 3, 157-240 (1964).
59. F. M. Matsunaga and K. Watanabe, "Total and Photoionization Coefficients and Dissociation Continua of O₂ in the 580-1070 Å Region," Science Light 16, 31-42 (1967).
60. K. Watanabe, "Ultraviolet Absorption Processes in the Upper Atmosphere," Adv. Geophys. 5, 153-221 (1958).
61. M. Ackerman, F. Biaumé, and G. Kockarts, "Absorption Cross Sections of the Schumann-Runge Bands of Molecular Oxygen," Planet. Space Sci. 18, 1639-1651 (1970).
62. L. C. Lee, T. G. Slanger, G. Black, and R. L. Sharpless, "Quantum Yields for the Production of O(¹D) from Photodissociation of O₂ at 1160-1770 Å," J. Chem. Phys. 67, 5602-5606 (1977).
63. R. D. Hudson, "Critical Review of Ultraviolet Photoabsorption Cross Sections for Molecules of Astrophysical and Aeronomic Interest," Rev. Geophys. Space Phys. 9, 305-406 (1971).
64. R. W. Ditchburn and P. A. Young, "The Absorption to Molecular Oxygen Between 1850 and 2500 Å," J. Atmosph. Terrestr. Phys. 24, 127-139 (1962).
65. F. J. Comes, F. Speier, and A. Elzer, "Photoionisationsuntersuchungen an Atomstrahlen. II. Der Ionisierungsquerschnitt des atomaren Sauerstoffs," Z. Naturforsch. 23A, 125-133 (1968).
66. G. L. Weissler, J. A. R. Samson, M. Ogawa, and G. R. Cook, "Photoionization Analysis by Mass Spectroscopy," J. Opt. Soc. Am. 49, 338-349 (1959).
67. E. Phillips, L. C. Lee, and D. L. Judge, "Absolute Photoabsorption Cross Sections for H₂O and D₂O from λ 180-790 Å," J. Quant. Spectrosc. Radiat. Transfer 18, 309-313 (1977).
68. V. H. Dibeler, J. A. Walker, and H. M. Rosenstock, "Mass Spectrometric Study of Photoionization. V. Water and Ammonia," J. Res. NBS-A. Phys. Chem. 70A, 459-463 (1966).
69. D. H. Katayama, R. E. Huffman, and C. L. O'Bryan, "Absorption and Photoionization Cross Sections for H₂O and D₂O in the Vacuum Ultraviolet," J. Chem. Phys. 59, 4309-4319 (1973).
70. K. Watanabe and A. S. Jursa, "Absorption and Photoionization Cross Sections of H₂O and H₂S," J. Chem. Phys. 41, 1650-1653 (1964).

71. K. Watanabe and M. Zelikoff, "Absorption Coefficients of Water Vapor in the Vacuum Ultraviolet," J. Opt. Soc. Am. 43, 753-755 (1953).
72. J. R. McNesby, I. Tanaka, and H. Okabe, "Vacuum Ultraviolet Photochemistry. III. Primary Processes in the Vacuum Ultraviolet Photolysis of Water and Ammonia," J. Chem. Phys. 36, 605-607 (1962).
73. G. A. West, "Cyanide Radical Molecular Electronic and Vibrational Chemical Lasers: Hydrogen Cyanide Polyatomic Chemical Lasers," Ph.D. Thesis, U. Wisconsin, Madison, Order No. 75-18,204 (1975).
74. R. S. Nakata, K. Watanabe, and F. M. Matsunaga, "Absorption and Photoionization Coefficients of CO₂ in the Region 580-1670 Å," Science Light 14, 54-71 (1965).
75. G. M. Lawrence, "Photodissociation of CO₂ to Produce CO(*a*³Π)," J. Chem. Phys. 56, 3435-3442 (1972).
76. H. Sun and G. L. Weissler, "Absorption Cross Sections of Methane and Ammonia in the Vacuum Ultraviolet," J. Chem. Phys. 23, 1160-1164 (1955).
77. K. Watanabe and S. P. Sood, "Absorption and Photoionization Coefficients of NH₃ in the 580-1650 Å Region," Science Light 14, 36-53 (1965).
78. K. Watanabe, "Photoionization and Total Absorption Cross Section of Gases. I. Ionization Potentials of Several Molecules. Cross Sections of NH₃ and NO," J. Chem. Phys. 22, 1564-1570 (1954).
79. B. A. Thompson, P. Hartek, and R. R. Reeves, Jr., "Ultraviolet Absorption Coefficients of CO₂, CO, O₂, H₂O, N₂O, NH₃, NO, SO₂, and CH₄ between 1850 and 4000 Å," J. Geophys. Res. 68, 6431-6436 (1963).
80. W. Groth, H. Okabe, and H. J. Rommel, "Die Primärprozesse der NH₃-Photolyse bei 1470 Å," Z. Naturforsch. 19A, 507-508 (1964).
81. H. Okabe and M. Lenzi, "Photodissociation of NH₃ in the Vacuum Ultraviolet," J. Chem. Phys. 47, 5241-5246 (1967).
82. P. H. Metzger and G. R. Cook, "On the Continuous Absorption, Photoionization, and Fluorescence of H₂O, NH₃, CH₄, C₂H₂, C₂H₄, and C₂H₆ in the 600- to 1000-Å Region," J. Chem. Phys. 41, 642-648 (1964).
83. T. Nakayama and K. Watanabe, "Absorption and Photoionization Coefficients of Acetylene, Propyne, and 1-Butyne," J. Chem. Phys. 40, 558-561 (1964).
84. R. I. Schoen, "Absorption, Ionization, and Ion-Fragmentation Cross Sections of Hydrocarbon Vapors under Vacuum-Ultraviolet Radiation," J. Chem. Phys. 37, 2032-2040 (1962).
85. H. Okabe, "Photodissociation of Acetylene and Bromoacetylene in the Vacuum Ultraviolet: Production of Electronically Excited C₂H and C₂," J. Chem. Phys. 62, 2782-2787 (1975).

86. G. Herzberg, Molecular Spectra and Molecular Structure. III. Electronic Spectra and Electronic Structure of Polyatomic Molecules (Van Nostrand Reinhold Co., New York, Cincinnati, Toronto, London, Melbourne, 1966).
87. J. E. Mentall, E. P. Gentieu, M. Kraus, and D. Neumann, "Photoionization and Absorption Spectrum of Formaldehyde in the Vacuum Ultraviolet," *J. Chem. Phys.* 55, 5471-5479 (1971).
88. E. P. Gentieu and J. E. Mentall, "Formaldehyde Absorption Coefficients in the Vacuum Ultraviolet (650 to 1850 Angstroms)," *Science* 169, 681-683 (1970).
89. J. G. Calvert and J. N. Pitts, Jr., Photochemistry (John Wiley & Sons, Inc., New York, 1966).
90. J. H. Clark, C. B. Moore, and N. S. Nogar, "The Photochemistry of Formaldehyde: Absolute Quantum Yields, Radical Reactions and NO Reactions," *J. Chem. Phys.* 68, 1264-1271 (1978).
91. L. J. Stief, B. Donn, S. Glicker, E. P. Gentieu, and J. E. Mentall, "Photochemistry and Lifetimes of Interstellar Molecules," *Astrophys. J.* 171, 21-30 (1972).
92. P. M. Guyon, W. A. Chupka, and J. Berkowitz, "Photoionization Mass Spectrometric Study of Formaldehyde H_2CO , $HDCO$ and D_2CO ," *J. Chem. Phys.* 64, 1419-1436 (1976).
93. S. Glicker and L. J. Stief, "Photolysis of Formaldehyde at 1470 and 1236 Å," *J. Chem. Phys.* 54, 2852-2857 (1971).
94. A. P. Lukirskii, I. A. Brytov, and T. M. Zimkina, "Photoionization Absorption of He, Kr, Xe, CH_4 , and Methylal in the 23.6-250 Å Region," *Opt. Spektr.* (Engl. Trans.) 17, 234-237 (1964).
95. R. W. Ditchburn, "Absorption Cross-Sections in the Vacuum Ultra-Violet. III. Methane," *Proc. Roy. Soc. London* 229A, 44-62 (1955).
96. R. Gorden, Jr., and P. Ausloos, "Gas-Phase Photolysis and Radiolysis of Methane. Formation of Hydrogen and Ethylene," *J. Chem. Phys.* 46, 4823-4834 (1967).
97. E. E. Barnes and W. T. Simpson, "Correlations Among Electronic Transitions for Carbonyl and for Carboxyl in the Vacuum Ultraviolet," *J. Chem. Phys.* 39, 670-675 (1963).
98. R. Gorden, Jr., and P. Ausloos, "Vapor-Phase Photolysis of Formic Acid," *J. Phys. Chem.* 65, 1033-1037 (1961).
99. S. Bell, T. L. Ng, and A. D. Walsh, "Vacuum Ultra-Violet Spectra of Formic and Acetic Acids," *J. Chem. Soc. Faraday Trans. (2)* 71, 393-401 (1975).
100. F. H. Field and J. L. Franklin, Electron Impact Phenomena (Academic Press, New York, London, 1970).

101. R. E. Connors, J. L. Roebber, and K. Weiss, "Vacuum Ultraviolet Spectroscopy of Cyanogen and Cyanoacetylenes," J. Chem. Phys. 60, 5011-5024 (1974).
102. M. Zelikoff and K. Watanabe, "Absorption Coefficients of Ethylene in the Vacuum Ultraviolet," J. Opt. Soc. Am. 43, 756-759 (1953).
103. D. F. Strobel, "The Photochemistry of Hydrocarbons in the Jovian Atmosphere," J. Atmos. Sci. 30, 489-498 (1973).
104. P. G. Wilkinson and R. S. Mulliken, "Far Ultraviolet Absorption Spectra of Ethylene and Ethylene-d₄," J. Chem. Phys. 23, 1895-1907 (1955).
105. R. Botter, V. H. Dibeler, J. A. Walker, and H. M. Rosenstock, "Mass-Spectrometric Study of Photoionization. IV. Ethylene and 1,2-Dideutero-ethylene," J. Chem. Phys. 45, 1298-1301 (1966).
106. D. R. Salahub and C. Sandorfy, "The Far-Ultraviolet Spectra of Some Simple Alcohols and Fluoroalcohols," Chem. Phys. Letters 8, 71-74 (1971).
107. R. P. Porter and W. A. Noyes, Jr., "Photochemical Studies, LIV. Methanol Vapor," J. Am. Chem. Soc. 81, 2307-2311 (1959).

Printed in the United States of America. Available from
 National Technical Information Service
 U.S. Department of Commerce
 5285 Port Royal Road
 Springfield, VA 22161

Microfiche \$3.00

001-025	4.00	136-150	7.25	251-275	10.75	376-400	13.00	501-525	15.25
026-050	4.50	151-175	8.00	276-300	11.00	401-425	13.25	526-550	15.50
051-075	5.25	176-200	9.00	301-325	11.75	426-450	14.00	551-575	16.25
076-100	6.00	201-225	9.25	326-350	12.00	451-475	14.50	576-600	16.50
101-125	6.50	226-250	9.50	351-375	12.50	476-500	15.00	601-up	

Note: Add \$2.50 for each additional 100-page increment from 601 pages up.

LAIL
CLASSIFIED
REPORT LIBRARY

JAN 25 1960

RECEIVED

